Master's Thesis

Master`s Degree Programme in Biomedicine
May 2021

Effects of polycyclic aromatic hydrocarbons (PAHs) on cell viability and gene expression related to neurite outgrowth in human neural stem cells undergoing differentiation

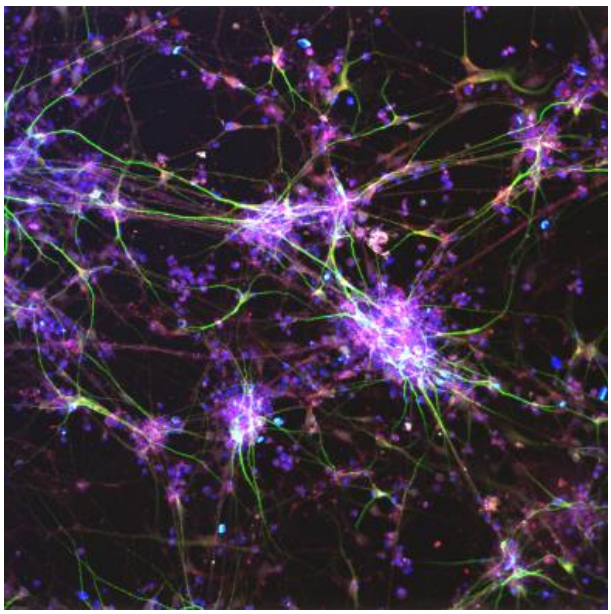

Inger Margit Alm

MABIO5900

60 ETC

Faculty of Health Sciences

OSLO METROPOLITAN UNIVERSITY
STORBYUNIVERSITETET

Effects of polycyclic aromatic hydrocarbons (PAHs) on cell viability and gene expression related to neurite outgrowth in human neural stem cells undergoing differentiation

Inger Margit Alm

Section of Toxicology and Risk Assessment, Department of Environmental Health

Norwegian Institute of Public Health

Supervisors: Oddvar Myhre, Jørn A. Holme, Ragnhild Paulsen
and Anna Jacobsen Lauvås

Master Thesis submitted for Master`s Degree in Biomedicine, 60 ETC

Faculty of Health Sciences

Department of Life Sciences and Health

May 2021
Oslo Metropolitan University

ACKNOWLEDGMENTS

The work presented in this thesis was carried out at the Section of Toxicology and Risk Assessment, Department of Environmental Health at the Norwegian Institute of Public Health (NIPH) from August 2020 until May 2021, as a part of the master's degree program in Biomedicine at Oslo Metropolitan University. All experimental work has been carried out under the supervision of MSc Anna Jacobsen Lauvås. My main advisor was Dr. Oddvar Myhre at the Section of Toxicology and Risk Assessment. Dr. Jørn Andreas Holme at the Section of Air Pollution and Noise, Professor Ragnhild Paulsen at the University of Oslo, and MSc Anna Jacobsen Lauvås were my co-advisors.

First, I would like to express my gratitude to Anna. You have been an amazing teacher and thank you for your patience, guidance, and for sharing laboratory experience and teaching me about the NSC model, it has not been just easy. I would also thank my co-student Malene Lislien for all the good times in the lab and for sharing experience and knowledge. I will truly miss all the good conversations and discussions we had together in the lab.

I would like to extend my gratitude to my advisors Oddvar and Jørn for giving me the opportunity to be a part of this exciting research, and for all shared knowledge and valuable feedback during the experimental and writing phase of this thesis. Thanks to Tone Rasmussen for always taking the time to find or answer whatever I asked for. I would also like to thank Ragnhild for sharing knowledge and help during this thesis.

Finally, I would like to thank my friends and family for their encouragement and support through this exciting and demanding year. It has not all been easy to work and write a thesis during a pandemic.

Oslo May 2021

Inger Margit Alm

ABSTRACT

Polycyclic aromatic hydrocarbons (PAHs) are widespread environmental pollutants formed under incomplete combustions of organic materials such as the burning of fossil fuels, domestic heating, automobile exhaust, cooking, and tobacco smoke. Some of the PAHs, like benzo[a]pyrene (B[a]P), are known for their carcinogenic, genotoxic, and reproductive toxic properties. Furthermore, concerns have been raised about the impact of PAHs on neurodevelopment and possibly neurodevelopmental disorders, since accumulating evidence in both animal and epidemiological studies points in the direction that PAH exposure can lead to adverse effects on the developing brain. PAHs are lipophilic compounds and when inhaled they can readily pass the placenta omitting the first path elimination in the liver. The fetus is therefore at high risk due to limited protection by an immature blood-brain barrier and because of the highly vulnerable dynamic complex processes during neurodevelopment. In this thesis, neural stem cells derived from human induced pluripotent stem cells were used. This model can mimic key neurodevelopmental differentiation processes, vital for normal brain development, which were assessed by changes in cell viability, gene expression, and protein markers. The neural stem cells were during differentiation to a complex neuronal network exposed to a wide concentration range of three PAHs, namely B[a]P, β-naphthoflavone (β-NF), and pyrene for up to 21 days. Effects on cell viability were measured with Alamar Blue™ Cell Viability assay after exposure for 1, 3, 14, and 21 days. Changes in expression of genes related to neurodevelopment were evaluated with real-time PCR after exposure for 3, 14, and 21 days. Protein markers were qualitatively investigated with immunocytochemistry and high content imaging after 14 and 21 days of exposure. The culture and differentiation processes developed as expected, determined by changes in morphology and gene expression in addition to the protein markers. Exposure to low concentrations of β-NF and pyrene increased cell viability, while higher concentrations of particular B[a]P caused cytotoxicity. Minor alternations were found in gene expression, and only one gene was statistically significantly changed upon exposure. Expression of the astrocyte marker *GFAP* was unexpectedly not detected. Protein expression of markers related to neurodevelopment was only qualitative and did not reveal any visible differences after PAH exposure up to 21 days. In conclusion, exposure to the PAHs increased cell viability at nanomolar concentrations of β-NF and pyrene, whereas micromolar concentrations of B[a]P caused a decrease. The neurite outgrowth marker *GAP43* was statistically significantly increased after 21 days of exposure to the three PAHs. No visible alterations in protein markers for neurodevelopment processes were observed.

SAMMENDRAG

Polysykliske aromatiske hydrokarboner (PAHer) er en stor gruppe av miljøforurensende stoffer/kjemikalier som dannes under ufullstendig forbrenning av organisk materiale. Utslipp ses i sammenheng med husholdningsoppvarming, bileksos, matlagning og tobakksrøyk. Noen PAHer, som benzo[a]pyren (B[a]P), er kjent for sin kreftfremkallende, gentoksiske og reproduksjonstoksiske egenskaper. Bekymring rundt mulige nevroutviklingsforstyrrelser indusert av PAHer, har blitt utrykt, etter akkumulerende bevis i både dyrestudier og epidemiologiske studier. PAHer er fettløselige forbindelser, og når de inhaleres, kan de passere morkaken og unngå første linje-elimineringen i leveren. Fosteret har derfor høy risiko for eksponeringen som følge av den umodne blodhjerne-barrieren og de svært sårbare og dynamiske prosessene under nevroutvikling.

I denne oppgaven ble nevrale stamceller utviklet fra human induserte pluripotente stamceller benyttet. Cellemodellen kan etterligne viktige prosesser i human nevroutvikling/hjerneutvikling og mulig endringer i slike prosesser ble undersøkt ved bruk av viabilitetsstudier, genuttrykk og proteinmarkører. Nevrale stamceller ble, under differensiering, til et komplekst nettverk av nevroner eksponert for ulike konsentrasjoner av PAHer i opptil 21 dager. PAHer som ble benyttet var B[a]P, β-naftoflavon (β-NF) og pyrene. Effekter på celleviabilitet ble målt med Alamar Blue™ etter eksponering i 1, 3, 14 og 21 dager. Endring i genuttrykk ble analysert med sanntids-PCR etter eksponering i 3, 14 og 21 dager. Proteinmarkører ble undersøkt kvalitativt med immuncytokjemi og visualisert med høyoppløselighetbilledtakning etter eksponering i 14 og 21 dager. Cellekulturen og differensieringsprosessen utviklet seg som forventet, som vist ved endringer i morfologi, genuttrykk og forekomst av proteinmarkører. Eksponering for lave konsentrasjoner av β-NF og pyren førte til en økning i celleviabilitet, mens høye konsentrasjoner av særlig B[a]P forårsaket cytotoksisitet. Mindre endringer ble funnet i genuttrykk, og kun et gen var statistisk signifikant endret etter eksponering. Genuttrykk av *GFAP* ble ikke funnet og bør videre undersøkes. Proteinutrykk av markører relatert til nevroutvikling og morfologi var kun kvalitativt vurdert, og ingen åpenbare forskjeller ble funnet etter PAH-eksponering i opptil 21 dager. Det konkluderes med at PAH-eksponering av nanomolare konsentrasjoner av β-NF og pyren økte celleviabiliteten, mens mikromolare konsentrasjoner av den mulige kreftfremkallende PAH-forbindelsen B[a]P forårsaket en reduksjon. Nevrittutvekstmarkøren *GAP43* ble statistisk signifikant økt etter 21 dager eksponering. Ingen åpenbare endringer i proteinutrykk ble observert.

ABBREVIATIONS

ADHD	Attention Deficit Hyperactivity Disorder
AhR	Aryl hydrocarbon Receptor
AO	Adverse Outcome
AOP	Adverse Outcome Pathway
ARNT	AhR nuclear translocator
ASD	Autism Spectrum Disorders
B[a]P	Benzo[*a*]pyrene
BBB	Blood-Brain Barrier
BDNF	Brain-Derived Neurotrophic Factor
BMM	Basement Membrane Matrix
BSA	Bovine Serum Albumin
cDNA	complementary DNA
CNS	Central Nervous System
CYP	Cytochrome P-450
DIV	Days of differentiation
DMEM/F12	Dulbecco`s Modified Eagle Medium F-12 Nutrient Matrix
DMSO	Dimethyl Sulfoxide
DNT	Developmental neurotoxicity
EC-JRC	European Commission Joint Research Centre
ECVAM	European Centre for the validation of Alternative Methods
GABA	Gamma Amino Butyric acid
GAP43	Growth associated protein 43

GFAP	Glial fibrillary acid protein
GST	Glutathione S-transferase
h	Hour
hESC	Human Embryonic Stem Cells
hiPSC	Human induced Pluripotent Stem Cells
IQ	Intellectual Quotient
LAF	Laminar-air flow
LOD	Limit of Detection
MAP2	Microtubule-associated protein 2
mRNA	messenger ribonucleic acid
ND	Neuronal Differentiation
NI	Neural Induction
NIPH	Norwegian Institute of Public Health
NMDA	N-Methyl-D-Aspartate
NRT	No Reverse Transcription control
NSC	Neural Stem Cell
NTC	Non-Template control
OECD	Organization for Economic co-operation and Development
PAH	Polycyclic aromatic hydrocarbon
PBS	Phosphate buffered saline
PBS+	Phosphate buffered saline with Ca^{2+} and Mg^{2+}
PCR	Polymerase Chain Reaction
PDL	Poly-D-Lysine

PM	Particulate matter
PSC	Pluripotent Stem Cell
PSD95	Post-synaptic Density Protein 95
RFU	Relative Fluorescence Unit
rGF	Basement Membrane Matrix reduced Growth Factor
ROS	Reactive Oxygen Species
RT	Reverse Transcriptase
S.E.M	Standard Error of mean
SD	Standard Deviation
SYP	Synaptophysin
TH	Tyrosine Hydroxylase
WHO	World Health Organization
XRE	Xenobiotic-responsive element
β-NF	β-Naphthoflavone

Table of Contents

1. INTRODUCTION

1.1 Background

Air pollution is a major cause of diseases, disability life years and deaths around the world. The World Health Organization (WHO) reported that over 80% of the world's population live in areas where air pollution exceeds the limit set by the WHO (6). Air pollution is a complex mixture of particulate matter (PM) and absorbed organic compounds originating mainly from anthropogenic sources (7). Polycyclic aromatic hydrocarbons (PAHs) are widespread environmental pollutants formed under incomplete combustions of organic materials such as burning of fuels, domestic heating, automobile exhaust, cooking, and tobacco smoke (8, 9). In air pollution PAHs are often present (9), however they can also occur in food (8, 9). Air pollution has been linked to health effects such as cardiovascular diseases, asthma, and lung cancer (10-14). There are accumulating studies in humans and animals that air pollutions also targets the brain and may lead to adverse effects on the central nervous system (CNS) such as dementia (15-18) and/or depression (19).

In children, air pollution has been associated with an increase in adverse neurodevelopment such as learning disabilities and lowered IQ (20), in addition to Autism Spectrum Disorders (ASD) (21), Attention Deficit Hyperactivity Disorder (ADHD) (7, 22, 23), and schizophrenia (24). In many of these studies, the authors suggest a possible role of PAHs on developmental neurotoxicity (DNT) effects. The developing brain in children and fetuses is suspected to be more vulnerable to perturbations by chemicals than the adult brain (3, 25, 26). The cause of neurodevelopmental disorders is, however, not fully known, and more mechanistic knowledge is also needed to support the association between air pollutants and DNT outcomes. A particular challenge in the evaluation of the DNT effects induced by exogenous chemicals is that the neurodevelopmental effects not only depend on dose and duration, but also on the developmental stage of the brain and the time of exposure (25, 27). It is additionally challenging to study the effects of environmental contaminants in pregnant women for obvious, ethical reasons.

1.2 Polycyclic aromatic hydrocarbons

Polycyclic aromatic hydrocarbons (PAHs) are a large group of environmental contaminants that have two or more fused benzene rings. They are made up of carbon and hydrogen atoms (8). PAHs can be divided into two groups, low and high molecular wight PAHs. The low molecular weight group consists of PAHs with two and three rings while the high molecular weight consists of PAHs with four or more rings (28). Hundreds of different PAHs are ubiquitously in the environment and the biological effects of a majority of these are still unknown. Many of them are exhibiting toxic, mutagenic, or/and carcinogenic effects (29). PAHs occurrence and emission have been substantial during the past centuries because of the large use of fuels for industry, heating, and transport (9). The most well-known PAH is the environmental carcinogen benzo[a]pyrene (B[a]P). Studies of this compound provide the majority of information on the health effects of PAHs (30).

1.2.1 Dietary and inhalation exposure

Human exposure to PAHs relies on different routes like through the respiratory tract by inhalation of contaminated air, dermal exposure to soil or other substances containing PAHs (9, 31). Another major route of exposure to PAHs in the general population is through ingestion of food and water containing PAHs. Of the total B[a]P exposure, 90% is originating from dietary sources. Smoking and cooking food at high temperatures like barbecuing, and frying is a major source of PAHs (31). Other food sources of PAH exposure are lipophilic meat, dairy products, and cereals (32). The highest dietary exposure to B[a]P is estimated to be 55 ng/kg-bw. B[a]P concentration in ambient air is in the ng/m^3 range, and activities such as cooking with oil or wood-burning may lead to air concentrations ranging from 20 to 100 µg/m^3 (30).

Another important contributor to PAH exposure in human is through inhalation. The major sources are coming from breathing out and indoor air, such as smoking cigarettes or/and breathing in smoke contaminated air. A cigarette contains 5.5 ng B[a]P and a daily smoker is consuming 15.1 cigarettes. Thus, the average smoker is exposed to 80 ng B[a]P in cigarettes per day, which accumulates into 1 ng/kg bw daily. For non-smokers in the general population, the dominant route of exposure to PAHs is trough food (30).

PAHs are widely distributed in the atmosphere and were one of the first atmospheric pollutants identified to be a suspected carcinogen (8). PAHs in the ambient air exist in both vapor phase

and/or absorbed into airborne PM. The atmospheric conditions like air temperature and humidity are influencing the properties of the individual PAHs. Low molecular PAHs are more volatile and therefore exist mainly in the gas phase. (33). High molecular PAHs occur mainly in the particulate phase because of their low vapor pressure (34). The concentration of the gas-phase PAHs increases in the summer season and the particulate phase PAHs are more dominant during winter (35).

PAHs have for a long time been studied for their carcinogenic properties, however, more recent studies indicate that these compounds are also capable of disrupting normal brain development (36). There is currently a lack of available evidence/information regarding PAHs potential to produce neural cell toxicity; one example of this is inhibition of enzymes involved in metabolism of neurotransmitters and other impairments in the nervous system (37).

1.2.2 Transfer of polycyclic aromatic hydrocarbons across biological barriers

When PAHs are inhaled, they omit the first path elimination in the liver and reaches the placenta un-metabolized to a greater extent compared to dietary exposure. PAHs are lipophilic compounds and can therefore readily cross the placenta and the blood-brain barrier (BBB) and exert adverse effects on the fetus (38). A positive correlation between high levels of PAHs and an increased risk for neural tube defects has been observed. High levels of PAHs are found in both maternal serum, umbilical cord serum and placenta samples (39). A correlation between maternal serum and umbilical cord serum indicates the occurrence of transplacental transfer from the mother to the fetus. Three rings PAHs dominate, and the PAHs can therefore possibly accumulate in the brain tissue without being metabolized. The placenta is a complex tissue and consists of many enzymes and transporter proteins. These transporter proteins can facilitate the transfer of chemicals, and likely influence the distribution and accumulation in the placenta. Moreover, it is proposed that the placenta can activate the metabolism of B[a]P by its very nature (38).

The BBB develops early in the embryonic period but is immature, and not completely formed until about 6 months after birth (40). The BBB is an efficient protector of the adult brain against exposure to many chemicals, although some chemicals have been demonstrated to pass through (41). The increased vulnerability of the developing brain extends through pregnancy, postnatally, and into early childhood. The PAHs can also pass into the breast milk and expose

the newborn by diet (42). Pyrene appear to be more abundant in breast milk for woman that are exposed to PAHs compared to the heaviest PAHs (43).

1.2.3 Metabolism of polycyclic aromatic hydrocarbons

Different organs, especially the lung and liver, have enzymes that can convert the PAHs to water-soluble metabolites that easily are eliminated from the body via urine and feces. The PAHs depend on metabolic activation to reactive intermediates to elicit toxic effects. The reactive metabolites have a short half-time and they may harm the cells at their site of origin. Metabolism may lead to either bioactivation to more toxic compounds or detoxification (44). The generation of free radicals such as Reactive Oxygen Species (ROS) can interfere with signaling pathways in the cells. Free radicals are continuously generated during normal metabolism and in response to exogenous environmental exposures, such as PAHs. Oxidative stress may be caused by the imbalance between ROS production and the present antioxidant defense system. The oxidative stress state has been implicated in a range of CNS disorders (45). Despite the metabolism and the formation of potential intermediates that can promote cell injury and toxicity, the oxidative metabolism of the PAHs is the pathway of detoxification and elimination (44).

The aryl hydrocarbon receptor (AhR) is a cytoplasmic receptor and has natural ligands. As several environmental contaminants including PAHs also may bind the receptor, its activity may be modified (46). By binding to the AhR, PAHs may induce their metabolism (47). The binding of PAHs is often causing an upregulation in Cytochrome P-450 (CYP)-enzymes and will result in an increased metabolization of many xenobiotics and increased levels of ROS (46, 48). Accordingly, this receptor plays an important role in modulating the toxicity of the PAHs and other environmental pollutants. However, it has also been shown to regulate neural differentiation in different models and is expressed in the early developmental stages and the expression increases throughout development in mice (49). Ligands of the AhR also affect genes involved in cell proliferation, cell cycle regulation, and inflammation (48). AhR protein has been found in both the human placenta and fetal tissues. However, a low level in the human fetal brain from the second trimester of pregnancy indicat that the AhR may not be active in undifferentiated neural stem cells (50).

There are three different signaling pathways downstream of the AhR, namely the classical genomic, the non-classical genomic, and the non-genomic pathway (51). The classical genomic

pathway of AhR is activated when an inducer such as B[a]P or/and β-naphthoflavone (β-NF), binds to the receptor. This induces a conformational change in the receptor, AhR dissociates from the complex and translocate from the cytoplasm into the nucleus where it interacts with the AhR nuclear translocator (ARNT) to form an AhR-ARNT complex, this complex binds to the xenobiotic-responsive element (XRE) in the promotor regions of target genes and regulate their transcription to control xenobiotic metabolism. XRE is found in the promotor region of various genes, several metabolizing enzymes like CYP, CYP1A1, CYP1B1, and glutathione S-transferase (GST) have multiple XRE sequences in the promotor region (46, 52).

The non-classical genomic pathway of AhR leads to the translocation into the nucleus where it interacts with other transcription factors (51), which affect genes involved in inflammation (48). The non-genomic pathway of AhR does not require the binding of ARNT. In this pathway, the receptor function as a signaling molecule and the responses involves activation of protein kinases and mediation of intracellular Ca^{2+} concentration responses, which secondary can activate genes (53). Neurotoxicity of AhR ligands has been suggested to be due to the non-genomic pathways when activated upon ligand binding to AhR and possibly the N-Methyl-D-Aspartate (NMDA) receptor. This may result in a cytoplasmic increase of calcium, and the generation of ROS (46). ROS production may be associated with oxidative stress which is observed in low-dose exposure to AhR ligands (PAHs).

1.3 Neurodevelopment

The developing brain undergoes complex and specific processes. The onset of development is three weeks after fertilization and continues for several years over the postnatal life. Neurodevelopment and related processes and time windows for vulnerability are illustrated in Figure 1. During this period different cellular processes like neurogenesis, migration, neuronal differentiation, apoptosis, synaptogenesis, and synaptic plasticity take place in a strictly controlled time frame and a regulated sequence (25). Evidence from animal studies have shown that during the critical phase of brain development, even exposure to low levels of environmental toxicants can disrupt the brain development and maturation (25, 41). If a brain developmental process is delayed or inhibited the consequences can be permanent (54, 55). The developing brain is less protected during fetal and early life compared to adults, and some chemicals can pass the biological barriers such as placenta and the BBB and gain access to the developing brain (56).

1.3.1 Human brain development

The embryonic period begins at conception and extends throughout week 8. By the end of the embryonic period, the basic structures of the brain and CNS are settled, and the major compartments of the central and peripheral nervous systems are defined. At the second week after conception, the embryo is a small oval-shaped, two-layered structure consisting of two cell types, epiblast, and hypoblast which give rise to all the cells in the human body (26). The epiblast cells will further differentiate into three primary stem cell lines, the endodermal line, mesodermal line, and ectodermal line (26, 40). The ectodermal line will give rise to the neural stem cells which can produce all cell types that make up the brain and the CNS (26). The next step in brain development is the formation of the neural tube.

On day 24 after conception, a small number of neural stem cells has formed in the region called the ventricular zone. These neural stem cells go through a massive symmetrical cell proliferation; every cell produces two neural stem cells which is leading to a massive increase in neural stem cells. On day 42 after conception, the neurogenesis starts, and the cell proliferation shift from symmetrical to asymmetrical meaning one stem cell produce one neural stem cell to maintain the balance between the two. Different populations of neurons arise in different regions of the brain. Gliogenesis is the generation of glial populations from neural stem cells (2). When neuronal stem cells differentiate, they leave the cell cycles in the G_0 phase and are called post-mitotic neurons. Neuronal migration brings different classes of neurons and astrocytes together so they can connect with the environment and each other. The neurons will migrate from the ventricular zone and out to the cortex where they will interact with each other to form neural networks. When the neurons have reached their destination, they start to extend axons and dendrites called neurites to communicate with each other (26). The neurons extend one axon away from the cell to the exterior environment, the tip of the axon has a growth cone that can sense the environment and help the axon to reach its target location. When reaching its target location by reaching the dendrites of other neurons, the axon will form synapses where neurotransmitters can be released and mediate signaling from the cell (26, 57). In the second trimester of pregnancy, see Figure 1, when the cells have reached their final destination synaptogenesis, dendritic sprouting, axon guidance and neural circuit formation are essential for normal brain development. Making these synaptic connections is important to set the stage for intracellular communication (58).

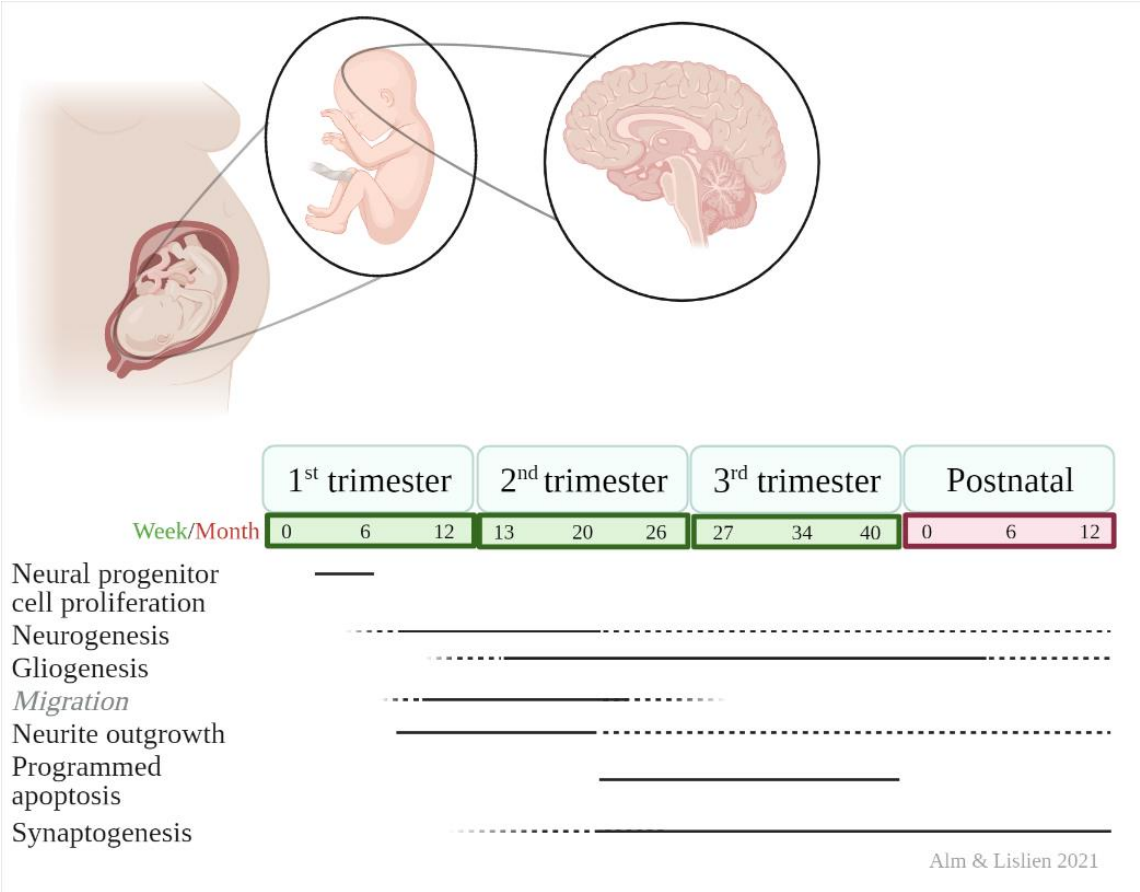

Figure 1: ***Overview of fundamental human neurodevelopmental processes and developmental time windows relevant for DNT testing.*** *It is assumed that toxicants like chemicals may cause DNT by disturbing or interfering with at least one of these processes for normal brain development identified from in vivo studies. The developmental time windows are divided into two: essential for neurodevelopment and vulnerable for perturbations with toxic impact (black line) and time windows were the process still occur, but when it is not particularly sensitive for perturbations (dotted line). Developmental processes measurable using the 2D NSC models (in black font) and other processes essential for neurodevelopment measurable with 3D in vitro models (grey italic). Figure created by Malene Lislien and Inger Margit Alm with BioRender.com in spring 2021 inspired by (2) and (3).*

Synapses are the neurons` main tool for communicating with each other and are essential for the processing of information and functioning of the nervous system as a whole. A synapse consists of two neurons, where a neurotransmitter can move from the presynaptic neuron across the synaptic cleft to the postsynaptic neuron. Neurons synthesize neurotransmitters and store them in synaptic vesicles which may be released at the terminals as a result of electric activity at the presynaptic neuron. At the postsynaptic neuron, the neurotransmitters can bind to receptors. Neurotransmitters especially gamma-aminobutyric acid (GABA) and glutamate are the most abundant secreted from neurons (57). Synapses continue to rearrange throughout the entire life and one neuron can have many thousands of dendrites which form synapses with many thousands of different neurons (26, 57). The formation of new synapses is called synaptogenesis. Synaptogenesis is guided by the growth cone localized on the tip of the axon.

The growth cone will sense other cells and signaling molecules located in its proximity to find the optimal space to initiate synaptogenesis (59). When contact between the pre and postsynaptic neuron is initiated signaling by voltage-gated ion channels in the presynaptic neuron activated. This will lead to an upregulation of neurotransmitter receptor-related genes in the postsynaptic neuron which further upregulate receptor in the synaptic area, and a depolarization of the neuron, and the transfer of the action potential to the postsynaptic cell (59). Dendritic spines will form on the postsynaptic neuron and are the first sign of early synapse formation, the dendritic spines are the main site for synapse transmission. Dendritic spines are membrane structures that protrude from the neuron (57).

1.4 Evidence for developmental neurotoxicity after polycyclic aromatic hydrocarbon exposure

There is growing evidence that early exposure to air pollutants from combustions sources such as PAHs induces growth impairments and disturbances of early neurodevelopment. Prenatal exposure to PAHs has been demonstrated to be correlated to reduced birth weight, and head circumference (60-63). The reduction of birth weight and head circumference are associated with a lower IQ, poor cognitive functioning, and delayed school performance (64). Epidemiological studies show an association between pre and postnatal exposure of PAHs and adverse effects on the developing brain (20, 22, 23, 65-68). Perera et al. published in 2006 the results from a cohort study on New York children from non-smoking African - American and Dominican mothers who were highly exposed to PAHs during pregnancy. The results showed that the children had a lower mental developmental index at 3 years of age. The odds of cognitive delay were also significantly higher for children exposed during pregnancy (69). The same authors reported an association between prenatal PAH exposure and impairments of child intelligence measured at the age of 5 years (20).

ADHD is one of the most common neurodevelopmental disorders among children. The disorder is characterized by impulsivity and lack of concentration, together with other common dysfunctions like compromised cognitive functions (70). ASD is a type of neurodevelopmental disorders characterized by impairment in social communication and interaction. Many studies have associated mutations in genes like *NRXN*, *NLGN*, *SHANK*, *TSC1/2*, *FMR1*, and *MECP2* to ASD. These genes encode for scaffolding proteins and other proteins involved in different aspects of the synaptogenesis, including synapse formation, synaptic transmission, and

plasticity. This suggests that the pathogenesis seen in ASD can be attributed to synaptic dysfunction (71).

In a cohort study from 2010 on pregnant, non-smoking healthy women in Poland, showed that prenatal exposure to PAHs affected children's cognitive development at 5 years of age (23). This is also supported by other studies (20, 22, 65). PAH exposure was associated with low IQ, anxiety, depression, and attention problems in addition to ADHD behavioral symptoms (66). Prenatal exposure to PAHs can be measured with PAH-DNA adducts in maternal blood or cord blood. The DNA adducts don't only reflect exposure but also absorption, metabolic activation, and DNA repair; they are additionally considered an individual dosimeter for PAH exposure (72). These biomarkers have been associated with a range of adverse neurodevelopmental outcomes in children (22, 65, 73).

Despite the human evidence that PAH exposure affects brain development, few studies have examined this in animals to support causality (74). Recent publications on neurotoxic effects of B[a]P were found in rats after oral administration of 0.02 mg/kg-bw-day, which resulted in neurobehavioral impairments (75). This dose is much lower than the level causing cancer and it was concluded that B[a]P and neurotoxicity had been largely overlooked in the risk assessment and B[a]P (and possibly other PAHs) induced neurotoxicity also may occur at a lower dose than B[a]P induced carcinogenicity (30). However, it is often challenging to prove that an association is due to causality between adverse effects and chemical exposure in epidemiological studies. Humans are continuously exposed to a range of chemicals and other factors may also influence the effects observed in epidemiological studies.

1.5 Developmental neurotoxicity testing

It is well established that humans are exposed to environmental contaminants, such as PAHs. Only a small percentage of these have been tested for DNT and it is an urgent need to develop models to assess neurodevelopmental effects of chemical exposures. DNT testing is not mandatory in either the US or the European Union for safety assessments for pesticides or industrial chemicals. An assessment of these is only performed when evidence of neurotoxicity is observed *in vivo* in adult rodents, and this may be insufficient since some neurodevelopmental processes and the immature BBB is not present in the adult brain (76). The *in vivo* tests according to regulatory guidelines require a high number of rodents, they are costly, is time consuming, and are not suitable for testing a large number of chemicals (77). Using an *in vitro*

method will be in line with the 3Rs principle (reduction, replacement, and refinement) (78). Replacement of animals has over the past years received much attention, particularly in the European countries. The creation of Norecopa (Norwegian national consensus platform on alternatives to the use of research animals) in Norway and the European Centre for the validation of Alternative Methods (ECVAM) at the European Commission of Joint Research Centre (EC-JRC) in Italy coordinated efforts in cell-based toxicity testing (79).

A paradigm shift in regulatory toxicology is to move away from phenotypic changes found in animals toward mechanistic *in vitro* assays using human cells (5). Takashi and Yamanaka showed already in 2006, the reprogramming of fibroblasts to pluripotent stem cells (PSC) in mice (80). The inducing of transcriptional factors to PSC derivates can be alternatives to studying-chemical-induced adverse effects in cancer cell models, as the cells may more closely mimic the physiological conditions of human tissue, and are therefore suitable for DNT testing (81). Human Embryonic Stem Cell (hESC) and human-induced Pluripotent Stem Cell (hiPSC) are the major types of models used in toxicity to study chemical-induced adverse effects. There are several ethical concerns regarding the hESC, test methods of regulatory testing will therefore unlikely be accepted due to ethical concerns, national laws, and regulations regulating the use of hESC (5). In Norway, the use of hESC is regulated by "Bioteknologiloven- the human use of biotechnology act" (82). The hiPSCs do not have the same regulations and ethical dilemmas as hESCs and are therefore considered a great alternative to the hESC (27).

1.5.1 Neural Stem Cells derived from Human-Induced Pluripotent Stem Cells

In this thesis hiPSC differentiated into neural stem cells (NSCs) to a mixed culture of post-mitotic neurons and glia cells with forebrain and cortical-like characteristics, and may also have midbrain specificity (5), see Figure 2, was used. This model recapitulates key processes relevant for neurodevelopment such as the commitment of neural progenitor cells, proliferation, migration, neural and glial differentiation, synaptogenesis, and neural network formation and function (27, 83), as seen in Figure 1. The model are therefore considered suitable for DNT, rather than adult neurotoxicity evaluation because they don't differentiate and function similarly to adult brain physiology (27).

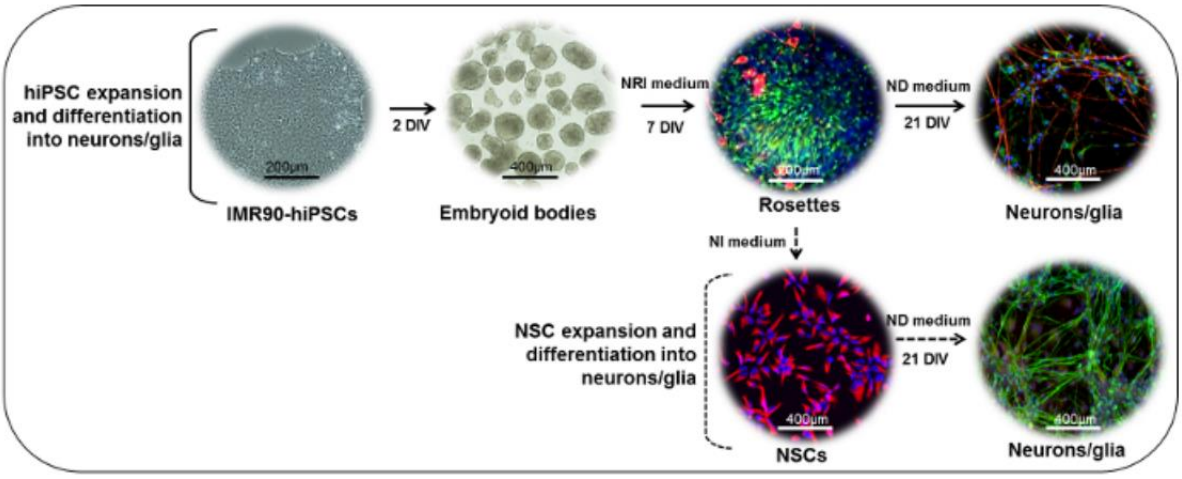

Figure 2: ***Schematic representation of the differentiation process from hiPSC to NSCs used in this thesis****. IMR90-hiPSC colonies can be cut into fragments to form embryoid bodies (EBs). After 2 days in vitro (DIV), EBs can be plated onto laminin or standard matrix-coated dishes and cultured in the presence of neuroepithelial induction (NRI) medium to generate neuroectodermal derivates (rosettes, here stained for nestin (green) and β-III-tubulin (red). Rosettes can be dissociated, collected, replated on laminin- or standard matrix-coated dishes, and further differentiated into mature neuronal (NF-200, red) and glial (GFAP, green) cells in the presence of neuronal differentiation (ND) medium. NSCs derived from rosettes can also be expanded in neural induction (NI) medium and further differentiated to form neuro and glia cultures. Figure obtained with permission from the author, Francesca Pistollato (5).*

Previous characterization of the NSC model during the differentiation process shows that expression of genes and proteins will change depending on the number of differentiation days. The NSC model is characterized by a high percentage of the neural stem cell marker, Nestin, and a low expression of the astrocyte marker Glial Fibrillary Acid Protein (*GFAP*) in undifferentiated cells. Both *GFAP* and nestin are intermediate filament proteins, nestin is a marker for immature neurons and is expected to decrease upon differentiation (5). *GFAP* is an important component of the cytoskeleton in astrocytes during development, changes in *GFAP* expression might alter the morphology of astrocytes, *GFAP* is known to be induced upon brain damage/CNS degeneration and is important in many CNS processes like cell communication and the functioning of the BBB (84). Further differentiation of the NSCs into more mature neurons and astrocytes is expected to give a nestin and *GFAP* expression of 10-15% and 20-30%, respectively after 21 days of differentiation. The cell cycle marker Ki67 will show a decrease after 21 days of differentiation, this indicates the neural progression into more mature subpopulations (5, 81).

Undifferentiated cells also express the neural marker β-III Tubulin and the microtubule-associated protein 2 (*MAP2*), a cytoskeletal protein mainly expressed in neurons. The expression of these increases during differentiation, where more mature neurons have MAP2 located in the cell body and dendrites and this makes MAP2 a marker for neurite outgrowth

(85). Growth associated protein 43 (*GAP43*) is a membrane-associated neuron-specific phosphoprotein, its expression is linked to neurite outgrowth and neural development. *GAP43* plays a critical role in the axonal growth and the functions of synapses during neurogenesis (86) and levels will increase during differentiation (81).

The NSC model has been shown to consist of large populations of GABAergic and glutamatergic neurons and a smaller proportion of dopaminergic neurons. After 21 days of differentiation, the culture is expected to contain approximately 30% glutamatergic, 15% GABAergic, and 10% dopaminergic neurons (81). The presence of glutamatergic and GABAergic cells indicates that the culture expressing forebrain and cortical-like characteristics and the presence of discrete proportions of dopaminergic neurons may resemble those present in the midbrain (5). Glutamate is an excitatory neurotransmitter in the CNS (87) and GABA is an inhibitory neurotransmitter (88). The release of excitatory and inhibitory signals regulates the activity of the postsynaptic neuron, and neurotransmission relies on the interconnection of neurons via synapses (87, 89). The balance between inhibitory and excitatory signals is important for the cortical function in the brain (88) and disturbance is associated with a variety of neurological disorders like ASD and schizophrenia (88, 90). In the human brain, dopaminergic neurons play an important role in motivation and memory, and loss is linked to Parkinson`s disease (91).

When neurons mature it also means the start of synaptogenesis and synapse formation which is an important part of the neurodevelopment (26, 57). The neurite length, electrical activity, and the expression of the postsynaptic marker have been shown to increase during differentiation (81). Synaptophysin (SYP) is a presynaptic marker (5) and Post-Synaptic Density protein (PSD95) a postsynaptic marker (92), both are markers for synaptogenesis. SYP is the most abundant membrane protein in synaptic vesicles, and it plays a role in vesicle fusion and neurotransmitter release after repeated stimulation (93). PSD95 is a scaffold protein found in glutamatergic neurons excitatory synapses and is encoded by the *DLG4* gene in humans. PSD95 is an essential component in glutamatergic transmission, synaptic plasticity, and dendritic spine morphogenesis during neurodevelopment. Dysfunction of the PSD95 during neurodevelopment has been associated with neurological disorders, such as the pathology observed in schizophrenia and ASD (92). This knowledge can therefore be used to evaluate toxicology effects on the developmental brain and nervous system (5).

1.5.2 Adverse Outcome Pathway

It is hypothesized that if a chemical at the concentration relevant for environmental exposure, affects at least one of the key neurodevelopment processes in a statistically significant manner it should be defined as a potential neurodevelopmental toxicant. These processes can be quantified by short or long-term exposure to a chemical or a mixture of chemicals (83). In regulatory toxicology, DNT is an important endpoint (94).

The Adverse Outcome Pathway (AOP) allows us to incorporate mechanistic toxicity pathways information into regulatory decisions. The AOP, see Figure 3 will generally start with a molecular initiating event which is triggered by an interaction between a chemical and the biological system which further leads to a key event.

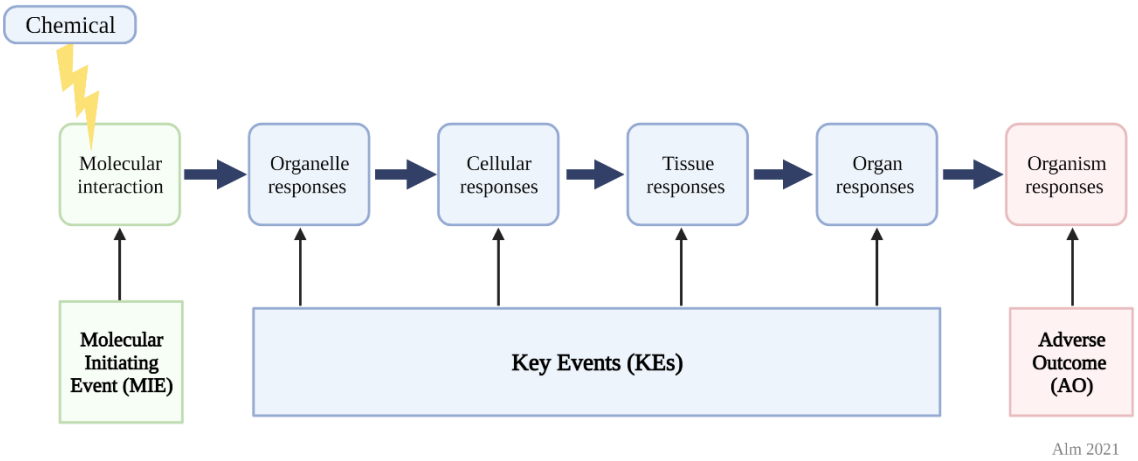

Figure 3: ***The Adverse Outcome Pathway concept.*** *A chemical initiating event leading to a series of key events that are connected leading to adverse outcome (AO) on the organism or population levels. Figure is created with BioRender.com by Alm 2021 and modified after (4).*

The cascade of key events will result in an Adverse Outcome (AO). The AO could be impairment in cognitive function such as learning and memory deficits, but also ADHD, ASD, and reduced IQ. This AO should be of regulatory relevance and has been tested *in vivo* on the organism or population level (4). The key events represent pathways of toxicity at various biological levels (organelle, cellular, tissue, and organ). These key events must be measurable (27), the NSC model can be differentiated into neurons and astrocytes and recapitulates most of the key events important in human brain development.

A major concern for DNT is the lack of understanding of the molecular initiating events that are causally responsible for triggering the cascade of the key events up to the AO observed in children. The use of *in vitro* methods such as the NSC model could therefore potentially

describe the causative relationship between molecular initiating events, key events, and AOs and be used to determine causation rather than correlation (94)

Most of the Organization for Economic co-operation and Development (OECD) endorsed AOPs for neurotoxicity/DNT are leading up to cognitive impairment in memory and learning in children as AO. The model is, therefore, suitable to test chemical exposure (DNTs) to biological systems leading up to a potential cause of impairment in cognitive function in children as seen in epidemiological studies (4). A battery of such tests based on mechanistic knowledge derived from the AOPs would boost confidence in their use, and taken together, would facilitate a paradigm shift toward mechanistically driven hazard identification and characterization (27).

1.6 Selections of polycyclic aromatic hydrocarbons

B[a]P is the most used and representative compound of PAHs and consists of five fused benzene rings as shown in Figure 4. International Agency for Research on Cancer and Environmental Protection Agency have determined that B[a]P is a probable human carcinogen and a known environmental carcinogen (95). It may bind to AhR but may additionally form DNA reactive metabolites. As a result, B[a]P induces gene mutations, chromosomal aberrations, and other types of genotoxic and carcinogenic linked effects. B[a]P is catalyzed by CYP-enzymes such as CYP1A1 and CYP1B1 to form B[a]P-7,8-diol, which may be further metabolized to the ultimate carcinogen, B[a]P-7,8-dihydrodiol-9,10-epoxide. B[a]P-7,8-diol may also be activated to various catechol's that form DNA adducts and ROS leading to oxidative damage (30). Current regulatory guidelines are based on B[a]P carcinogenic potential. There are numerous other PAHs with low mutagenic potential that are often found in concentrations way higher than B[a]P. Their effects are less well characterized than those of B[a]P. Both B[a]P and other PAHs forms several metabolites which are often poorly characterized (96).

β-NF is a PAH consisting of fused benzene rings, see Figure 4. It is not commonly found in nature but used in the project for the mechanistic reason as a non-toxic AhR agonist. β-NF activates the AhR classical-genomic pathway resulting in increased CYP-enzymes and genes for detoxification (97).

Pyrene is a PAH and consists of four fused benzene rings, see Figure 4. Pyrene is one of the most common PAHs found in outdoor air. It is found in concentrations higher than B[a]P but

is not listed as a human carcinogen (9). There is evidence of pyrene activating the AhR non-genomic pathway by Ca^{2+} signaling (52). Pyrene exposure has been associated with asthma in children and cardiovascular diseases.

A study done on detecting blood levels of PAHs in exposed children from India, found low levels of B[a]P and high levels of non-carcinogenic such as pyrene. They hypothesized that exposure to PAHs that are not classified as hazardous but are present in higher concentrations in the atmosphere posed a health risk (98). Low molecular weight PAHs are the predominant compounds found in the placenta and maternal umbilical cord serum. The lower-weight PAHs are more likely to pass from the mother to the fetus (38).

The selection of PAHs to this thesis is therefore partly based on occurrence in air, blood, placenta, and fetus, but also partly on their different properties. B[a]P forms reactive metabolites and a trigger for the AhR classic genomic pathway. β-NF is a strong AhR trigger of the classic genomic pathway, while pyrene is an activator of the non-genomic pathway.

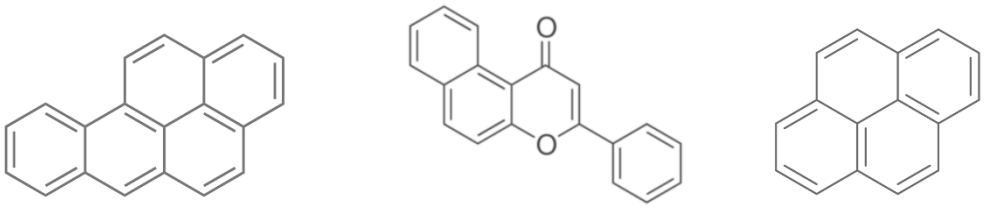

Figure 4: ***Structures of the polycyclic aromatic hydrocarbons (PAHs) used in this thesis****. The PAHs used in this study consisted of four to five fused benzene rings. Three different types of PAHs were selected namely benzo[a]pyrene, β-naphthoflavone and pyrene: 1: known to be differently abundant in outdoor air, indoor air and food, 2: known to have different properties and sizes and 3: known to affect cells via different mechanisms. Figure made with biorender.com by Alm 2021.*

2 AIM OF STUDY

This master thesis is a part of a larger project aiming at establishing the Neural Stem Cell (NSC) model at The Norwegian Institute of Public Health (NIPH). The NSC is an animal-free human *in vitro* system capturing processes relevant to human brain development. The model is developed as a part of the paradigm shift in toxicology towards a non-animal approach; and is a mixed culture of neurons and astrocytes.

As a part of the overall NIPH project, I first participated in an experiment with the aim to clarify the function of the NSC model in our laboratory.

i. Characterizing the morphological changes in the culture by microscopy
ii. Optimizing assay for cell viability
iii. Establishing assay for gene expression related to differentiation
iv. Establishing assay for immunocytochemistry for protein/enzyme markers of differentiation using high content imaging

Epidemiological studies indicate that exposure to polycyclic aromatic hydrocarbons (PAHs) may have neurodevelopmental effects. Current evidence is limited regarding mechanisms involved and their relative potency. Hence, our primary hypothesis is that various PAHs change neurodevelopmental processes as seen in the human NSC model. If so, this can give information regarding relative potency and possible mechanisms involved.

NSCs were exposed to three different types of PAHs (B[a]P, β-NF, and pyrene). We hypothesized that exposure of these three different PAHs gives changes in:

i. Cell viability
ii. Gene expression of markers related to neurodevelopment
iii. Protein markers related to neurodevelopment and morphology
iv. Cellular responses via different mechanisms

Markers related to neurodevelopment include proliferation, differentiation, synaptogenesis, and neurite outgrowth.

3 MATERIALS AND METHODS

The experiments in this master thesis were conducted at the NIPH and were part of a larger establishing project aiming to assess the transferability of the NSC model from the EC-JRC. Protocols for cell culturing of the NSC were originally developed at EC-JRC where the cell model was developed. As a consequence of this, all assays were therefore not pre-established for experiments at NIPH and had to be optimized before use. Part of the experiments conducted was validated using information and protocols from EC-JRC as a reference point and any changes were assed thoroughly in collaboration with NIPH.

3.1 Reagents and chemicals

See Appendix 1 for more detailed information on the chemicals and reagents used in this thesis.

3.2 Neural Stem Cells

IMR90 fibroblast was reprogrammed into hiPSC at I-Stem (France) by viral transduction of *Oct4* and *Sox1*, two transcription factors by using pMIG vectors (99). For experiments in this thesis neural stem cells (NSCs) derived from hiPSC-line IMR90 was used and kindly provided by the EC-JRC, the differentiation process to NSC are detailed described in (5) and seen in Figure 2. NSCs cultured in 2D were incubated at 37 °C in 5% CO_2 and humidified atmosphere.

Cell culture work was done in a cell lab with a sterilized Laminar-Air Flow (LAF) bench using standard aseptic technique. This involves applying the strictest rules to minimize the risk of infection and to provide a safe barrier between the sterile environment and the microorganisms in the environment. The aseptic technique needs to be used constantly when performing cell work (100). Lab coat and glows were worn, and gloved hands were sprayed with 70% ethanol. Sterile pipettes, cell culture flask and, cell plates were used. All the equipment put into the LAF-bench was washed with 70% ethanol. Bottles with reagents were never left open in the hood longer than necessary.

3.2.1 Cell culturing

Information regarding cryopreservation, maintenance of cells, cell culture medium with supplements and growth factors and, coating of labware is described in detail in Appendix 2.

NSCs were cryopreserved in CryoStore Cell cryopreservation media (C2874-100ML, Sigma-Aldrich, Germany) containing 10% dimethyl sulfoxide (DMSO) at -150 °C. Before cultivation, the cells were rinsed free for DMSO. After thawing, cells were cultured in Basement Membrane Matrix (BMM) Matrigel (354234, Corning, USA) coated Falcon™ Tissue culture Treated flasks (353135, Falcon, USA) in Neural Induction (NI) medium consisting of DMEM/F12-medium (31331028, Thermo Fisher, USA) with supplements and growth factors. Cell medium was changed three times a week, cells were routinely split at 90-100% confluency by enzymatic dissociation using trypsin.

NSCs were differentiated into a mixed culture of neurons and astrocytes on poly-D-lysine (PDL)-96 well plates (354461, Corning, USA) coated with Matrigel Basement Membrane Matrix reduced Growth Factor (354230, Corning, USA) (rGF). After the expansion of NSCs in the NI medium, the medium was changed to Neuronal Differentiation (ND) medium consisting of Neurobasal medium (21103049, Thermo Fisher, USA) with supplements and growth factors. Growth factors were added fresh to avoid degradation and medium change was done twice a week. Thawing of cryopreserved cells and coating of labware are described in more detail in Appendix 2.

3.2.2 Cell passaging

NSCs were passaged by enzymatic dissociation with trypsin. Trypsin-EDTA (0.5%) (15400054, Thermo Fisher, USA) was diluted 1:10 in phosphate-buffered saline (PBS) (pre-warmed). The old cell medium was aspirated, and cells were incubated in the trypsin solution at 37 °C for 2 min to detach the cells from the coated surface. Trypsin was inactivated by mixing the dissolved cell suspension 1:2 with Defined Trypsin Inhibitor (R007100, Thermo Fisher, USA) at 37 °C. The cell suspension was then centrifuged for 4 min 30 sec at 130g and the supernatant was aspirated and gently resuspended in NI medium, and gently mixed. The cells were counted on an automatic cell counter (LUNA-II™, Logos Biosystems, South Korea) using a 1:2 mix of cell suspension and Trypan Blue (T8154-100ML, Sigma-Aldrich, Germany) to determine cells/mL. The cells were seeded in NI medium in BMM pre-coated flasks for future passages at a density of 10-13000 cells/cm^2 or rGF pre-coated PDL-plates at a density of 21000 cells/cm^2 and 12000 cm^2 in 96-well and 24-well plates, receptively.

3.3 Preparations of polycyclic aromatic hydrocarbon dilutions

The PAHs used in this study were benzo[*a*]pyrene (B[a]P), β-naphthoflavone (β-NF), and pyrene all from Sigma-Aldrich and dissolved in DMSO (D4540-100ML, Sigma-Aldrich, Germany). A scientist at NIPH prepared the master stock solutions ($20x10^{-3}$ M) of each PAH. Working stocks were prepared in glass vials at concentrations 1000 times higher than the final exposure concentrations in the ND medium of giving a final concentration of 0.1% DMSO, see Appendix 3 for preparations. The vials were stored at -80 °C and fresh dilutions in the ND medium were prepared for each medium change. In all experiments, exposure started when inducing differentiation to neural cells (DIV0). Experiments with PAHs had DMSO (0.1%) as solvent control.

3.4 Alamar Blue Viability assay

Alamar Blue assay™ was used to investigate cell viability after chemical treatment of NSCs undergoing differentiation. Alamar Blue™ assay is a fluorometric analysis measuring mitochondrial dehydrogenase activity of cells, which reflects the metabolic activity of the cells. Resazurin is the active ingredient in Alamar Blue and acts as an intermediate electron acceptor in the electron transport chain whiteout interfering with normal metabolic activity. Resazurin is a water-soluble, non-toxic blue non-fluorescent dye, which is permeable to cellular membranes. When resazurin enters the living cell it will be reduced to the pink highly fluorescent resorufin emitting light at 590 nm (101), see Figure 5. Depending on time, resorufin will achieve equilibrium with dihydroresorufin, this is a colorless, non-fluorescent product leading to fluorescence decreases (101, 102). The color change can be measured as absorbance or fluorescence, for greater sensitivity (103). The fluorescence measured reflects the metabolic activity and is proportional to the number of living cells. Non-viable and damaged cells will

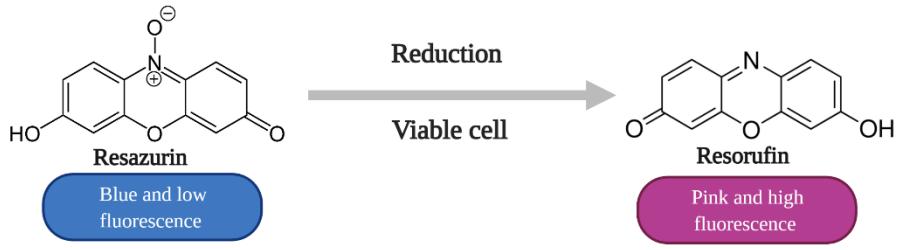

*Figure 5: **Illustration of Alamar Blue™ assay**. The viable cell can reduce the blue non-fluorescence resazurin to the pink high fluorescence resorufin which can be measured as absorbance or fluorescence. Created by Alm 2021 using BioRender.com.*

have lower metabolic activity and to a lesser degree reduce resazurin and give a lower fluorescence signal. (101, 102).

3.4.1 Optimization of Alamar Blue assay for assessment of cell viability

The protocol for Alamar Blue™ was optimized by investigating the effect of incubation time, cell density, and substrate concentration on cell viability measurements for further experiments, as well as to investigate whether cell density affected the cell viability. NIPH and EC-JRC use resazurin reagents from different manufactures. NIPH from Invitrogen and JRC from Promega. Since these manufacturer's protocols are slightly different, it was needed to compare and optimize these for further experimental use. A defined cytotoxic concentration of $1x10^{-3}$ M glycidamide was used as a positive control for 80-90% cell death (unpublished pilot study). Two substrate concentrations of Alamar Blue™ were chosen to compare the protocols. The validation and optimization of the Alamar Blue™ assay were performed by trained personnel at NIPH and the student projects, performed in parallel, were aimed for training in cell cultivation for the NSC model and further validation. Although identical projects were performed, data was collected individually and was not a result of cooperation.

The recommended cell density by EC-JRC in a 96-well plate is 7000 cells/well (210000 cells/cm^2), 96-well plates with 7000 cells/well were seeded in presence to NI medium, as described in 3.2.2. When cells are kept in NI medium the cells dived every 24 h and the proliferation will decrease and eventually stop after changing to ND medium, by the cells reaching $G_{0,}$ a terminal state where cell division is uncommon (104). To investigate the effects on cell densities on Alamar Blue™ assay and because the differentiation process and the Alamar Blue™ assay is sensitive to cell density, we cultured the cells for 1 and 2 days before starting differentiation and exposure in ND medium for 1 and 3, or 1 and 5 days, respectively, see Figure 6. The purpose was to find the best time for cell proliferation to detect changes in cell viability after 1-5 days of differentiation. The chemical treatments started simultaneously with differentiation on days of differentiation (DIV0). The optimization performed by NIPH included several cell densities, 7000, 10500, and 14000 cells/well for a more controlled assessment of the cell densities impact.

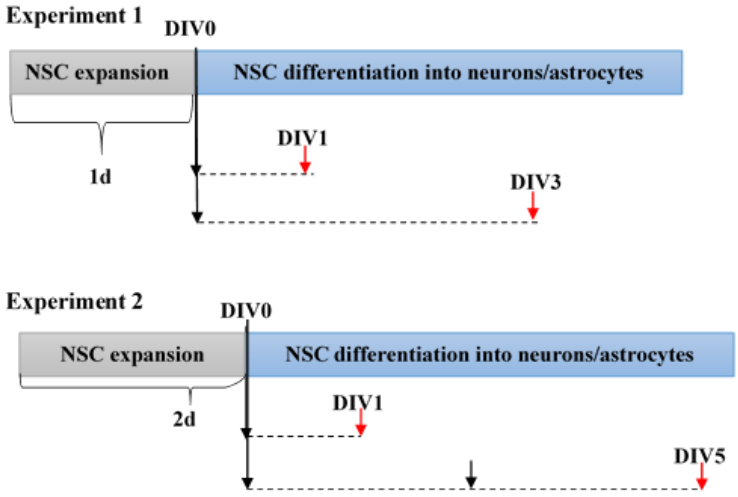

Figure 6: ***Experimental design for optimization of Alamar Blue assay.*** *The optimization was divided into two experiments (experiment 1 and experiment 2). Experiment 1: cells proliferated for 1 day before differentiation for 1 and 3 days whit or without glycidamide. Experiment 2: cells proliferated for 2 days before differentiation for 1 and 5 days whit or without glycidamide. Medium change from NI medium to ND medium is represented with a red frame, additionally, a medium change for DIV5 was performed on day 5 due to longer exposure time. Alamar Blue measurements are presented with a blue frame. Abbreviations: DIV = days of differentiation*

When cells had differentiated for either 1, 3, or 5 days in ND medium whit or whiteout glycidamide ($1x10^{-3}$ M), cells were incubated with Alamar Blue™ Cell Viability reagent (DAL1025, Invitrogen, USA) in a final dilution of 1:10 (Invitrogen) or 1:6 (Promega) dilution to compare the commercial protocol from the Alamar Blue assay from Invitrogen (1:10, NIPH) with the one from Promega (1:6, EC-JRC), see Table 1 and plate layout in Appendix 4. A blank consisted of ND medium only was included to eliminate background fluorescence from the medium and the plate, and a negative control consisted of ND medium and Alamar Blue™ reagent in a final dilution of 1:10 and 1:6 was included. The cells were then incubated at 37 °C, 5% CO_2 for 8 h, and fluorescence was measured every hour on gain 850 at excitation at 520-540 nm and an emission wavelength at 580-600 nm with CLARIOstar plate reader (BMG LABTECH, Germany).

Table 1: ***Alamar Blue dilution™ for assessment of optimization project.*** *The amount of Alamar Blue™ added to each well in a 96-well plate was calculated from the dilution used, 1:6 or/and 1:10 which was used dependent on the pre-existing ND medium with cells in the well. Blank included the total volume in wells for both dilutions, 1:6 and 1:10 dilution, respectively.*

Alamar Blue™ Dilution	**1:6**	**1:10**
	Volume pr well (µL)	
Volume of cells + ND medium	135	135
Added Alamar Blue™	27	15
Negative control (ND medium + Alamar Blue™)	135 + 27	135 + 15
Total Volume	162	150
Blank (ND medium)	162	150

3.5 Cell viability

Alamar Blue™ was used to assess the possible impact on the cell viability in NSCs undergoing differentiation by measuring mitochondrial dehydrogenase activity after exposure to different concentrations of the three PAHs (B[a]P, β-NF, and pyrene). The impact of possible alternations in cell viability was important for further mechanistic studies on gene and protein markers related to neurodevelopment.

3.5.1 Experimental design

NSCs were seeded in rGF pre-coated PDL-plates at a density of 21000 cells/cm^2 as described in 3.2.2. After proliferating for 1 day (14 and 21 days) and 4 days (1 and 3 days), the cells were exposed to B[a]P, β-NF, and pyrene in ND medium, ensuring exposure through the whole differentiation period as shown in Figure 7. Different time points of proliferating were performed to ensure a high enough cell density in each well. Exposure started on differentiation day 0 (DIV0).

For exposure of the NSCs, dilutions of the three PAHs were set up with the concentrations $2x10^{-5}$, $1x10^{-5,}$ $3x10^{-6}$, $1x10^{-6}$, $3x10^{-7}$, $1x10^{-7}$, $3x10^{-8}$, $1x10^{-8}$, $3x10^{-9}$, $1x10^{-9}$, $3x10^{-10}$ M in total eleven concentrations, as described in 3.3 and Appendix 3. Because of the limited water solubility of the PAHs, all test agents were dissolved in DMSO. When sub stocks were added to ND medium it was diluted to a final concentration of 1:1000 ensuring a final DMSO concentration of 0.1% in both exposed and solvent control.

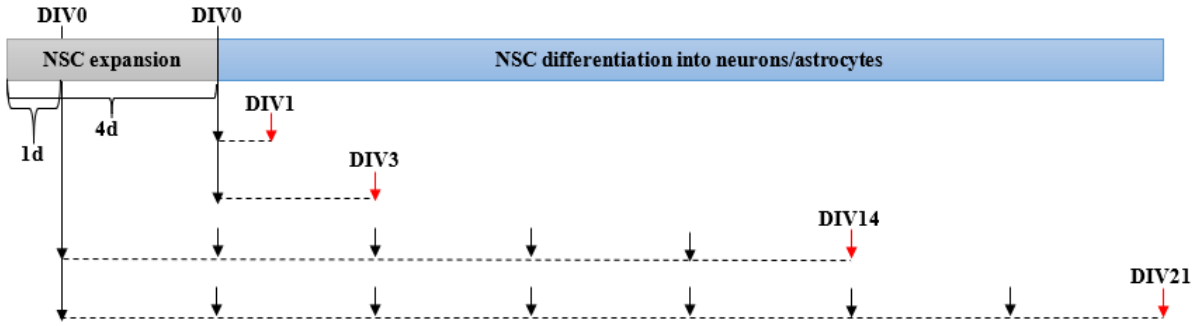

Figure 7: ***Exposure regime of cell viability assessment after PAH exposure.*** *The cells differentiated and exposed for 14 and 21 days were proliferated for 1 day. The cells differentiated and exposed for 1 and 3 days proliferated for 4 days. Exposure started on differentiation day 0 (DIV0). Black arrow indicates medium change and red arrow indicate analysis with Alamar Blue or collecting of sample for other analysis.*
Abbreviations; DIV: days of differentiation and exposure

Exposure of cells for 21 days was performed after the determination of concentrations for further experiments. The cells were therefore only exposed to three concentrations for each PAH. The cells exposed to B[a]P and pyrene were exposed to the concentrations $1x10^{-5}$, $1x10^{-6}$, and $1x10^{-7}$ M. Cells exposed to β-NF were exposed to the concentrations $1x10^{-6}$, $1x10^{-7}$, and $1x10^{-8}$ M because of poor solubility of β-NF.

Cell controls were also included, containing only ND medium and cells to control for no toxic effects of DMSO. The plate layout for the exposure and differentiation is shown in Appendix 4. For the cells which differentiated and were exposed for 14 and 21 days, medium change was done twice a week with refreshing of exposure. Exposure in the medium was prepared fresh for every medium change.

After 1, 3, 14, and 21 days of combined differentiation and exposure the cells were incubated with 1:10 dilution of Alamar Blue™ Cell Viability reagent for 3 h and 30 min at 37 °C and, fluorescent signal was read at 520-540 nm/580-600 nm (excitation/emission) using CLARIOstar (BMG LABTECH, Germany) as described in section 3.4. A negative control consisted of ND medium + Alamar Blue™ reagent (1:10 dilution) was included, see plate layout in Appendix 4. The results were normalized to solvent control and corrected to the negative control to eliminate background fluorescence caused by reagent in medium (105).

3.6 Gene Expression of neural markers related to neurodevelopment using real-time polymerase chain reaction

Gene expression analyses were performed on NSCs exposed to the PAHs undergoing differentiation to elicit effects on neural markers related to neurodevelopment. The process of gene expression is reliant on multiple steps. First, reverse transcription by using a reverse transcriptase enzyme to convert RNA to complementary DNA (cDNA). Second, polymerase chain reaction (PCR) to amplify the cDNA, and third detection and quantification of the signal using fluorescent probes.

The TaqMan real-time PCR is based on the 5`nuclease chemistry, which uses a TaqMan probe, labeled with a fluorochrome in the 5`end (in our assay FAM) and a quencher at the 3`end which repress the fluorescence emitted by the fluorochrome when it is close to the fluorochrome. The TaqMan probe is designed to anneal to the target sequence which is located between the unlabeled forward and reverse primers. During the start of the PCR, the temperature is raised allowing the double-stranded cDNA to denature. The probe is intact and the quencher at the 3`end will inhibit the fluorochrome by absorbing all the signal coming from the fluorochrome at the 5`end (106). In the next step, the temperature is lower allowing the primers and the probe to anneal to their target sequence. Taq polymerase will synthesize a new strand by using the unlabeled primers and the template, Taq polymerase has exonuclease activity and will cleave the probe and separating the fluorochrome from the quencher (107). This results in a fluorescence signal proportional to the amount of PCR product in the sample (106).

3.6.1 Experimental design

Cells were trypsinized and replated in rGF pre-coated PDL-plates at a density of 21000 cells/cm^2 as described in 3.2.2. For the determination of possible effects of B[a]P, β-NF, and pyrene on markers related to neurodevelopment, three differentiation and exposure time points were selected. The cells exposed to B[a]P and pyrene were exposed to $1x10^{-5}$, $1x10^{-6}$, and $1x10^{-7}$ M, and the cells exposed to β-NF, the concentrations were $1x10^{-6}$, $1x10^{-7}$, and $1x10^{-8}$ M because of poor solubility of β-NF, see plate layout in Appendix 4. Dilutions of the various PAHs were prepared as described in 3.3 and Appendix 3. Exposure in the medium was prepared fresh for every medium change. Samples were collected after 3, 14, and 21 days of differentiation and exposure.

3.6.2 RNA isolation

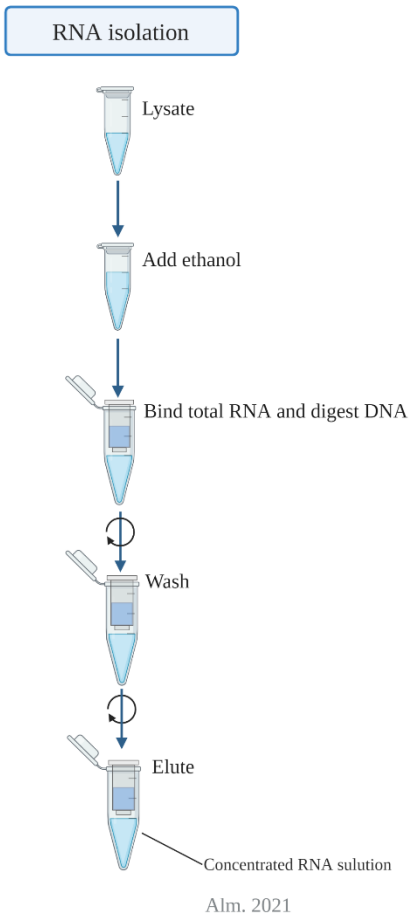

Figure 8: ***RNA isolation with Qiagen RNaesy Mini kit (1)****. Created using BioRender.com.*

RNA from the NSCs was isolated with RNeasy Mini Kit (74106, Qiagen, Germany) (1) according to the supplier's protocol with some modifications, see Figure 8. RNA isolation was performed to get purified RNA which could further be used in cDNA synthesis following real-time PCR analysis of neural markers. All RNA work was done in an RNase-free environment in a LAF-bench cleaned with water and 70 % ethanol. RNase away, a RNase inhibitor, was used to clean pipettes and other equipment used in the RNA isolation procedure. UV-light was applied in the LAF-bench for 10 min after use to sterilize the hood to prevent contamination.

The cells were lysed by adding 75 µL of RLT lysis buffer to each well after removal of ND medium following incubation at room temperature for 5 min. The lysate was pipetted to a QIAshredder column and centrifuged for 5 min at 12000 g. The QIAshredder only had room for 700 µL, depending on the number of replicates wells in the plate, the lysate was centrifuged once or twice with equal aliquots to not exceed the maximum volume of the QIAshredder column. The lysate was stored at -80 °C until RNA isolation. Frozen lysates were thawed at room temperature and mixed with an equal volume of 70 % ethanol and transferred to a RNeasy Spin column (spin column) and centrifuged. All centrifugation steps were performed at ≥ 8000 x g for 30 sec to 1 min except where noted. The flow-through left in the collection tube after a washing step was always discarded after centrifugation leaving total RNA bound to the membrane in the spin column. Ethanol was added to the lysate to bind the RNA to the spin column. As the column only had the capacity of 700 µL the column had to be filled and centrifuged twice or three times with successive aliquots. The spin-column was then washed with RW1 buffer and treated with DNase I (10 µL DNase stock solution + 70 µL RDD buffer) in 15 min incubation at room temperature. After incubation, the spin column membrane was washed once with RW1 buffer and twice with RPE buffer. The second wash with RPE centrifuged for 2 min, the long centrifugation ensured that no ethanol was carried over in the RNA elution. Centrifugation after the RPE wash was done to eliminate any possible carryover

from the RPE Buffer. After elimination of RPE, 50 µL RNAse and DNase-free H_2O was added directly to the center of the spin column membrane and centrifuged for 1 min to elute RNA. Isolated RNA samples were stored at -80 °C before real-time analyses.

3.6.3 Nucleic acid quality control

Following isolation, the yield and purity of all RNA samples were determined by the use of the Nanodrop 1000 Spectrophotometer (Thermo Fisher, USA). Nanodrop measures the absorbance of light and finds the quality and the quantity of the nucleic acids in the sample. Nucleic acids absorb light at 260 nm, proteins, and phenols at 280 nm, and carbohydrates and salts at 230 nm. The software of Nanodrop 1000 calculates the ratios between these three wavelengths and indicates the purity. Pure RNA is expected to have an A260/280 ratio of ~2.0 and an A260/230 ratio of 1.8-2.2. If the A260/230 ratio is below 2.0 it indicates that contaminants are present in the sample (108). The spectrophotometer was blanked with RNAse-free water and each sample was performed with 1.0 µL of the sample. Measurements of sample absorbance gave the ratios of A260/289 and A260/230 and the concentration in ng/µL. All samples < 80 ng/µL were concentrated with Eppendorf Concentrator plus™ (Eppendorf, Germany) with the program V-AQ, 60 °C for 10 min. This ensured efficient and gently vacuum concentration of RNA (109), samples were measured with Nanodrop 1000 after up-concentration.

3.6.4 cDNA synthesis

To perform real-time PCR analysis RNA was transcribed to cDNA by reverse transcription (cDNA synthesis) using reverse transcriptase (RT) enzyme. cDNA synthesis was performed using High Capacity cDNA Reverse Transcription kit (4368814, Applied biosystems, USA). Samples with the highest A230/260 ratio were chosen for cDNA synthesis to ensure that contaminants such as salts did not inhibit the real-time PCR.

The RNA samples were thawed and diluted using RNase and DNase-free H_2O to contain 1000 ng RNA as input for the cDNA synthesis. 12.5 µL diluted RNA was reverse transcribed to cDNA with 12.5 µL master mix containing RT buffer, dNTPs, random primers, and MultiScribe™ Reverse Transcriptase enzyme, see Table 2. It was also included a No Reverse Transcription control (NRT) without the enzyme to control for genomic DNA. The total reaction volume was 25 µL for one sample and the cDNA synthesis was run using CFX 96™

Real-Time System (Bio-Rad, Germany) with a 10 min warm-up at 25 °C for primer annealing, synthesis for 2 h in 37 °C, and a 5 min enzyme deactivation. After synthesis cDNA was stored in a freezer (-20 °C) before gene expression analysis with real-time PCR.

Table 2: ***Preparation to cDNA synthesis master mix and NRT control*** *Master Mix components and volumes to be added to make Master Mix for each sample for cDNA synthesis.*

	Volume per sample (µL)	**NRT sample (µL)**
10 X RT Buffer	2.0	2.5
25 X dNTP mix	1.0	1.0
10 X RT Random Primers	2.5	2.5
10 X MultiScribe™ Reverse Transcriptase	1.25	
RNase and DNase free H_2O	5.25	6.5
Diluted RNA (1000 ng)	12.5	12.5
Total volume	**25**	**25**

Abbreviations; NRT = No Reverse Transcription control, RT=Reverse Transcriptase

3.6.5 Real-time PCR

All cDNA samples were diluted 1:25 at the same time and stored at -20 °C to minimize the number of thaw-freeze cycles of cDNA. TaqMan Master Mix (4369016, Applied biosystems, USA) and TaqMan Gene expression assay (4331182, Applied biosystems, USA), see Table 4, was mixed and prepared fresh for every run in a designated hood, and mixed with prediluted cDNA to a final concentration of 1:50, see Table 3. The real-time PCR efficiency and cDNA concentration were previously determined by personnel at NIPH by running a dilutions series on pooled cDNA. All real-time PCR reactions were run in triplicates, and the plate setup allowed for simultaneous measurement of all samples (three different time points, three different concentrations, three different PAHs) for one gene. 10 µL of each sample was transferred in triplicates to a Hard-Shell 384-Well PCR plate (#HSP3805, Bio-Rad, Germany), sealed, and centrifuged for 1 min at 12000 x g before loaded to the CFX 384™ Real Time-systems (Bio-Rad, Germany). To verify that the PCR runs were valid, whiteout contamination all real-time PCR runs were included No Template Control (NTC) and NRT. PCR amplification conditions consisted of 40 cycles with a limit of detection (LOD) of 35 cycles with primer annealing and elongation at 60 °C.

Table 3: ***Preparation of Master Mix to real-time PCR analyses for each sample (triplicate) for each run.*** *Total volume is listed for in total 110 samples for each run in a 384-well plate*

	Per sample (triplicate)	**Volume total**
TaqMan Gene expression assay	2.1 µL	235.0 µL
TaqMan Master Mix	21.0 µL	2350 µL
cDNA template	7.8 µL	
RNase and DNase free H_2O	9.8 µL	

The point at which a fluorescent signal increases and goes beyond the set threshold for background fluorescence is known as the quantification cycle (Ct). More starting material gives a low Ct value indicating high numbers of the target sequence and vice versa for high Ct value (110). The ΔΔCt method is used to normalize the Ct values by comparing them with one or more reference genes and compare to control (unexposed) (111).

In total eight genes were investigated with gene expression including two reference genes, *ACTB* and *GAPDH*. The genes were selected based on their relevance to neurodevelopment processes such as differentiation and synaptogenesis. An overview of the genes analyzed is listed in Table 4 with the cellular target, assay ID, and supplier.

Table 4: ***Primer information for TaqMan Gene expression assay used for real-time PCR analysis.***

Gene	**Gene function/ cellular target**	**Assay ID**	**Supplier**
ACTB	Reference gene	Hs01060665_g1	Thermo Fisher
AHR	Aryl hydrocarbon receptor	Hs00169233_m1	Thermo Fisher
DLG4	Synaptogenesis/ Post-synaptic density protein 95	Hs01555367_m1	Thermo Fisher
GAP43	Mature neurons/ Expressed in the presynaptic terminal	Hs00967138_m1	Thermo Fisher
GAPDH	Reference gene	Hs02786624_g1	Thermo Fisher
GFAP	Astrocytes	Hs00909233_m1	Thermo Fisher
MAP2	Mature neurons and neurite outgrowth	Hs00258900_m1	Thermo Fisher
NES	Neural stem cells	Hs04187831_g1	Thermo Fisher

3.7 Immunocytochemistry of protein markers related to neurodevelopment

Protein markers related to neurodevelopment were assessed with immunocytochemistry by High Content Imaging (HCI). Immunocytochemistry is used to detect and quantify proteins in tissue and cell samples based on the binding of a specific primary antibody. The primary

antibody will bind directly to the antigen (target). Secondary antibodies that are specific for the primary antibodies with attached fluorophores are added to mark the primary antibody and the target antigen. Using HCI the fluorescent signal can be detected and quantified to determine relative amounts and distributions of proteins in tissue and/or in cells (112, 113)

3.7.1 Experimental design

NSCs were trypsinized and plated in rGF coated µ-Plate 24 well black (82406, Ibidi, Germany) plates at a density of 12000 cells/cm^2 as described in 3.2.2. After 1 day expansion medium was changed to ND medium (DIV0) to start differentiation and exposure to the three PAHs. NSCs were exposed to B[a]P and pyrene with the concentrations 1x10^{-5}, 1x10^{-6}, and 1x10^{-7} and with β-NF with concentrations 1x10^{-6}, 1x10^{-7}, and 1x10^{-8} M prepared fresh in ND medium and changed twice a week. A solvent control containing 0,1% DMSO corresponding to the total DMSO concentration was included. Stock solutions were prepared as described in 3.3. Two differentiation and exposure time points were chosen 14 and 21 days as shown in Figure 7. The time points were chosen to detect possible effects on protein markers related to neurodevelopment after exposure with the selected concentrations of the selected PAHs.

3.7.2 Fixation and staining of neural stem cells

NSCs was fixated using formaldehyde, the cells die and become fixated in their current state upon treatment. Fixation is used to preserve the cells for analysis while maintaining their structure and cell integrity, preserve protein, carbohydrates, and other macromolecules in the cell (114)

After 14 and 21 days of combined differentiation and exposure to the PAHs, the cells were fixed with 4% formaldehyde (47609-250ML, Sigma Aldrich, Germany) for 10 min after removal of the ND medium. Formaldehyde was aspirated completely, and the cells were washed twice with PBS with Ca^{2+} and Mg^{2+} (PBS+). The cells were permeabilized with 0.1% Triton-X-100 (93442-100ML, Sigma Aldrich, Germany) and 3.5% bovine serum albumin (A7979-50ML, Sigma Aldrich, Germany) (BSA) made in PBS+ for 15 min at room temperature. After permeabilization the cells were incubated in a blocking buffer consisting of 3.5% BSA made in PBS+ for at least 15 min at room temperature, to prevent nonspecific binding of antibodies. After the blocking step, the cells were incubated with primary antibodies

diluted in 3.5% BSA at determined dilutions as listed in Table 5 at 4 °C overnight. The plate set-up consisted of 6 wells per concentration, in the two first wells the cells were stained with MAP2, TH, and GABA. In the two next wells, the cells were stained with MAP2, SYP, and PSD95, and in the two last wells, the cells were stained with Ki67 and nestin. This ensured that no primary antibodies from the same species were used in the same well, see plate layout in Appendix 4. The plates were sealed with parafilm to avoid evaporation during incubation. The following day primary antibodies were recovered and reused up to three times. Cells were washed twice with PBS+ and incubated for 1 h at room temperature in darkness with Dyelight-conjugated secondary antibodies (1:500, Thermo Fisher, USA) and nuclei counterstained with 1 µg/mL DAPI (Thermo Fisher) diluted in 3.5% BSA, see Table 6. After incubation in darkness cells were washed twice in PBS+ and stored in PBS+ at 4 °C in darkness before analysis.

Table 5: ***Primary antibodies used in staining for immunocytochemistry following visualization with high content imaging.***

Primary antibodies and staining solutions	**Cellular target/ protein function**	**Dilution**	**Antibody species**	**Catalog number**	**Producer**
GABA	GABAergic neurons	1:200	Mouse	A0310	Sigma Aldrich
Ki67	Cell cycle marker	1:300	Rabbit	MAB4190	Merck
MAP2	Committed neurons and neurite outgrowth	1:5000	Chicken	ab5392	Abcam
Nestin	Neural stem cells	1:200	Mouse	N5413-100UG	Sigma Aldrich
PSD95	Synaptogenesis	1:300	Mouse	ab13552	Abcam
SYP	Synaptogenesis	1:200	Rabbit	AB14692	Millipore
TH	Dopaminergic neurons	1:400	Rabbit	AB152	Millipore

Table 6: ***Secondary antibodies used for staining for immunocytochemistry following visualization with High Content Imaging.***

Secondary antibodies	Dilution	Catalog number	Producer
DAPI	1:1000	62248	Thermo Fisher
Goat Anti Mouse IgG H&L (DyLight® 550) preadsorbed	1:500	ab96880	Abcam
Goat Anti-Chicken IgY H&L (DyLight® 488) preadsorbed	1:500	ab96951	Abcam
Goat Anti-Rabbit IgG H&L (DyLight® 650)	1:500	ab96902	Abcam

3.7.3 High Content Imaging

High Content Imaging was performed by Vigdis Sørensen (Ph.D.) specialist in light microscopy at the Institute of Cancer Research at Oslo University Hospital, The Norwegian Radium hospital at their advanced light microscopy core facility. Immunocytochemistry was visualized by HCI on a Nikon ECLIPSE Ti2-E microscope equipped with CSU-WI spinning disk confocal unit, Prime BSI sCMOS camera, and 405 nm, 488 nm, 561 nm, and 638 nm lasers. Multichannel images random fields of view for each well were captured and analyzed using NIS-Element AR Analysis software and/or Fiji/ImageJ. Images presented are maximum intensity projections of Z-sections adjusted by linear brightness-contrast.

3.8 Data analysis and statistics

Data were visualized with graphs prepared using GraphPad Prism v.5 (GraphPad Software Inc., USA). Statistical analysis was performed with JMP Pro 15.2.0 (SAS Institute Inc., USA) and GraphPad Prism v.5. Statistical significance was assessed by the Wilcoxon sign rank test for comparison cell control vs. DMSO control. Wilcoxon/Kruskal Wallis test with Steel Method as post-test was used for cell viability and gene expression. For all graphs, an asterisk (*) indicates a significant difference *$p < 0.05$, **$p < 0.01$ and ***$p < 0.001$ from defined control group.

3.8.1 ΔΔCt Method

Calculations of relative gene expression for the gene of interest were assessed using the ΔΔCt method. The real-time PCR reaction was run for 40 cycles and fluorescent emission was recorded for every cycle and the quantification cycle (Ct) value was determined by CFX Manager Software (Bio-Rad Laboratories, USA). The average Ct values for three independent

experiments were calculated for each condition. The average Ct value of two reference genes, *ACTB* and *GAPDH*, was determined. ΔCt was determined by subtracting the average Ct value for a given condition (target gene) with the average Ct value of two reference genes for the same given condition. The ΔΔCt was determined by subtracting ΔCt of the given condition with the ΔCt of the control. The equations are shown below and ΔΔCt was visualized in graphs by using GraphPad Prism 5.

ΔCt (sample) = Ct (target gene) – Ct (average of reference genes)

ΔΔCt = ΔCt (sample) - ΔCt (control)

4 RESULTS

4.1 Neural stem cells undergoing differentiation

The differentiation process from undifferentiated cells toward a complex neurite network is shown in the phase-contrast microscopic pictures presented in Figure 9. As illustrated in Figure 9, and from a subjective impression obtained after a visual examination of a large number of cultures, it seems as cells density increased somewhat as a function of differentiation time. In the undifferentiated cells, cytoplasmic outgrowth was short and few, an appearance similar to ordinary stem cells. With increasing time in differentiation medium, it was observed an increased length of cytoplasmic outgrowth from most cells, possibly representing outgrowth and formation of a more complex neurite network. It should also be noted that an increased number of dead cells was seen during the differentiation processes, as exemplified in the picture after 14 and 21 days of differentiation.

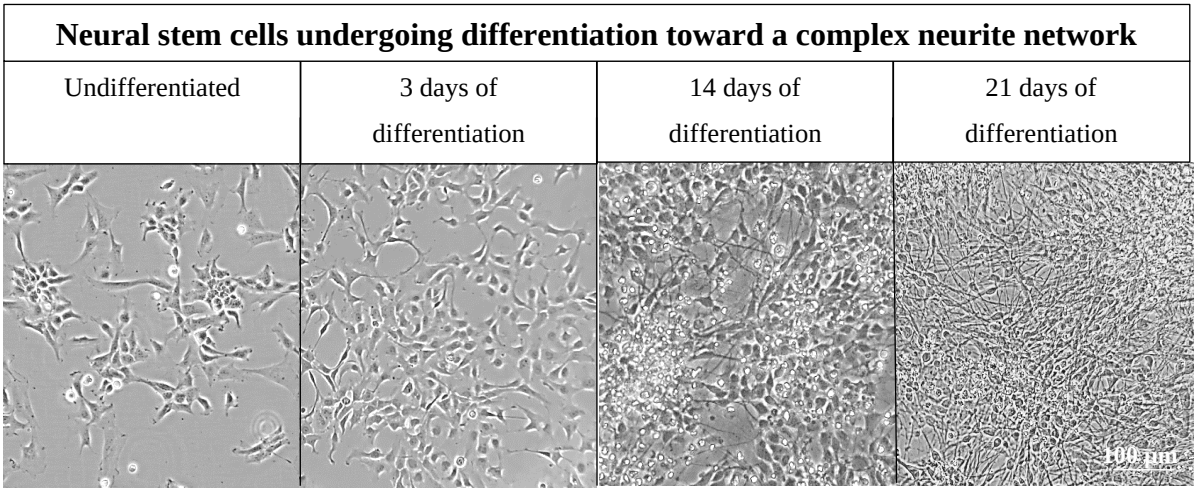

Figure 9: ***Neural stem cells (NSCs) undergoing differentiation toward a complex neurite nettwork****. NSCs was differentiated in the precence of differentiation (ND) medium in up to 21 days. The phase-contrat images show undifferentiated cells and cells undergoing differentiation for 3, 14 and 21 days, Scale bare is set to 100 µm.*

4.2 Optimization of Alamar Blue assay for assessment of cell viability

To examine whether different cell densities, incubation time, and substrate concentration have an impact on the Alamar Blue assay, an optimization of the assay was performed. Different dilutions of substrate were used to compare protocol from EC-JRC (1:6 dilution) (115) and NIPH (1:10 dilution) (116). Cell viability was measured as the relative fluorescence in differentiating cells exposed to the test substance (glycidamide) when compared to control cells as a function of time.

The fluorescence values increased with incubation time up to 8 h as shown in Figure 10. In control cells, the 1:6 dilution showed a steeper increase in fluorescence when compared to the 1:10 dilution. No difference in fluorescence was seen in cells exposed to the test substance glycidamide comparing the two dilutions. The 1:6 dilution showed a larger difference between control and glycidamide exposed cells than the 1:10 dilution.

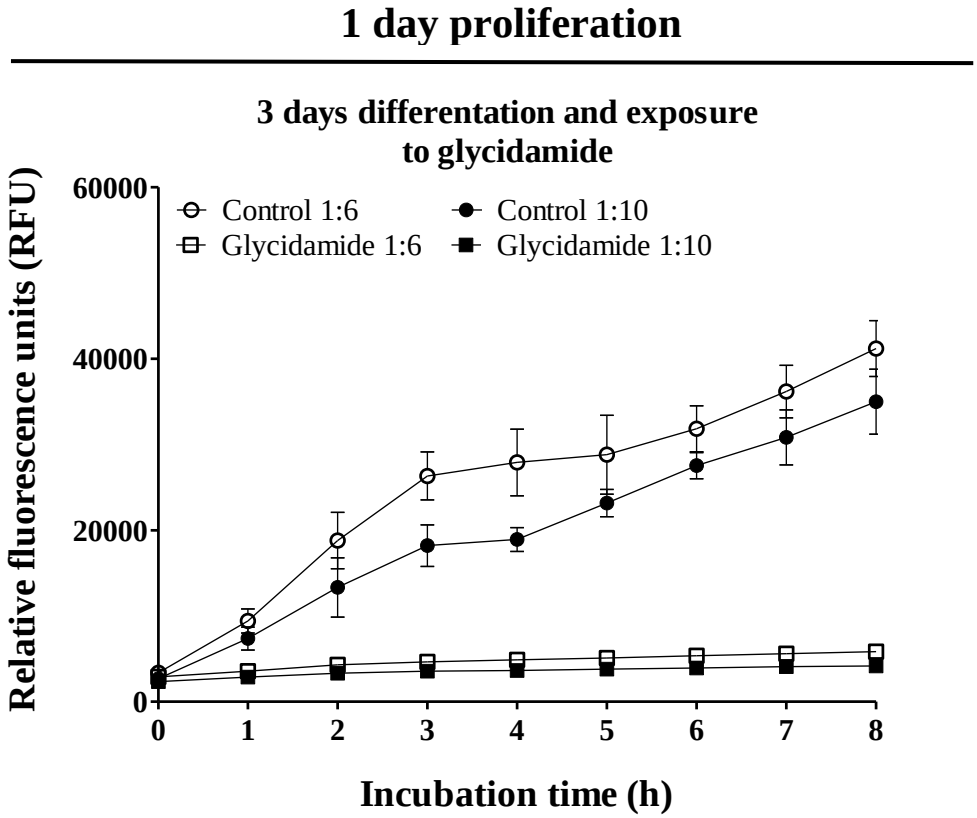

Figure 10: ***Relative fluorescence as a function of incubation time with 1:6 or 1:10 dilution of Alamar Blue****. NSCs proliferated for 1 day and differentiated for 3 days with or without exposure of 1x10^{-3} M glycidamide before incubated with 1:6 or 1:10 dilution of Alamar Blue and with measurement every hour up to 8 h. Data is presented as the mean value ± SD of one experiment.*

The percentage reduction of resazurin in cells exposed to 1x10^{-3} M glycidamide normalized to control after up to 8 h of incubation with Alamar Blue™ is shown in Figure 11. NSCs exposed to glycidamide for 3 (B) and 5 days (D) showed a reduction of resazurin at an earlier time point than cells exposed for 1 day (A and C). When cells proliferated for 2 days (C and D), which give a higher cell density, a more rapid reduction of resazurin was seen, when compared to their respective one day of proliferation (A and C). The reductions of resazurin between control and exposed cells using 1:6 dilution was larger than using the 1:10 dilution for cells proliferating for 2 days and 1 day combined differentiation and exposure to glycidamide (C). An overall reduction below 50% was seen after 8 h of incubation for all conditions. Using, 1:6 dilution the curve more rapidly flattened when compared to 1:10 dilution, the curve has flattened after 4 h

of incubation (Figure 11 C and D). Based on our results shown in Figure 11, a dilution of 1:6 seems to be the most sensitive dilution for detection of cell viability at various days of proliferation/differentiation/treatment and time points.

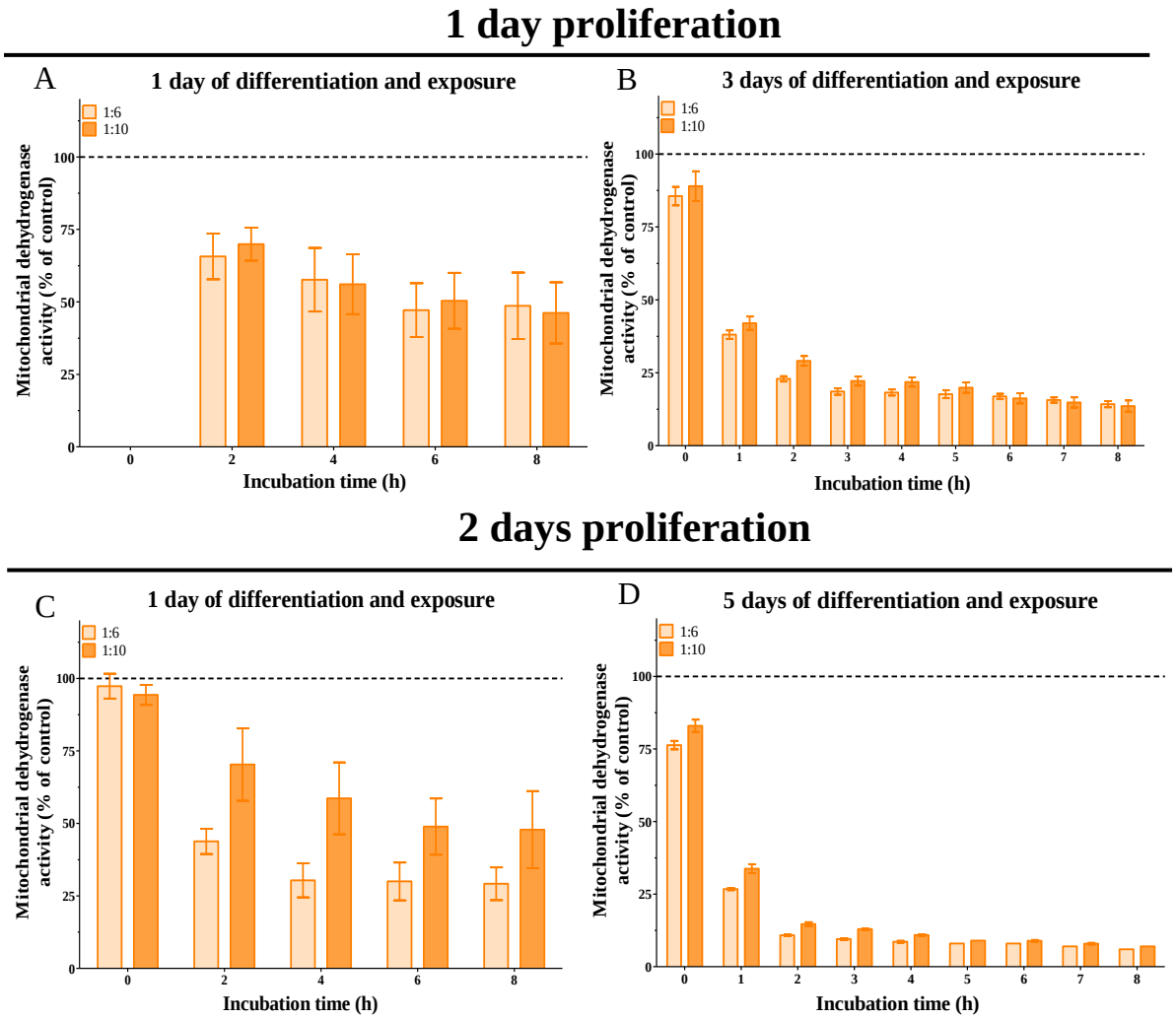

Figure 11: ***Reduction of resazurin by mitochondrial dehydrogenase as a function of incubation time with Alamar Blue™ reagent.*** *All plates were seeded with 7000 cells/well in a 96-well plate and proliferated for one (A, B) or two days (C, D) days before stating differentiation and exposure with or whiteout 1x10^{-3} M glycidamide. NSCs were exposed while undergoing differentiation for 1 (A, C), 3 (B) or 5 days (D). After differentiation with or without exposure to 1x10^{-3} M glycidamide, cells were incubated with 1:6 (light orange) and 1:10 (dark orange) dilution of Alamar Blue and relative fluorescence were measured. Data are presented as mean value ± SD normalized to control of one experiment.*

Optimization performed by personnel at NIPH is shown in Figure 12. Results are presented as percentage reduction of resazurin in NSCs exposed to 1x10^{-3} M glycidamide normalized to control with different seeding densities after up to 8 h incubation with Alamar Blue™. Cells exposed to glycidamide for 3 (B) and 5 days (D) showed a higher reduction of resazurin compared to cells exposed for the corresponding 1 day (A and C). The reduction of resazurin

seen in cells proliferating for 1-day before 1-day exposure with glycidamide was more marked (A) when compared to corresponding cells proliferating for 2 days (C).

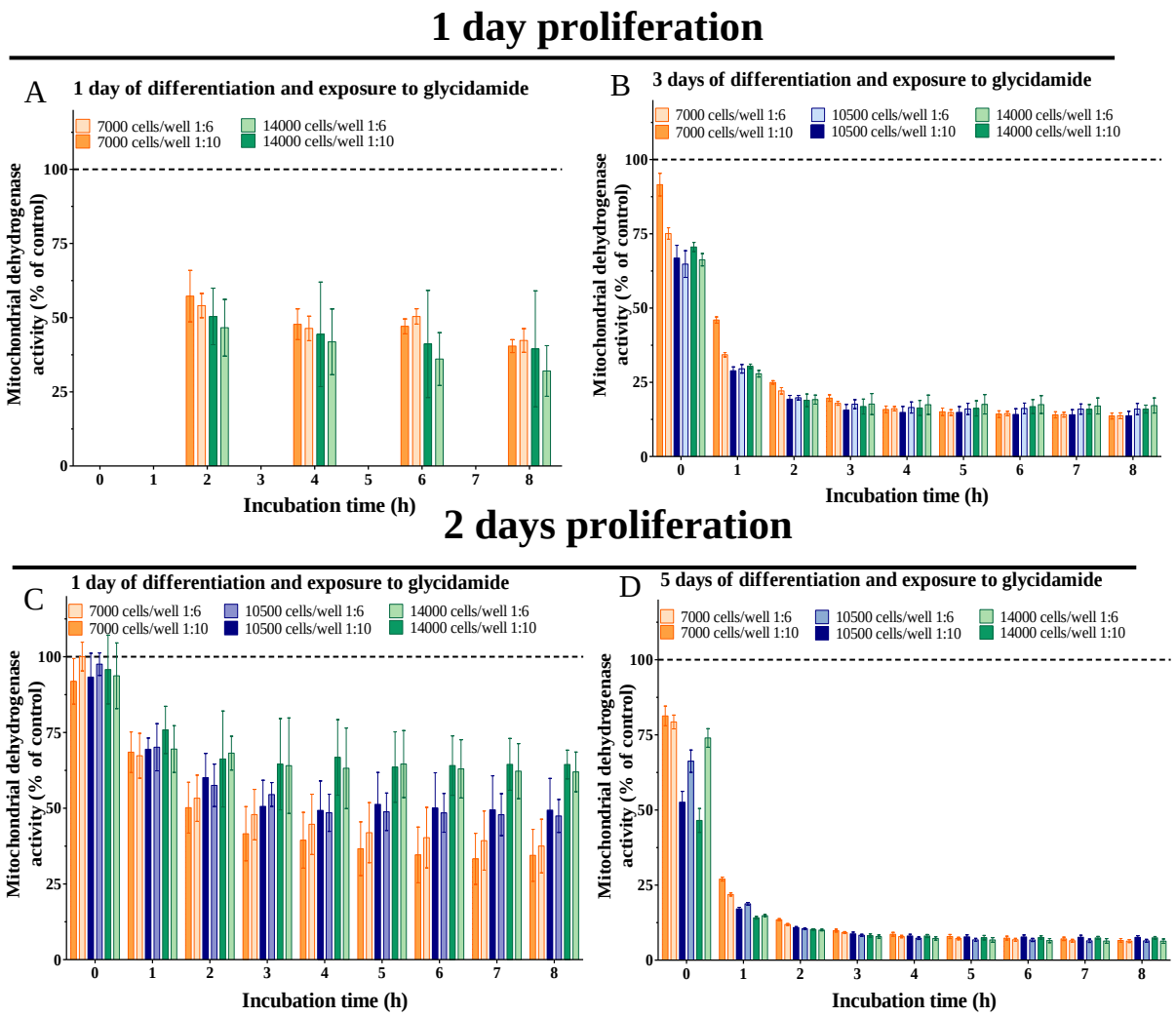

Figure 12: ***Reduction of resazurin by mitochondrial dehydrogenase as a function of incubation time with Alamar Blue™ reagent.*** *As a part of a more detailed validation of the Alamar Blue assay by the NIPH, were 96-well plates seeded with different seeding densities 7000 (orange), 10500 (blue) and 14000 (green) cells/well and proliferated for one (A, B) or two days (C, D) days before stating differentiation and exposure with or whiteout 1x10^{-3} M glycidamide. NSCs were exposed while undergoing differentiation for 1 (A, C), 3 (B) or 5 days (D). After differentiation with or without exposure, cells were incubated with 1:6 (light) and 1:10 (dark) dilution of Alamar Blue™ and measured up to 8 h. Data are presented as mean value ± SD normalized to control of one experiment.*

Differences in cell densities had an impact on the reduction of resazurin as shown in Figure 12 A and C after 1 day of exposure to glycidamide. After 3 and 5 days of exposure, the differences showed no impact of the reduction of resazurin (B and D). Little or no difference between the reduction of resazurin using 1:6 and 1:10 dilution at various cell densities was seen. Based on these results incubation time of 3 h and 30 min was chosen. Furthermore, the 1:10 dilution was concluded to be sufficient for good sensitivity for further experiments with the NSC model.

4.3 Cell viability after exposure to polycyclic aromatic hydrocarbons

Cell viability after exposure to B[a]P, β-NF and pyrene were tested using Alamar Blue™ assay. The aim was to determine cell viability after exposure and define non- and low cytotoxic concentrations on different time points (1, 3, 14, and 21 days of differentiation) for further mechanistic studies on neurodevelopment. None of the PAHs tested caused any marked changes in morphology at any of the concentrations tested, as seen by microscopic examination, and illustrated in Figure 13.

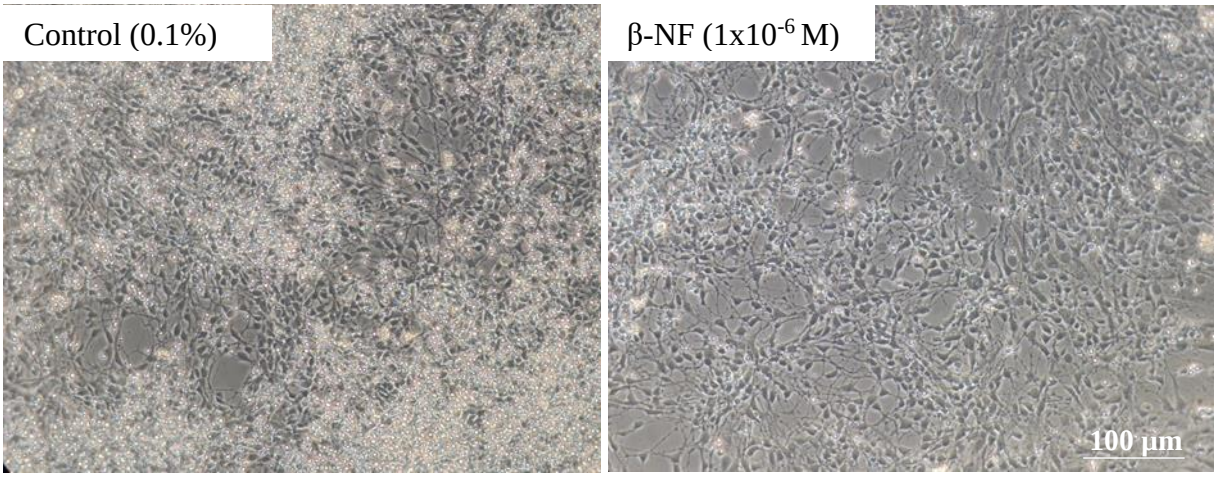

Figure 13: ***A representative phase contrast image showing control (0.1% DMSO) and NSCs exposed to 1x10^{-6} M of β-NF for 14 days of differentiation.*** *Scale bare is set to 100 µm.*

As PAHs are very lipophilic and poorly soluble in cell culture medium, they were first dissolved in DMSO. NSCs exposed to 0.1% DMSO for 1, 3, and 14 days of differentiation did not result in any significant changes in cell viability when compared with non-exposed controls at any of the time points investigated, as shown in Figure 14. DMSO at this dilution was therefore accepted as solvent control for further experiments with the PAHs.

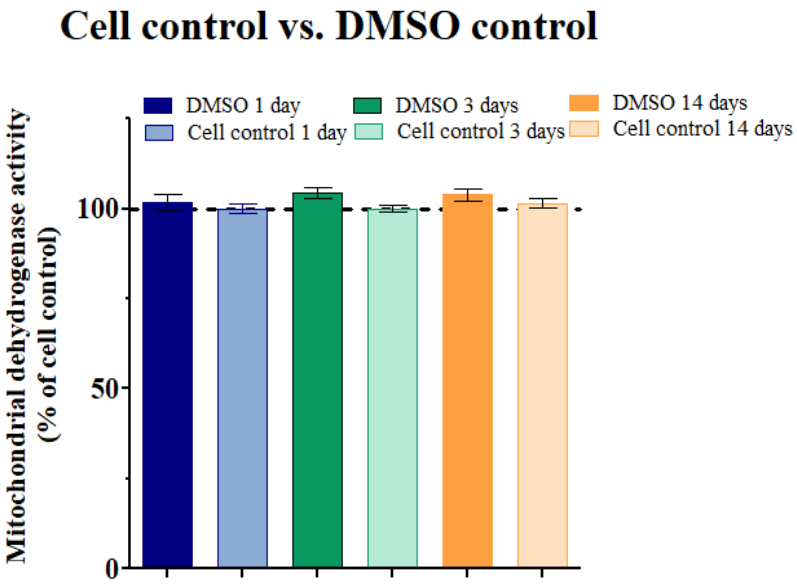

Figure 14: ***Effects on NSCs exposed to 0.1% DMSO undergoing differentiation.*** *Cells were exposed to 0.1% DMSO for 1 (blue), 3 (green), and 14 (orange) days of differentiation compared unexposed cells (cell control). Mitochondrial dehydrogenase activity was assessed with Alamar Blue™. Data are presented as mean value ± S.E.M of four independent experiments. All data were normalized to their respective cell control for comparison.*

4.3.1 Effects of benzo[a]pyrene on cell viability in NSCs undergoing differentiation

NSCs exposed to a wide range of concentrations of B[a]P undergoing differentiation for 1, 3, 14, and 21 days are shown in Figure 15. A small significant increase of 10% in cell viability was most prominent after 1 day of exposure and was seen at concentrations $3x10^{-7}$, $1x10^{-6}$, and $3x10^{-6}$ M compared to control (A). After 3 days the viability of the cells was closer to the control level compared to 1 day of exposure, although a significant increase of 6% was seen for $3x10^{-7}$ M (B). The increase seen after 1 and 3 days of exposure was no longer evident after 14 days of exposure (C). The highest and second-highest concentration showed a marked significant decrease of 20-30% in cell viability and appeared to be most cytotoxic. The lowest concentration ($3x10^{-10}$ M) also showed a significant decrease in cell viability which was the trend (although not statistically significant) for all time points (1, 3, 14 days). After 21 days of exposure, only three concentrations were tested, and all concentrations showed a significant decrease in cell viability (D). The highest concentration ($1x10^{-5}$ M) showed a decrease of 20% compared to the control. No difference in % control was observed comparing $1x10^{-5}$ M for 14 and 21 days of exposure. A decrease in cell viability was seen between 1 and 21 days of exposure for the same concentrations.

Benzo[*a*]pyrene

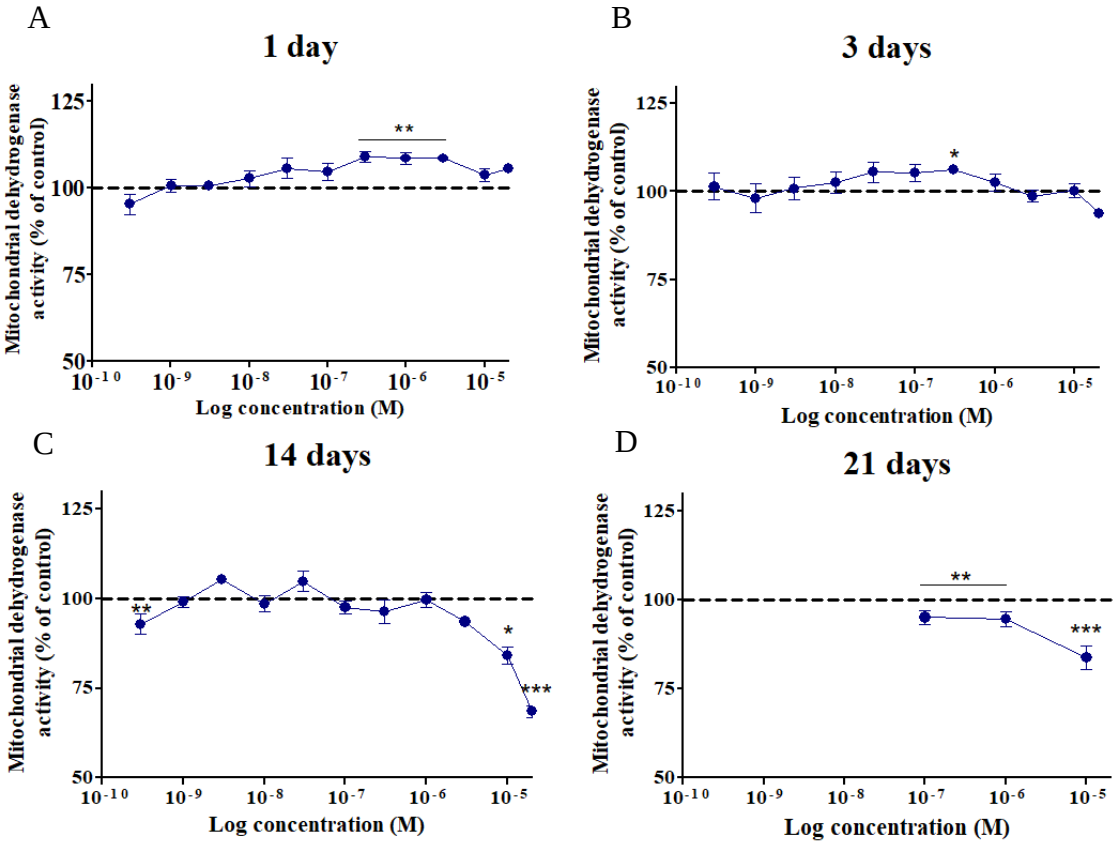

*Figure 15**: Effects of benzo[a]pyrene exposure on cell viability for NSCs undergoing differentiation assessed with Alamar Blue™.** NSCs were exposed for 1 (A), 3 (B), 14 (C) and 21 days (D) undergoing differentiation**.** Data are presented as mean value ± S.E.M. of four independent experiments. All data are normalized to the mean of solvent control (0.1% DMSO, dotted line), for their respective time points. Asterisks indicate a statistically significant difference compared to solvent control assed with Kruskal Wallis with Steel Method as post-test (*= p< 0.05, **=p<0.01 and ***=p<0.001)*

4.3.2 Effects of β-naphthoflavone on cell viability in NSCs undergoing differentiation

Effect on cell viability after exposure to different concentrations of β-NF for 1, 3, 14, and 21 days of differentiation are shown in Figure 16. Cell viability significantly increased upon 1 day of exposure, up to 11% for concentrations ranging $1x10^{-8}$ to $1x10^{-5}$ M (A) compared to control. A further significant increase was observed after 3 days of exposure, an increase of 10-20% compared to control (B). This increase was not seen for the two lowest concentrations. In contrast to 1 and 3 days exposure, 14 days of exposure showed a significant decrease in cell viability for the highest concentration tested (C). The increase in cell viability observed after 1 and 3 days was not observed after 14 days, however, a non-significant increase was seen for the lower part of the concentration spectrum. No significant changes in cell viability were found

for cells differentiated and exposed for 21 days (D). Although, not a significant increase was seen for the lowest concentration, and a decrease in cell viability was seen for the highest concentration. A decrease in cell viability was seen when comparing 1 and 21 days of exposure for the same concentrations. β-NF crystals were seen in the culture medium when adding β-NF dilution for $2x10^{-5}$ M and half the amount for $1x10^{-5}$ M. The visualization of crystals may indicate that β-NF has not been taken up by the cells.

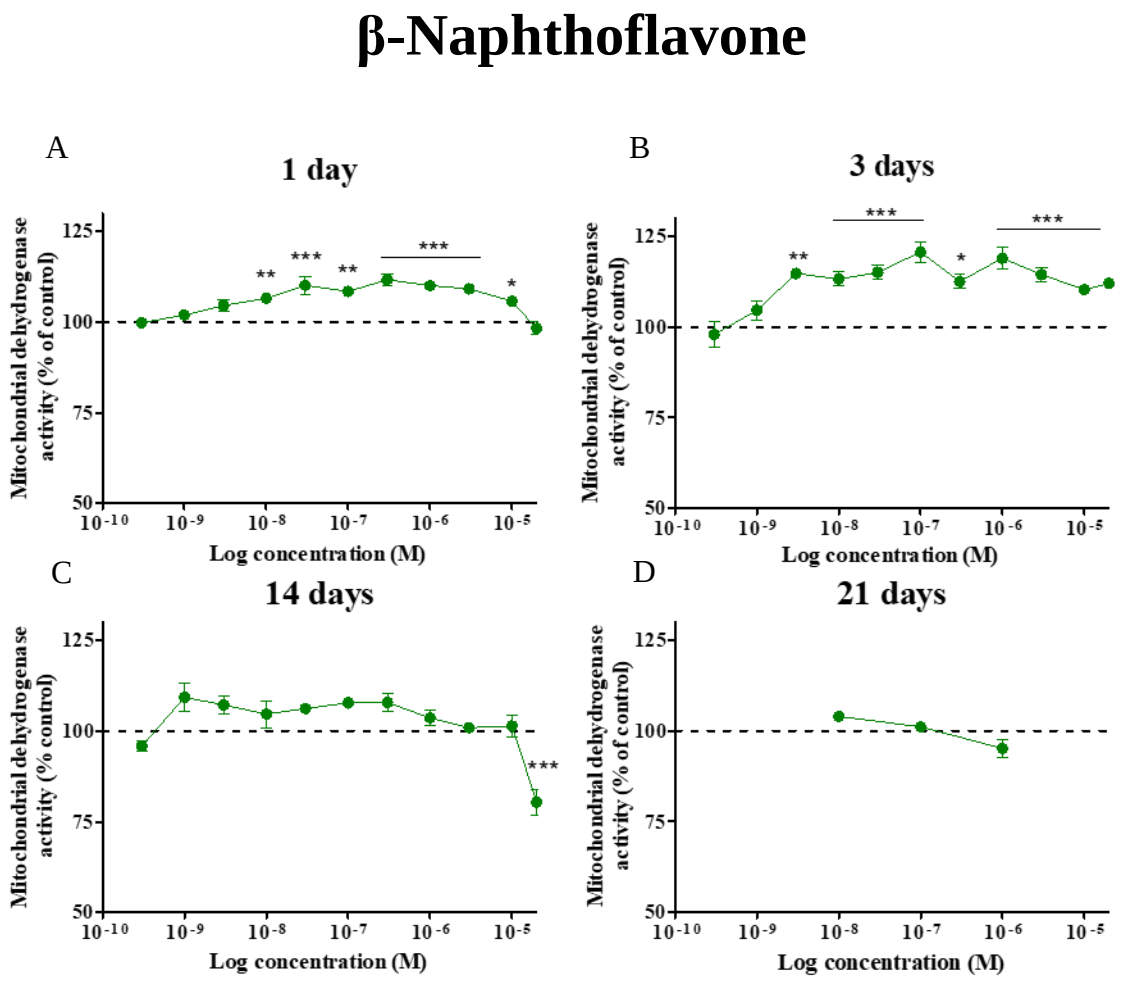

Figure 16: ***Effects of β-naphthoflavone exposure on cell viability for NSCs undergoing differentiation assessed with Alamar Blue™.*** *NSCs were exposed for 1 (A), 3 (B), 14 (C) and 21 days (D) undergoing differentiation. Data are presented as mean value ± S.E.M. from four independent experiments. All data are normalized to the mean of solvent control (0.1% DMSO, dotted line), for their respective time points. Asterisks indicate a statistically significant difference compared to solvent control assed with Kruskal Wallis with Steel Method as post-test (*= p< 0.05, **=p<0.01 and ***=p<0.001)*

4.3.3 Effects of pyrene on cell viability in NSCs undergoing differentiation

Cells exposed to different concentrations of the low weight PAH, pyrene for 1, 3, 14, and 21 days undergoing differentiation are shown in Figure 17. Already after 1 day of exposure, a significant increase in cell viability was observed (A). A 10-20% significant increase in

mitochondrial dehydrogenase activity was seen for concentrations ranging from $1x10^{-8}$ to $3x10^{-6}$ M. After 3 days of exposure a significant increase of 10-16% was observed for all concentrations, except the lowest and highest where the cell viability was closer to control levels (B). After 14 days of continuous exposure showed the highest concentration ($2x10^{-5}$ M) a 16% decrease in cell viability (C). All concentrations, except $1x10^{-9}$, $3x10^{-9}$, $3x10^{-8}$, and $2x10^{-5}$ M were observed close to the control level after 14 days of exposure. Upon continuous exposure for 21 days, no change in cell viability was seen (D). The increase seen after 1 day is not seen after 21 days for the same concentrations, indicating a decrease.

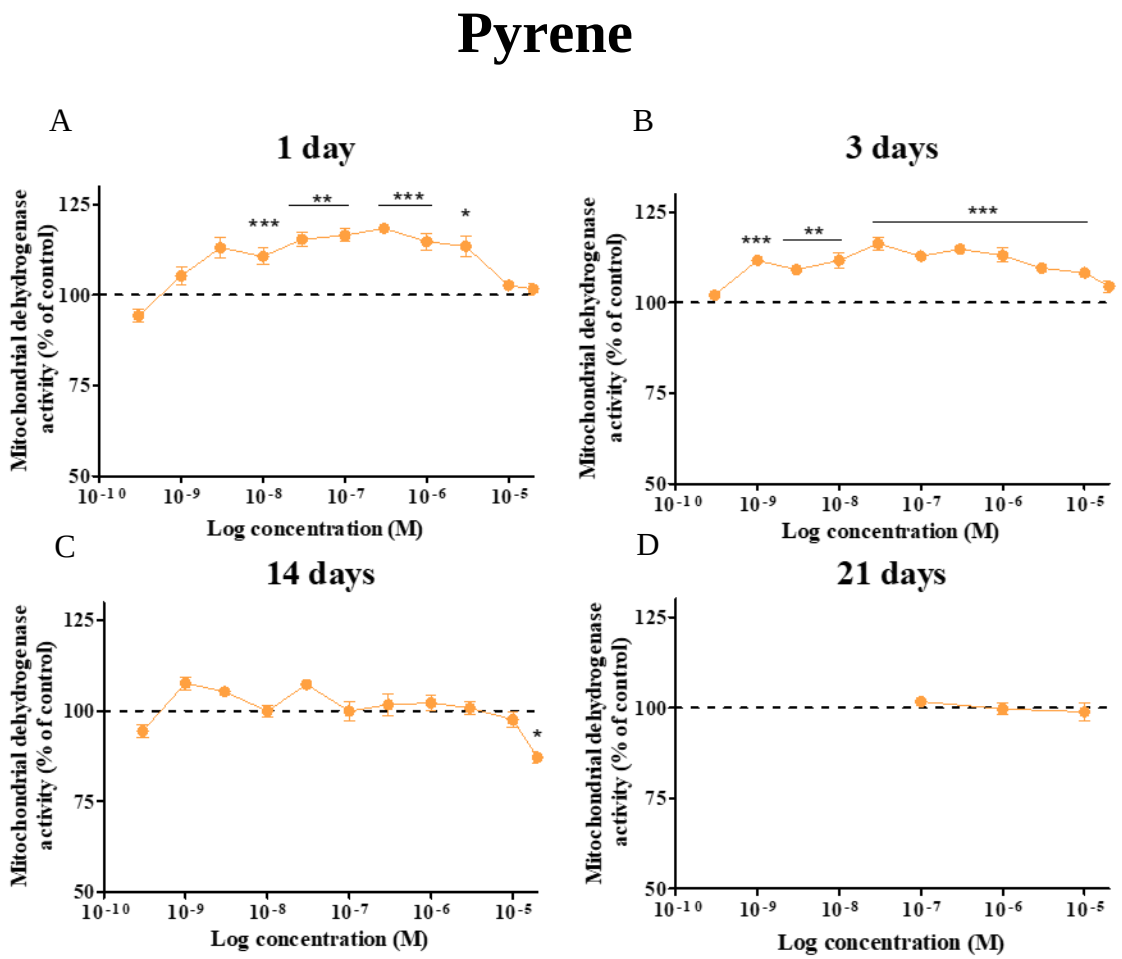

Figure 17: ***Effects of pyrene exposure on cell viability for NSCs undergoing differentiation assessed with Alamar Blue™.*** *NSCs were exposed for 1 (A), 3 (B), 14 (C) and 21 days (D) undergoing differentiation. Data are presented as mean value ± S.E.M. of four independent experiments. All data were normalized to the mean of solvent control (0.1% DMSO, dotted line), for their respective time points. Asterisks indicate a statistically significant difference compared to solvent control assed with Kruskal Wallis with Steel Method as post-test (*= p< 0.05, **=p<0.01 and ***=p<0.001).*

4.3.4 Edge effect

During incubation, it was discovered a difference between the relative fluorescence (RFU) output for wells in the edge of the 96-well plate (cell control in the vertical column) compared to wells inside the plate (cell control in the horizontal row). To verify this and exclude the possibility for artifact due to variations in culturing conditions we specifically tested if unexposed cells seeded at the edge column of the dish gave a different fluorescence than an inner row. As can be seen from the data presented in Figure 18. A cell control placed at the edge of the plate had a lower fluorescence output than cell control placed inside the plate. Figure 18 B shows relative fluorescence units for two sets of cell controls when the entire plate was framed with PBS to avoid any possible artifact due to evaporation of liquid. No change was seen between the vertical column and horizontal row when the plate was framed with PBS. The difference observed was controlled for by normalizing the concentration laying in the periphery of the plate to solvent control wells laying in the periphery of the plate.

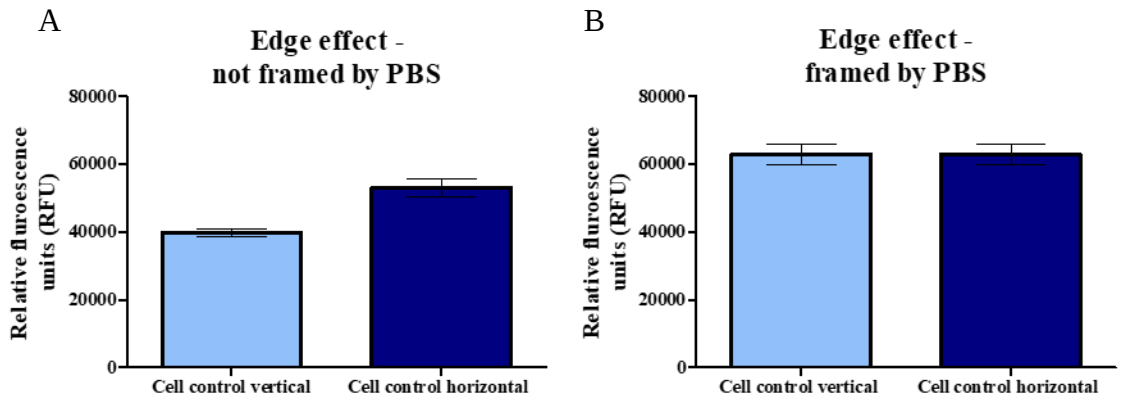

Figure 18: ***Edge effect before and after framing the 96-well plate with PBS****. Relative fluorescence units are measured with Alamar Blue. A: Cell control vertical was placed at the edge of the plate and cell control horizontal was placed inside the plate. B: Cell control vertical and cell control horizontal was placed in a plate framed with PBS. Data are presented as mean ± S.E.M. of three independent experiments.*

4.4 Gene expression of neural markers related to neurodevelopment

As a part of an ongoing project at the NIPH with the aim to characterize the NSCs undergoing differentiation, a gene expression of *MAP2* and *AHR* were assessed for NSC undergoing differentiation for 28 days as shown in Figure 19.

The relative mRNA gene expression is normalized to the reference genes *ACTB* and *GAPDH* and calibrated to undifferentiated cells (DIV0) to show the gene expression during

differentiation. Neural differentiation was confirmed with a significant upregulation of *MAP2* compared to undifferentiated cells for all time points (A). A marked progressive increase of *MAP2* expression was seen with a 4-fold change after 28 days of differentiation which indicates differentiation into more mature neurons. Since *AHR* has been shown as an important regulator for neural differentiation in different models, was the *AHR* gene expression a part of the characterization of the NSCs undergoing differentiation. Upregulation of *AHR* occurred from 14 to 28 days of differentiation, although not significant (B).

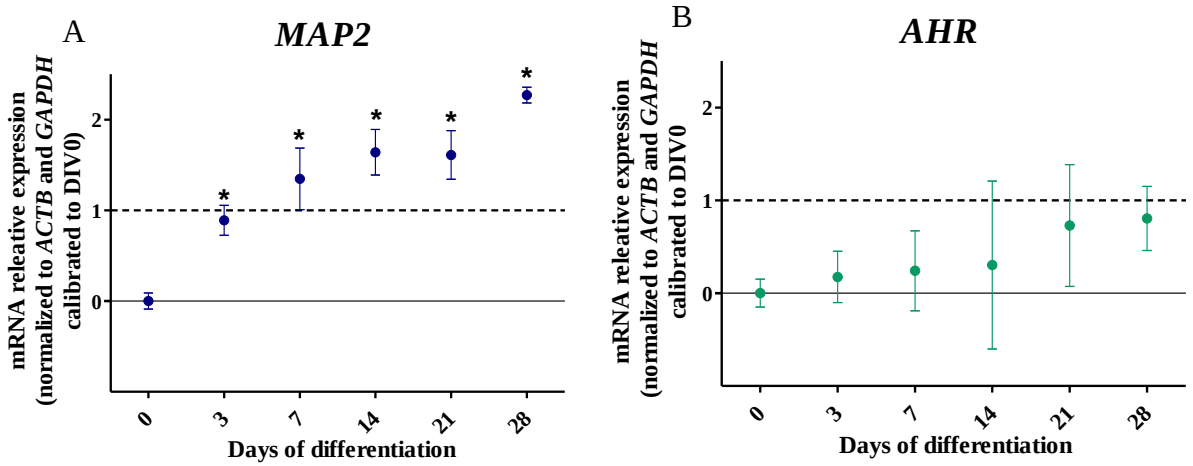

Figure 19: ***Gene expression of neural markers on NSC undergoing differentiation for up to 28 days without exposure.*** *Results from an ongoing characterization of the NSC model at NIPH performed by trained personnel. Gene expression of A: MAP2 and B: AHR were normalized to reference genes ACTB and GAPDH and calibrated to DIV0 (undifferentiated cells, represented by line) (ΔΔCt method). Data are presented as mean ± S.E.M. of three independent experiments with three technical replicates. Significant difference relative to control, * p < 0.05 was determined by Kruskal Wallis with Steel method as post-test.*

The Gene expression aimed to determine if PAH exposure of NSCs undergoing differentiation to 21 days affected markers related to neurodevelopment. The concentrations selected were defined as low-cytotoxic and no-cytotoxic as a result from the cell viability assessment. The most prominent result of the cell viability study indicated that less differentiated cells gave a stronger response to the exposure than more mature cells. Based on these results, differentiation, and exposure for 3, 14, and 21 days were chosen for further mechanistic study on gene expression of markers related to neurodevelopment. The expression levels were estimated and normalized based on the relative mRNA expression of the reference genes *ACTB* and *GAPDH* and calibrated to control.

The gene *GFAP* failed to show amplification within LOD set for our real-time PCR analysis, data are therefore not presented.

4.4.1 Effects of benzo[a]pyrene on gene expression in NSCs undergoing differentiation

NSCs were exposed to B[a]P with three concentrations ($1x10^{-5}$, $1x10^{-6}$, and $1x10^{-7}$ M) for 3, 14, and 21 days of differentiation, normalized to *ACTB*, and *GAPDH* and calibrated on control are shown in Figure 20. The gene expression of the neural stem cell marker, *NES* showed a minor upregulation after 14 days of exposure, with a 2-fold increase for $1x10^{-5}$ M, although not significant (A). *MAP2* showed no significant difference from control for any concentration or time point investigated (B). After 14 days of exposure to B[a]P, a minor upregulation was

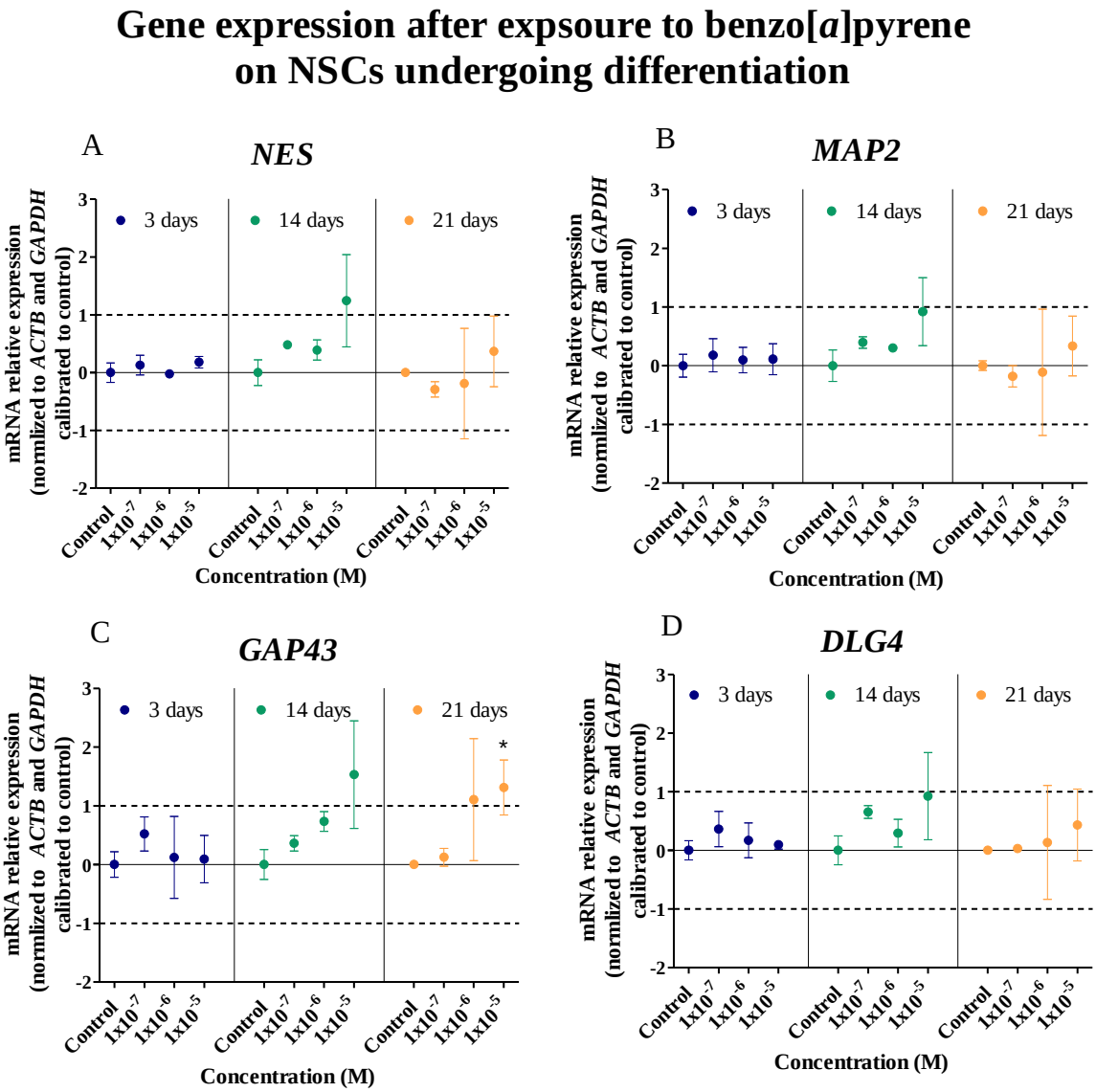

Figure 20: ***Effects on gene expression of four genes related to neurodevelopment after exposure to B[a]P on NSCs undergoing differentiation for 3 (blue), 14 (green) and 21 (orange) days.*** *NSCs were exposed to three concentrations ($1x10^{-5}$, $1x10^{-6}$ and $1x10^{-7}$ M) of B[a]P and 0.1% DMSO (solvent control). Gene expression of A: NES, B: MAP2, C: GAP43 and D: DLG4 were normalized to reference genes ACTB and GAPDH and calibrated to solvent control (represented by line) for respective time points (ΔΔCt method). Data are presented as mean ± S.E.M. of three independent experiments with three technical replicates. Significant difference relative to control, * $p < 0.05$ was determined by Kruskal Wallis with Steel method as post-test.*

observed. The gene expression of the neurite outgrowth marker *GAP43* was observed with a concentration-dependent increase after 21 days of exposure, with $1x10^{-5}$ M significantly ($p < 0.05$) increased with a 2-fold change (C). A concentration-dependent increase was observed after 14 days of exposure, although not significant. The gene expression for synaptogenesis marker *DLG4* did not show any significant up or down regulations at any concentration or time points tested (D). B[a]P seems to induce a slight concentration-dependent increase after 21 days of exposure.

4.4.2 Effects of β-naphthoflavone on gene expression in NSCs undergoing differentiation

NSCs were exposed to three concentrations ($1x10^{-6}$, $1x10^{-7}$, and $1x10^{-8}$ M) of β-NF undergoing differentiation for 3, 14, and 21 days as shown in Figure 21. The mRNA expression is normalized to *ACTB* and *GAPDH* and calibrated to control. The neural stem cell marker *NES* were observed with an upregulation for all concentrations at every time point tested', although not significant (A). The concentration-dependent upregulation was most apparent after 14 days of exposure; however, a 2-fold change increase was seen for the highest concentration after 21 days. Gene expression of *MAP2* showed no significant difference compared to control for the different time-points tested (B). A minor upregulation was seen after 3 days of exposure following a 2-fold change increase after 21 days to $1x10^{-6}$ M. *GAP43* was observed with a significant ($p < 0.05$) upregulation with a 2-fold change for $1x10^{-6}$ M after 21 days of exposure (C). A minor upregulation was seen after 3, 14, and 21 days. *DLG4* showed a trend of a slightly concentration-dependent increase after 3 days of exposure, with a modest increase for the highest concentration, however, no significant change was seen for neither of the concentrations and time points tested (D). An overall upregulation was also seen after 14 and 21 days of exposure, most prominent after 21 days with a 2-fold change increase with $1x10^{-6}$ M.

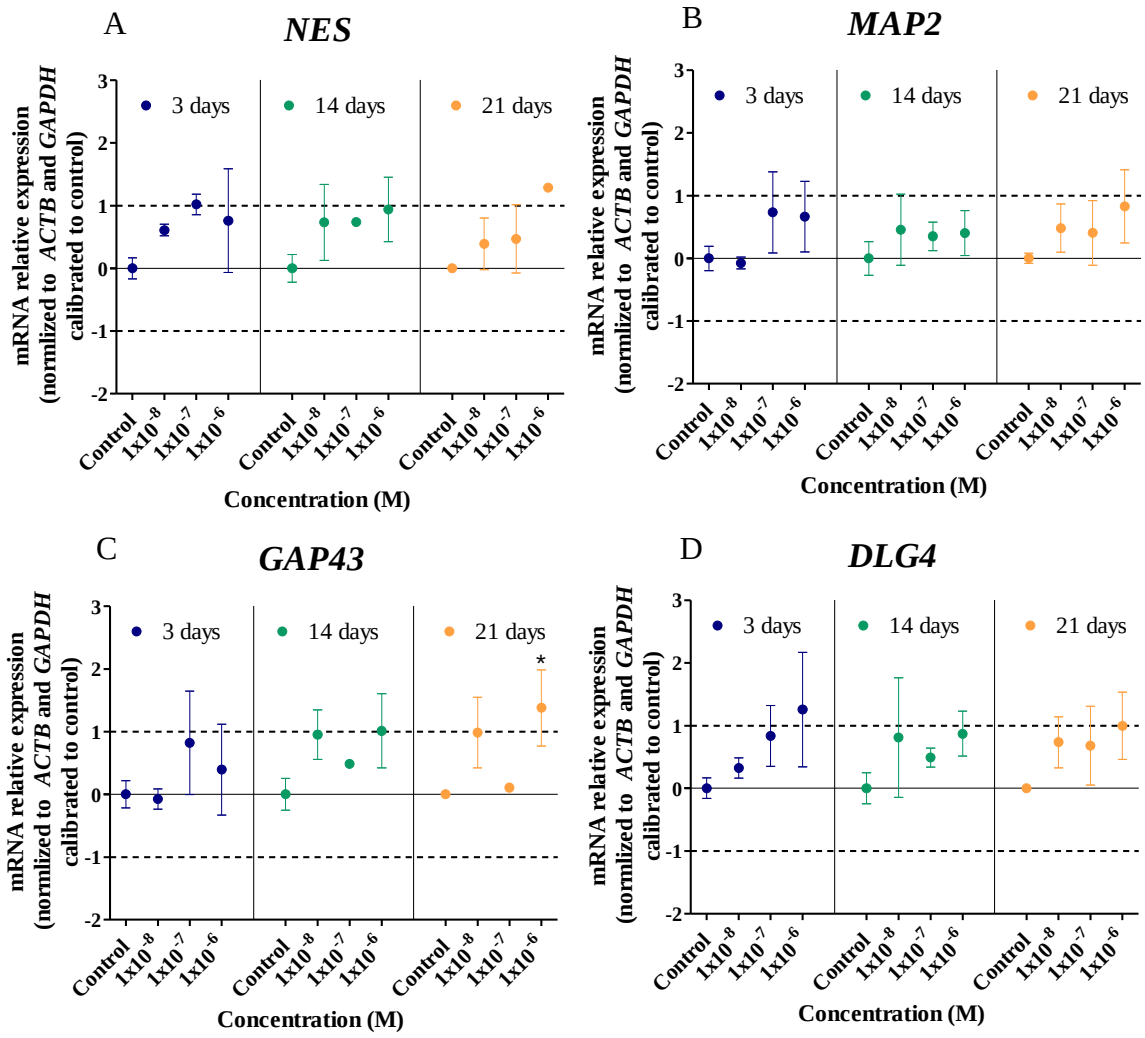

Figure 21: ***Effects on gene expression of four genes related to neurodevelopment after exposure to β-NF on NSCs undergoing differentiation for 3 (blue), 14 (green) and 21 (orange) days.*** *NSCs were exposed to three concentrations ($1x10^{-6}$, $1x10^{-7}$ and $1x10^{-8}$ M) of β-NF and 0.1 % DMSO (solvent control). Gene expression of A: NES, B: MAP2, C: GAP43 and D: DLG4. All genes were normalized to reference genes ACTB and GAPDH and calibrated to solvent control (represented by line) for respective time points (ΔΔCt method). Data are presented as mean ± SEM of three independent experiments with three technical replicates. Significant difference relative to control, * $p < 0.05$ determined with Kruskal Wallis with Steel method as post-test.*

4.4.3 Effects of pyrene on gene expression on NSCs undergoing differentiation

NSCs were exposed to three concentrations ($1x10^{-5}$, $1x10^{-6}$, and $1x10^{-7}$ M) of pyrene undergoing differentiation for 3, 14, and 21 days, normalized to *ACTB* and *GAPDH*, and calibrated to control as shown in Figure 22. Gene expression of *NES* did not show any significant up- or downregulating for any concentration or time point tested (A). After 14 and

21 days of exposure, a 2-fold change was observed for $1x10^{-5}$ M, with a slightly concentration-dependent increase after 21 days of exposure. No significant difference was observed for *MAP2* expression at any of the concentration and time points tested (B). Pyrene seemed to induce a concentration-dependent upregulation after both 14 and 21 days of exposure. *GAP43* expression was statistically significantly ($p < 0.05$) upregulated for $1x10^{-6}$ M with a 2-fold change of gene expression after 21 days of exposure (C). No other concentrations and time points tested were significantly different. The gene expression of *DLG4* showed no significant difference for any concentration or time points investigated (D). A minor upregulation was seen after 3 days followed by a 2-fold increase after 14 days of exposure for $1x10^{-5}$ M.

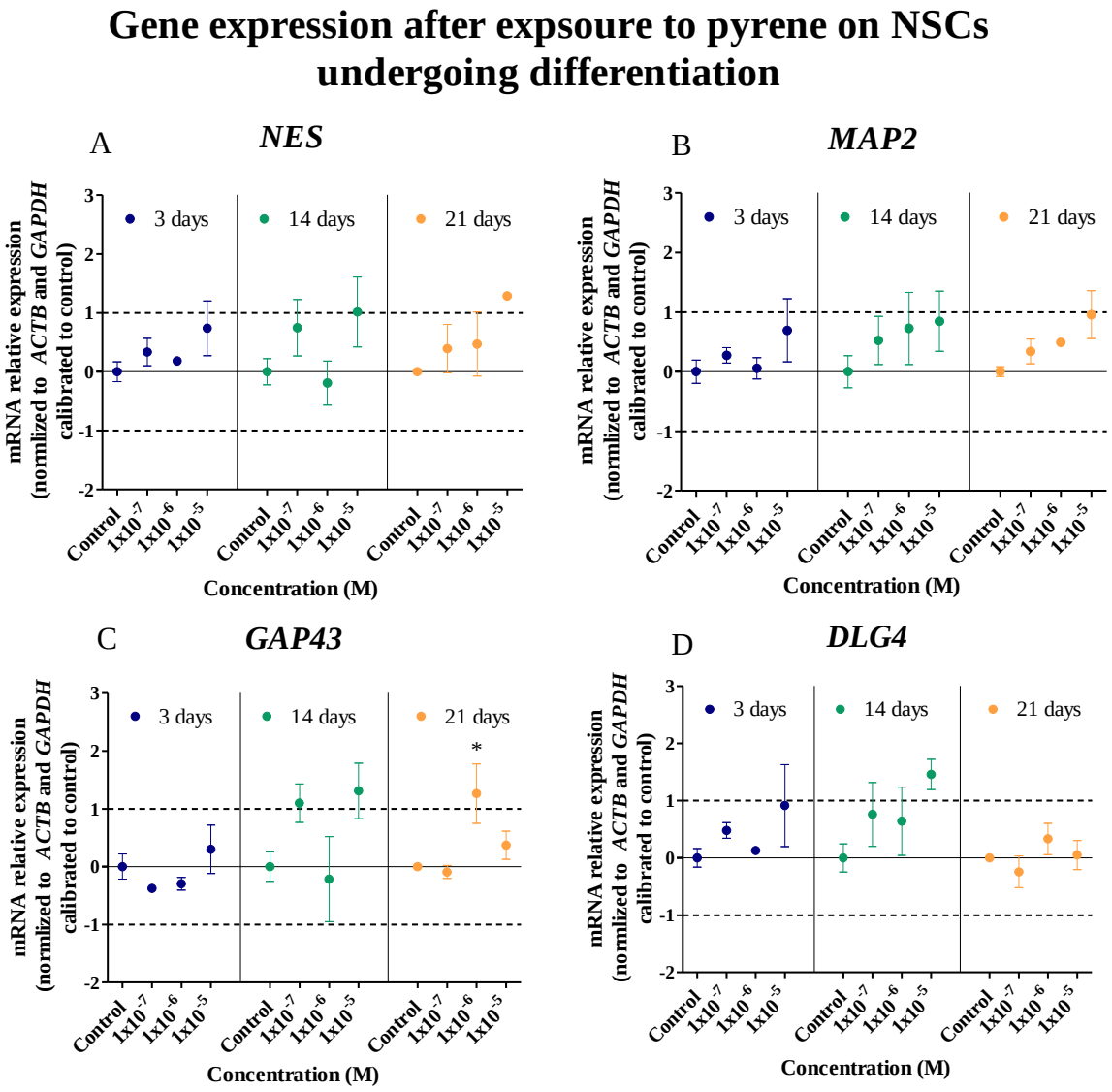

Figure 22: ***Effects on gene expression of four genes related to neurodevelopment after exposure to pyrene on NSCs undergoing differentiation for 3 (blue), 14 (green) and 21 (orange) days****. NSCs were exposed to three concentrations ($1x10^{-5}$, $1x10^{-6}$ and $1x10^{-7}$ M) of pyrene and 0.1% DMSO (solvent control). Gene expression of A: NES, B: MAP2, C: GAP43 and D: DLG4. All genes were normalized to reference genes ACTB and GAPDH and calibrated to solvent control (represented by line) for respective time points (ΔΔCt method). Data are presented as mean ± S.E.M. of three independent experiments with three technical replicates. Significant difference relative to control, * $p < 0.05$ determined with Kruskal Wallis with the non-parametric test Steel method.*

4.4.4 *AHR* gene expression after exposure to polycyclic aromatic hydrocarbons

AHR gene expression of NSCs exposed to three concentrations of B[a]P, β-NF, and pyrene undergoing differentiation for 3, 14, and 21 days are shown in Figure 23. mRNA expression is normalized to the reference genes *ACTB* and *GAPDH* and calibrated to control. There were no statistically significant alterations in the *AHR* gene expression for either B[a]P (A), β-NF (B), or pyrene (C) for any concentration or time points investigated. Although not significant, a 2-fold change was observed after 14 days of exposure to $1x10^{-5}$ M of B[a]P (A). The PAH B[a]P seemed to induce a minor concentration-dependent increase after 21 days of exposure. A minor

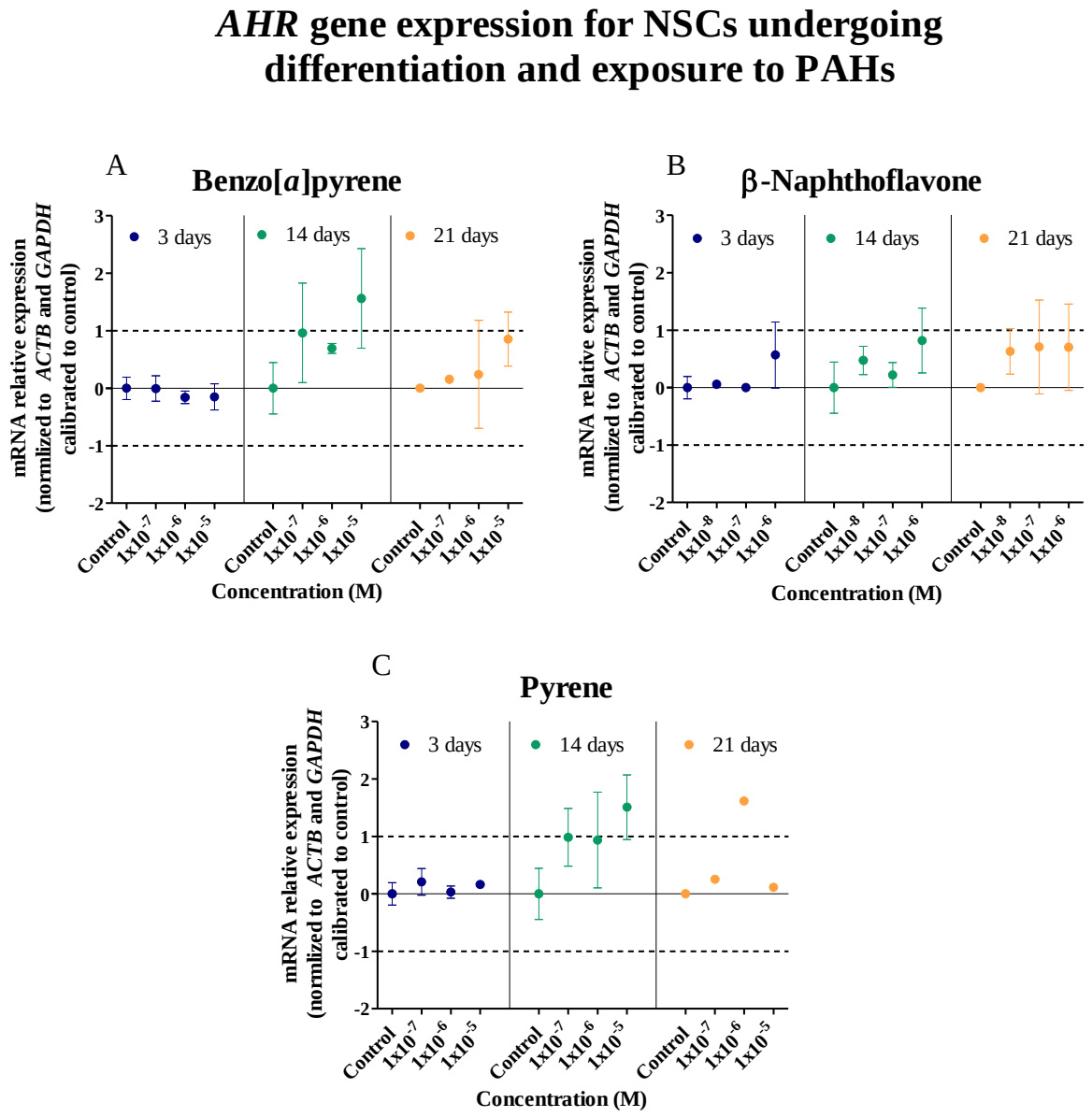

Figure 23: ***mRNA relative expression of AHR after exposure to PAHs for NSCs undergoing differentiation for 3 (blue), 14 (green) and 21 days (orange).*** *NSCs were exposed to three concentration of each PAH and 0.1 % DMSO (solvent control). AHR gene expression was normalized to ACTB and GAPDH and calibrated to control (represented by line) for respective time points (ΔΔCt method). All data are presented as mean ± S.E.M. of three independent experiments. Significant difference relative to control, * $p < 0.05$ determined with Kruskal Wallis with the non-parametric test Steel method.*

upregulation was seen for $1x10^{-6}$ M after 3 days, followed by an overall upregulation after 21 days for all concentrations after exposure to β-NF (B). Pyrene seemed to cause a concentration-dependent increase after 14 days of exposure, with a 2-fold change for the highest concentration ($1x10^{-5}$ M) tested (C).

4.5 Immunocytochemistry of protein markers related to neurodevelopment

Immunocytochemistry with high content imaging was performed to get a qualitative visualization of protein markers related to neurodevelopment and morphology. Immunocytochemical images are visualized in Figure 24 and 26 for NSCs undergoing differentiation for 14 and 21 days with or without exposure to the PAHs.

The NSCs were stained with antibodies, Ki67, nestin, MAP2, SYP, PSD95, TH, and GABA, as well as DAPI used for counterstaining of the cell nucleus. The images are merged by using several antibodies per well.

After 14 and 21 days of differentiation with or without exposure to the PAHs, B[a]P, β-NF and pyrene, cells were stained with antibodies for visualization. A illustrated the protein markers were detected in both control and exposed cells, no apparent difference was seen. The visualization of the neural stem cells marker, nestin (white) is localized in the cytoskeleton found and widely distributed in the axons, Ki67 (red) a cell cycle marker, located in the cell nuclei, and DAPI (blue) for the cell nucleus, used for counterstaining the cells (Figure 24 and 26 A). Neurons and neurite outgrowth were visualized with an expression of microtubule associated protein 2 (MAP2, green) widely distributed in the cell body and dendrites (Figure 24 and 26 B). Synaptogenesis-related proteins were envisioned with synaptophysin (SYP, white) and post-synaptic density protein 95 (PSD95, red) (Figure 24 and Figure 26 B). The presence of dopaminergic and GABAergic neurons was confirmed with the expression of tyrosine hydroxylase (TH, white) and gamma-aminobutyric acid (GABA, red) (Figure 24 and Figure 26 C).

A minor visible increase in the intensity of nestin together with Ki67 can be observed for all PAHs tested compared to control (Figure 24 A). MAP2 seemed to be observed with an increase in intensity upon exposure to pyrene when comparing to control (Figure 24 B and C). β-NF seemed to induce a visible increase in intensity for the dopaminergic marker, TH compared to control (C). However, no apparent visible difference was seen between control and exposed

cells in protein expression related to synaptogenesis and neural differentiation for the other PAHs following 14 days of differentiation (B and C).

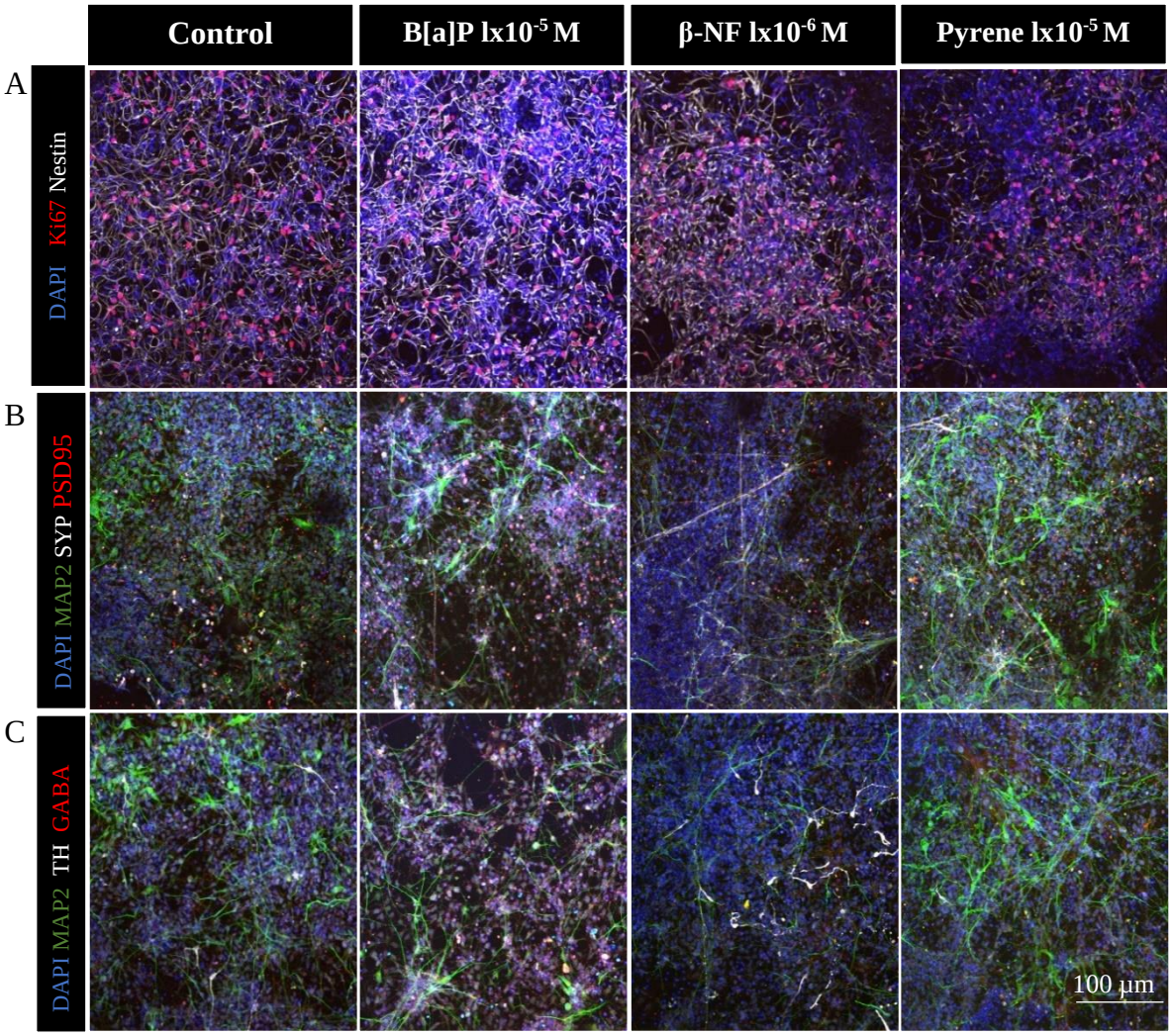

Figure 24: ***Visualization of qualitative immunocytochemical images of protein markers related to differentiation, neurite outgrowth and synaptogenesis of NSCs undergoing differentiation for 14 days****. Cells were stained for nestin (white) and Ki67 (red) (A), MAP2 (green), SYP (white), PSD95 (red) (B), MAP2 (green), TH (white) and GABA (red) (C) in NSCs undergoing differentiation with or without exposure to B[a]P (1x10^{-5} M), β-NF (1x10^{-6} M) and pyrene (1x10^{-5} M) for 14 days. DAPI (blue) was used for visualization of the nucleus. Scale bare is set to 100 µm.*

Upon differentiation for 21 days with or without exposure, no apparent visible difference was seen for nestin and Ki67 expression when compared to control (Figure 26 A). A visible difference in intensity of MAP2 was observed after exposure to pyrene (B). No other protein markers were observed different expressed after exposure to the PAHs compared to control. Staining of GABAergic neurons (GABA) and the post-synaptic protein (PSD95) resulted in weak staining for both exposed and unexposed cells (control). The weak staining is exemplified in unexposed cells shown in Figure 25.

When comparing unexposed cells for 14 and 21 days of differentiation a visible increase in MAP2 can be observed from 14 to 21 days. The presence of nestin is confirming the presence of the NSCs even up to 21 days of differentiation (Figure 26 A). The observed visible increase in the intensity of MAP2 upon pyrene exposure for 14 days was followed by a further observed increase after 21 days of exposure. No apparent difference was seen between the other PAHs tested from 14 to 21 days of exposure.

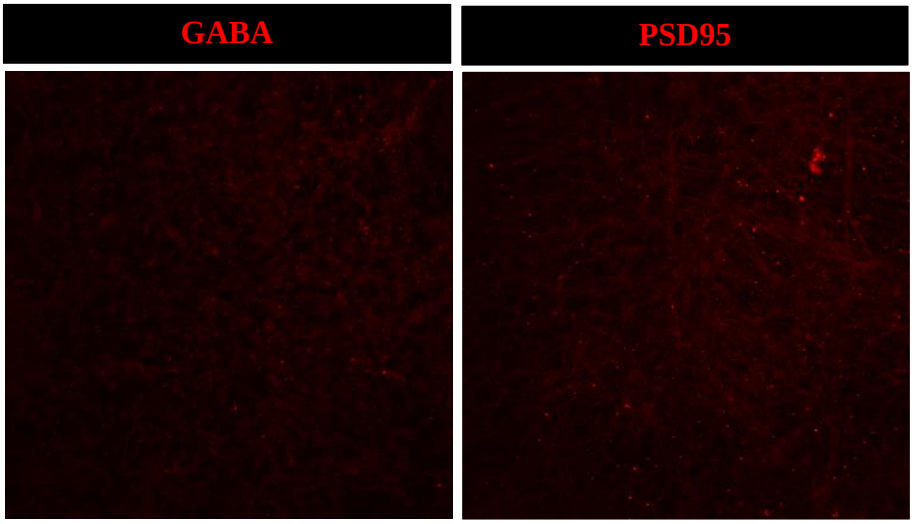

Figure 25: ***Visualization of immunocytochemistry staining for GABA and PSD95 in NSCs undergoing differentiation for 21 days****. Poor staining of the marker for GABAergic neurons (GABA) and the synaptogenese related protein (PSD95). Scale bar is set to 100 µm.*

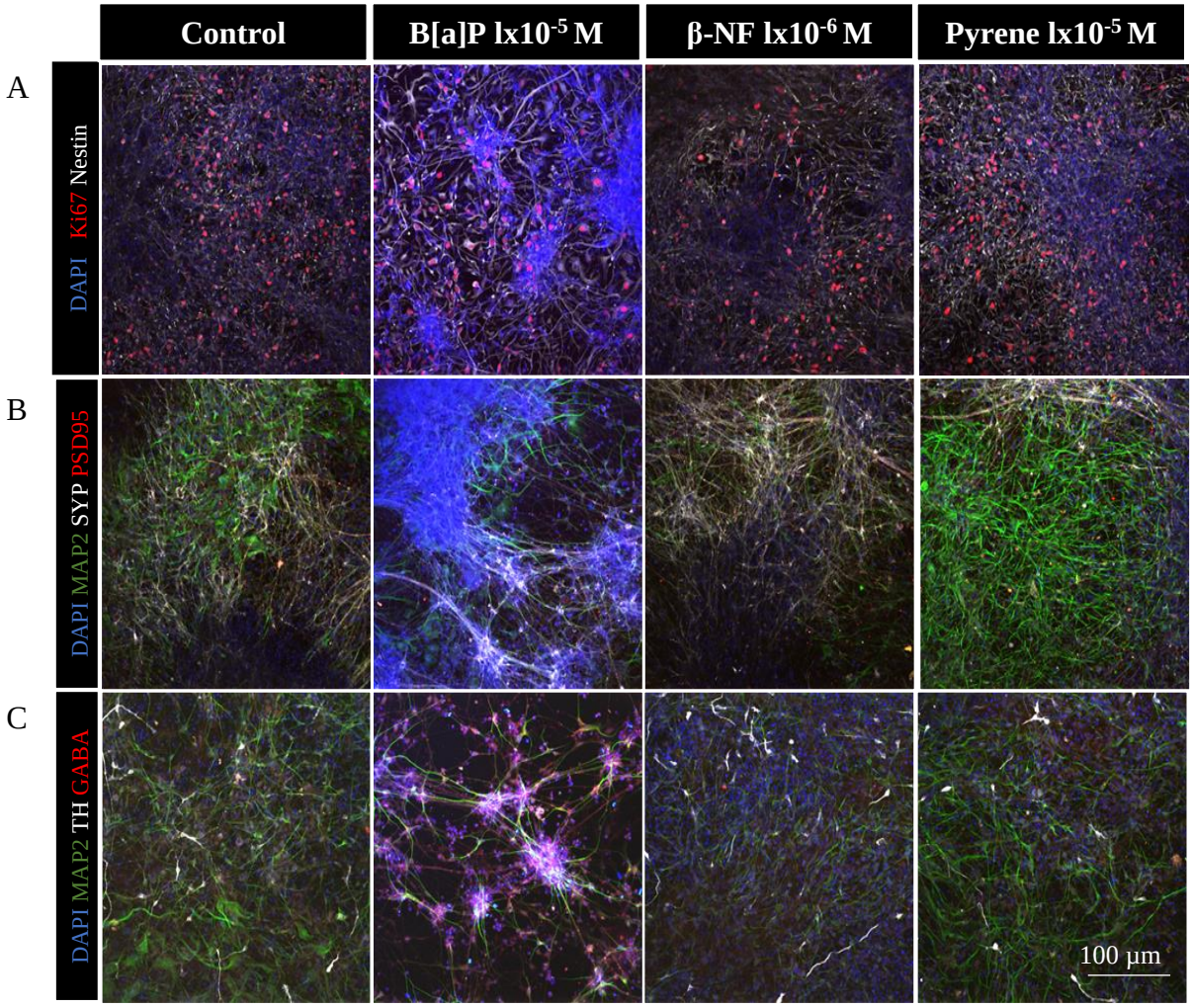

Figure 26: ***Visualization of qualitative immunocytochemical images of protein markers related to differentiation, neurite outgrowth and synaptogenesis of NSCs undergoing differentiation for 21 days.*** *Cells were stained for nestin (white) and Ki67 (red) (A), MAP2 (green), SYP (white), PSD95 (red) (B), MAP2 (green), TH (white) and GABA (red) (C) in NSCs undergoing differentiation with or without exposure to B[a]P (1x10^{-5} M), β-NF (1x10^{-6} M) and pyrene (1x10^{-5} M) for 21 days. DAPI (blue) was used for visualization of the nucleus. Scale bare is set to 100 µm.*

5 DISCUSSION

Accumulating evidence of both animal studies and epidemiologic research point in the direction that PAH exposure can lead to adverse effects on the developing brain (20, 22, 23, 65-68). However, the neurodevelopmental processes and mechanisms underlying the potential neurodevelopmental toxicity of pre and/or post-natal PAH exposure are not fully understood. The overall goal of this master thesis was to elucidate how the three selected PAHs (B[a]P, β-NF, and pyrene) affected human NSCs undergoing differentiation to a complex neurite network, a differentiation process which previously has been described in other laboratories by microscopic characterization, microelectrode array (MEA), and expression of genes and protein markers (5, 77, 81)

We report that the NSCs differentiated into a mixed culture and formed complex networks, with an increased expression of *MAP2* and *AHR*, which are, commonly used markers of differentiation and neurite outgrowth (5, 46, 81). The most interesting finding was that both β-NF and pyrene at low concentrations showed a marked upregulation of mitochondrial activity at the early stages of differentiation, most probably reflecting an increased number of cells. At higher non-physiological concentrations increased toxicity at the longest exposure time(s) could be seen, with B[a]P as the most potent. Gene expression analysis after exposure to the PAHs releveled only minor changes, however, some concentration-dependent increases could be observed. A few genes showed a change close to or above 2-fold change, and only the expression of one gene (*GAP43*), a neurite outgrowth marker, was significantly different from control. For most genes, a 2-fold change is the lowest level considered to be biological relevant, although there are exceptions and lower trends could also be of biological importance (117). Immunocytochemical visualization of protein markers showed a qualitative protein expression, which is in line with a study on the NSC model (81). NSCs derived from hiPSC is a relevant model for studying DNT effects in humans, this is due to that the model does not exhibit tumor-growth properties that may affect the responses upon chemical exposure. The model is suitable to test DNT effects because they can mimic key neurodevelopmental processes which are critical for normal human brain development, challenges with interspecies differences and extrapolation are therefore not relevant. The presence of neurons possessing forebrain and cortical-like features when undergoing differentiation makes it suitable to investigate perturbation related to cognitive impairments observed as an adverse outcome in epidemiological studies (2, 76).

Our results suggest some differences regarding effects on cell viability between the different PAHs, with pyrene having effects on viability at rather low concentrations. Most PAHs cross the placenta due to their lipophilic solubility and possibly accumulate in the fetal brain, since the BBB are not fully developed before 6 months after birth, and most of the fetal life is occurring with an immature BBB (38, 118). Inhaled PAHs metabolize to a smaller degree and will therefore reach the fetus unmetabolized. Both high and low molecular PAHs are found in the air. Pyrene is the predominant compound found in the placenta and maternal umbilical cord serum due to high exposure and is, therefore, likely to transfer in larger amounts from the mother to the fetus (38). As pyrene affects viability at early differentiation steps, while AhR is expressed at the later in cellular development, the mechanisms involved are still uncertain.

5.1 Neural stem cells differentiated into a mixed culture as expected

The culture of NSCs was examined using phase-contrast microcopy when undergoing differentiation, as seen in (Figure 9). This was done to ensure that the cells in the culture developed as expected and to ensure reliable results with this NSC model. Only a minor observable change was seen after differentiation for 3 days, a complex neurite network combined with the dead, possibly apoptotic cells appears upon further differentiation which is a normal process. The appearance corresponds nicely with phase-contrast images previously published in a study at EC-JRC (83). Apoptosis is a normal process that occurs during neurodevelopment and is discarded by immune cells *in vivo*. Since this mechanism cannot be repeated *in vitro* in our cell system, apoptotic cells are visualized as bright cells attached to living cells. Thus, the NSCs seemed to differentiate as expected and it was considered as a reliable model for further experiments.

5.2 Optimization of Alamar Blue assay

Optimization of Alamar Blue™ assay was done to assess the impact of incubation time, substrate concentration, and cell densities with glycidamide as the test substance. All conclusions are based on visual inspection of the data only. The optimization project`s conclusion is mainly based on the findings of the supervisor`s validation at NIPH. This is due to differences in cell densities caused by inexperience with cell cultivation, which resulted in less accurate student project performance.

After 3-4 h of incubation with Alamar Blue™, the development of fluorescence measured by mitochondrial dehydrogenase activity becomes stable for every cell density and time-point tested (Figure 12 B and D). The various cell densities were used to investigate differences in confluence during an experiment. When seeding density of 7000 cells/well were allowed to proliferate for 1 day, it results in the recommended cell density for experiments with the NSC model (5), as well as 14000 cells/well allowed to proliferate for 2 days will represent a nearly confluent well. An observable difference was seen after 1 h incubation between 7000 and 14000 cells/well with a 1:10 dilution of Alamar Blue™. Measurement of cell viability after 1 h incubation could therefore result in a false difference in viability caused by the difference in cell density. Thus, an incubation time of 3-4 h was chosen for further experiments which are sensitive enough to detect changes regardless of cell density.

Shorter exposure (1 day) to $1x10^{-3}$ M glycidamide affected the cells negatively but did not result in complete cell death, as seen in Figure 11 and 12, and verified by visual inspection of cells after Alamar Blue™. Longer periods of exposure (3 and 5 days) result in fairly complete cell death (80%) for all cell densities (Figure 12 B and D). Although, less cell death is observed for the higher cell densities (14000 cell/well) (Figure 12 C). This correlates with findings found by Wu et al. (2020), who found a negative correlation between high cell densities and low cytotoxicity (119). Based on these findings a hypothesis can be that high cell densities can protect against exposure to chemicals up to a certain point.

The larger difference between control and unexposed cells in the reduction of resazurin for 1:6 dilution and 1:10 dilution (Figure 10), were reduced and almost negligible when normalizing the exposed cells to control Figure 11. While the reduction of resazurin between control and exposed cells using 1:6 dilution in the student project was larger than using the 1:10 dilution for cells, this was not the case in the experiment for the validation performed by NIPH (Figure 12). Based on this and the recommendation in the protocol 1:10 dilution was concluded to be adequately sensitive for our cell model, clearly differentiating between exposed and unexposed cells. An Alamar Blue™ dilution of 1:10 and incubation time of 3-4 h was chosen for further experiments. The conclusion from the optimization experiment is based on the results obtained by the NIPH optimization.

5.3 Effects of polycyclic aromatic hydrocarbons on cell viability

Cell viability was investigated to assess the possible impact of the PAHs (B[a]P, β-NF, and pyrene) on NSCs undergoing differentiation and was measured with Alamar Blue™. Cell injury/death is an important key event in the AOP) framework (94). As most of the literature regarding PAHs is focused on the carcinogenic B[a]P forming highly reactive metabolites (30), we also examined two other PAHs. β-NF was chosen due to its strong agonist properties to AhR receptor through the classic-genomic pathway and pyrene was chosen as an activator of the AhR by non-genomic pathway. Notably, AhR is a receptor suggested to be important in neurodevelopment (46). PAHs are abundant components in air pollution (9) and the fetus can be exposed via the mother.

Most, interestingly, low concentrations of the PAHs after 1 and 3 days of exposure seemed to cause an increase in cell viability as judged by Alamar Blue assay (Figure 15-17 A and B). The increase was not observed as constant for all concentrations of B[a]P (Figure 15 A and B) and was more marked following β-NF (Figure 16 A and B) and pyrene exposure. This suggests that the increased values seen were mediated by receptors and not due to reactive metabolites. High concentrations of the B[a]P and β-NF resulted in a decrease in cell viability with B[a]P being the most cytotoxic PAHs tested. Whiteout knowing the level of CYP-enzymes, it is difficult to know if the toxicity is due to reactive metabolites, receptor binding, or possibly unspecific effects on cellular membranes due to lipophilicity.

Alamar Blue™ measures metabolic activity in living cells by fluorescence, and the observed effects by this assay can therefore be many. The increase in mitochondrial dehydrogenase activity may be due to an increased reduction of resazurin to resorufin by an increase in metabolic/mitochondrial activity triggered by the PAHs. The increase seen can also be due to an increase in cell number, due to reduced apoptosis, increased proliferation, and/or reduced differentiation. The decrease observed in mitochondrial dehydrogenase activity, may be caused by cell death or cells with reduced metabolic activity, as the assay does not separate dead cells from metabolic inactive cells (101).

Slotkin and Seilder (2009) found an increase in cell number after exposing PC12 cells undergoing differentiation to B[a]P (120). They suggested that the increase could be a delay in the transition from cell replication to neurodifferentiation. This was confirmed with an impairment in differentiation markers and a reduced cell size. This increase was not found in proliferating PC12 cells (126). An increase upon exposure to β-NF was also seen in human

neuroblastoma (SH-SY5Y) cells, however, the increase was not further investigated (123). The increase in mitochondrial dehydrogenase activity observed in our study after 1 and 3 days of exposure, most likely could be due to a similar increase in cell number and/or an impairment in the differentiation process implicating an increased proliferation of the NSCs. If so, this could be an interesting finding, which could be further investigated. If the increase in mitochondrial dehydrogenase activity is due to an increase of living cells, the effects on neurodevelopment will be determined by which cellular process is disturbed. An increase in living cells may affect neurodevelopment, an unbalanced cell proliferation/apoptosis may affect the normal development of the nervous system (121). An excess of neurons has been associated with neurodevelopment disorders like ASD. In a study comparing children with ASD, 67% more neurons were found in the prefrontal cortex compared to children without the disease (122). To confirm the increase in cell number, cell counting and DAPI staining with immunocytochemistry should be performed. However, the increase in cell viability observed could also be a response to oxidative stress elicited by the chemicals upon the metabolism of the PAHs by bioactivation with CYP-enzymes (44). This bioactivation can cause upregulation in mitochondrial activity. CYP-enzymes has been detected in the NSC model, although first at later differentiation steps (77).

Mitochondria are essential for cell viability and cell function, as their main roles are ATP production, metabolism of ROS, regulation of Ca^{2+}, and apoptosis (101, 102). Mitochondria are thought to play an important role in the development of the nervous system because key processes like NSC proliferation, neurite outgrowth, and synaptic activity require a high amount of energy, and the mitochondria fuel these processes (123). Neurons are especially sensitive to metabolic, distributional, and structural changes of the mitochondria. Changes in the mitochondria can affect synapses that can lead to impairment of memory (124). Defective mitochondria can enhance the overproduction of ROS and lead to damage within the cell and cell death. Neurons are cells with high energy requirements (125) and mitochondrial impairment has been suggested to play a central role in both B[a]P and β-NF induced cytotoxicity (126, 127). The mitochondria also play an important role in the regulation of various apoptotic processes including those induced by toxicants (123). It is found direct evidence that B[a]P induces apoptotic death of proliferating cerebral neurons, by upregulation of pro-apoptotic members (126) and an increase in ROS production upon exposure (125). Exposure to rat cortical neurons enhanced the caspase-3 activity and induced cytotoxicity to the cells after β-NF exposure (127). Similarly, the same decrease in cell viability was observed in

a study with proliferating primary glioblastoma cells (128). Excessive apoptosis in childhood has been associated with ASD, and an increase in apoptosis could impair neurodevelopment and possibly lead to ASD (129). In our study, however, the decrease in cell viability was first seen after long-term exposure to concentrations probably not relevant for human exposure. It is tempting to speculate that the decrease in mitochondrial dehydrogenase activity is due to an excess of apoptosis induced by the PAHs, and if higher concentrations had been included, we would probably have observed more cell death.

Our results indicate that the more mature cells are more resistant to the PAHs which by extending the exposure time, the observed increase in cell viability almost reverted to control levels for the lowest concentrations. Post-mitotic neurons possibly have better detoxification mechanisms and can therefore resist apoptotic stimuli (130). When comparing cells exposed for 1 day to cells exposed for 14 days, a decrease in cell viability was observed. The same concentrations inducing an increase in early differentiated cells were observed to give a decrease in more mature cells, however, this may be due to the continuous exposure for mature cells. This is in line with a study investigating methylmercury in hESC by differentiation, where they found that low concentrations were more cytotoxic to mature neurons than their unmatured counterpart (131). The PAHs are lipophilic compounds and the accumulation of PAHs is seen in fat tissue and the brain (132). The exposure regime in our cell system can mimic continuous exposure. It could therefore be hypothesized that the decrease in cell viability and the increased sensitivity for the PAHs seen in mature cells is due to the accumulation of the PAHs in the cell system. This is in line with what is reported *in vivo*, as the PAHs are lipophilic compounds they may also accumulate in the cells in particular cell and organelle membranes.

No obvious differences in cell densities were seen for any of the concentrations at any time points. It may be that the decrease seen in mitochondrial dehydrogenase activity is due to mitochondrial impairment and metabolic inactive cells. This could be due to that the decrease seen is not more than 30%. During differentiation of NSC mitochondria is been found to be prone to oxidative damage that can result in mutations. Accumulation of mutations has been found to impair NSCs ability to differentiate properly into neurons (133). Mitochondrial dysfunction is a common key event in neurotoxicity and has been linked to the key event named cell injury/death. In turn cell injury/death is a known key event in many AOPs related to neurotoxicity including impairment of important cognitive function like memory and learning (94). Mitochondrial dysfunction has been suggested to be associated with ASD (134).

5.3.1 The viability of cells was not affected by DMSO

DMSO is often used to dissolve lipophilic compounds like PAHs and pesticides for *in vitro* testing (135, 136). It is generally accepted that DMSO concentration ≤ 0.1% is harmless for the cells (137) and 0.1% DMSO has been used on the cell model in previous experiments conducted with this model (81, 83, 138). This is in line with our result where DMSO did not affect the cell viability when compared to cell control (only ND medium) for all time points. No morphological change was seen when examined in the microscope (Figure 14). Higher concentrations of DMSO have been shown to cause a reduced number of neurites, nuclear fragmentation, cell number, and survival (137). DMSO (0.1 %) as solvent control was used for all experiments with cells on PAH exposure in this thesis.

5.4 Background for concentrations chosen for mechanistic studies

There is a need for assessment of DNT markers after exposure to environmental contaminants (i.eg PAH exposure) with concentrations mimicking the real-life exposure in a model reflecting early brain development in humans since adverse effects after B[a]P exposure are associated with lower doses than cancer endpoints (30). Several epidemiological studies associate PAH exposure with adverse effects on neurodevelopment (20, 22, 23, 65-68). Daily inhalation of B[a]P is estimated to 0.15-32 ng/day, however higher doses when exposed to indoor sources such as cooking can be observed. The PAHs have been shown to have a high placental transfer (38) and the fetus is unprotected due to the immature BBB (118). The exposure could continue post-natal as well, since PAHs are found in breast milk (42). However, the extrapolation of *in vitro* concentrations based on *in vivo* studies is difficult (and out of scope for this master thesis) and therefore concentrations selected for further mechanistic studies were based on the impact of the PAHs on cell viability. The concentrations chosen were mainly based on the results from cell viability after B[a]P exposure (Figure 15) due to the extensive literature on this PAH, where continuous exposure caused a larger decrease in cell viability. The highest concentration selected was, therefore, $1x10^{-5}$ M for B[a]P and pyrene because after 14 days of exposure it is determined as a low-cytotoxic concentration with no more than a 30% decrease in cell viability for B[a]P, and it will give a high enough RNA output. For intermediate and lowest concentration, $1x10^{-6}$ and $1x10^{-7}$ M was selected, respectively for B[a]P and pyrene. The same concentrations were not selected for β-NF, due to observation of precipitation in the culture medium after exposure in the cell viability experiment. Therefore, for β-NF exposure concentration of $1x10^{-6}$, $1x10^{-7}$, and $1x10^{-8}$ M were chosen.

5.5 Effects of polycyclic aromatic hydrocarbons on gene expression of neural markers

As a part of an establishing project of the NSC model at NIPH gene expression of *MAP2* and *AHR* was assessed for NSCs undergoing differentiation for up to 28 days. The marker for mature neurons, *MAP2* showed a progressive increase upon differentiation as expected with a statistically significantly 2-fold change after 3 days of differentiation followed by a 4-fold change after 28 days of differentiation compared to their undifferentiated counterpart (Figure 19 A). The AhR has been shown to be an important regulator for neural differentiation in different models (46). The expression of the *AHR* gene indicated a time-dependent upregulation on NSCs undergoing differentiation for 28 days (Figure 19 B). These results indicate that the model developed and differentiated as expected and this supports that the gene expression results are trustworthy.

We analyzed the gene expression of markers related to neurodevelopment, such as differentiation, neurite outgrowth, and synaptogenesis. The gene expression of *GAP43* was the only gene found statistically significantly upregulated compared to control for all three PAHs. Effects of low and non-cytotoxic concentrations showed only minor effects with some trends close to or ± 2-fold change (Figure 20-23). It should be noted that variation in the dataset and between the experiments was observed, however, there are some trends that possibly could indicate biological relevance. The overall effects seen were most prominent for long-term exposure, which may indicate that the chemicals are more harmful to continuous exposure during differentiation into mature neurons.

A trend indicating an upregulation of the neural stem cell marker, *NES*, after exposure to β-NF and was observed for all time points, with a 2-fold increase for the highest concentrations after 21 days of exposure (Figure 21 and 22 A). The trend towards an increase in *NES* can indicate a higher presence of NSCs this could be in concordance with the increase seen in mitochondrial dehydrogenase activity judged by the Alamar Blue assay for β-NF and pyrene (Figure 16 and 17). The study conducted by Slotkin and Seilder (2009), support our suggestion that the increase could be due to an increase in cell number, possibly of immature cells due to an increase in proliferation of NSCs (120). On the contrary, this study was elucidating B[a]P, and a concentration-dependent upregulation was only seen after 14 days. It could be that other PAHs like β-NF and pyrene can provoke the same changes upon exposure. An increase in nestin expression has also be associated with brain injury in rats (139), which may indicate that the

PAHs cause damage which further gives a tendency toward upregulation of *NES* by repairing the damage, although further research is needed to confirm this.

The gene expression of *MAP*, encoding a microtubule associated protein, mainly expressed in neurons and a marker for dendrites and neurite outgrowth (85) showed a trend towards an upregulation upon exposure. The trend was most apparent for β-NF (Figure 21 B), and pyrene was the only PAH causing a trend toward an upregulation in concentration and time-dependent manner (Figure 22 B). The increase in *MAP2* is associated with differentiation (85). However, the increase seen after exposure could be due to an increase in cell number which correlates with the increase found for *NES* after exposure to β-NF and pyrene in concordance with the cell viability measurements.

A trend indicating upregulation of *GAP43*, a growth-associated protein and a marker for neurite outgrowth, found on the axonal terminals (86), was observed for all PAHs which was most prominent after 14 and 21 days of exposure (Figure 20-22 C). The upregulation was not seen as prominent for pyrene, as for B[a]P and β-NF. A correlation between inhibition of neurite outgrowth and induction of *GAP43* has been reported, with an upregulation of *GAP43* after exposure of pesticides to PC12 cells undergoing differentiation (140). As mentioned, pesticides are also chemicals possessing DNT properties (27). *GAP43* mRNA expression was by this study reported to be a relevant DNT endpoint by correlation with expressional changes to neurite outgrowth (140). In contrast, a study on neurite outgrowth found only minimal effects upon exposure for 72h to PAHs, but they suggested that it could be due to poor metabolism capacity in the cell system or short time exposure (141). *GAP43* is highly expressed during the early stages of synaptogenesis and neurite outgrowth, as well as neurotransmitter release. *GAP43* is also expressed when neuronal axons are damage during brain development or regeneration (86). One explanation could be that the upregulation seen in our study is due to, that the axons are damaged by the exposure to the PAHs, and upregulation of *GAP43* is induced. However, to confirm this more research is needed.

After NSCs undergoing differentiation to 21 days, an overall increase was observed for all time points for the synaptogenesis-related gene *DLG4* after exposure to β-NF (Figure 21 D). The increase was also seen prominent after 14 days for B[a]P (Figure 20 D) and pyrene (Figure 22 D). Mutations in the protein PSD95 coded by the gene *DLG4* have been associated with susceptibility for ASD and schizophrenia (92). It is thought that overexpression of PSD95 is shifting the expression of NLG1 another scaffolding protein, from inhibitory to excitatory

synapses, that may give a decrease in inhibitory synapses and that the ratio between inhibitory and exhibitory synapses gets disturbed (71). This can indicate impairment in synaptogenesis and the neurons ability to communicate with other brain regions. An increased number of dendritic spines can occur with overexpression of PSD95 and lead to altered synaptic transmission and the cognitive impairment seen in patients with ASD (92). Our study indicates an upregulation of *DLG4*, although not significant, but it seems like a trend. It is therefore alluring to suggest that if we had calculated the PSD95 and SYP protein expression with high content imaging it could have confirmed altered expression of PSD95.

Over 80% of the genes which play an important role in early neurodevelopmental differentiation and function, are high-risk genes associated with ASD. These are genes particularly involved in neurite outgrowth and synapse formation (142). The indication of upregulation in genes related to these processes could explain an increased differentiation induced by the PAHs which could alter the differentiation process and could by suggestion possibly be implicated in the ASD pathology.

5.5.1 *AHR* gene expression

AhR activation mediates the expression of *CYP* genes related to metabolism, detoxification, and apoptosis (46). AhR activation has been suggested to be one of the etiological mechanisms essential for PAHs effects (143), where they are acting as AhR ligand. PAHs can have a toxic mode of action by activating the AhR where this receptor plays an important role in the metabolism of the PAHs (46). If the exposure to AhR ligands occurs at a critical neurodevelopmental window, interference with the AhR function may impair neurodevelopment (30). This is supported by evidence were overactivation of AhR in neuroblastoma cells leads to uncontrolled neural differentiation such uncontrolled differentiation may disrupt the strict-controlled neurodevelopment (48).

The expression of the *AHR* gene showed a time-dependent upregulation of NSC undergoing differentiation for 28 days (Figure 19 B). This is in line with what has been found in the NSC model in an earlier study (138). At early time points, there is a low expression of the *AHR*, which is in line with our results showing a lack of increase after 3 days of exposure (Figure 23). The lack of increase after 3 days of exposure and the 2-fold upregulation for the highest concentrations after 14 days suggest that the induction of AhR mediated toxicity induced by PAHs occur at a later stage in the differentiation process. A study by Davidsen and Lauvås et al. (2021) observed the same when testing *AHR* gene expression after exposure to POPs for the

same time-points, and they suggested the same (138). This may reflect changes found related to neurodevelopment. To further examine the effects of the activation of the AhR, genes activated upon AhR ligand binding should be investigated, *CYP1A1* is a gene target for the AhR (46) and is present in the NSC model (77). By investigating *CYP1A1* or other AhR targets genes a confirmation of the AhR activation could be done and elicit the AhR agonist properties. β-NF agonist properties may be reflected by the overall upregulation close to 2-fold for all concentrations (Figure 23 B) but should be further investigated to confirm and may use higher concentrations.

The decrease in mitochondrial dehydrogenase activity upon exposure to $1x10^{-5}$ M of B[a]P for 14 and 21 days (Figure 15 C and D), corresponds with the upregulation of *AHR* (Figure 23 A) These results are in line with that *AHR* and *CYP1A1* activation are reported to correlate with neurotoxicity from these compounds (46). It can therefore be suggested that the non-decrease in cell viability seen after 1 and 3 days of exposure (Figure 15 A and B) is due to low expression or null expression of the AhR at early time points and can also be explained by the and lower Nrf2/ARE signaling pathway activation (81) than in the more differentiated NSC culture.

The *NMDA* gene and function are shown to be altered upon B[a]P exposure in rodents (144-147). There are currently no data available suggesting that the NMDA is affected upon B[a]P exposure in humans (30). The AOP framework may be used to interpret the current finding by highlighting the various key event. The binding of ligand such as PAHs to the AhR may lead to changes in the gene regulation of NMDA receptor subunits and disturbed Ca^{2+} homeostasis, which may impair the BDNF signaling and lead to memory and learning deficits (30). Altered function of the NMDA may give an increase in BDNF which may induce the presynaptic release of glutamate, cell injury, dendritic aberrations, and further upregulation of synaptogenesis. This can further lead to an increase in neural network function that is affecting learning and memory as seen in epidemiological studies (148). This could possibly and be tempting to speculate that the upregulation seen in *GAP43* together with the minor, not significant upregulations seen in *DLG4* and *MAP2* could be of relevance. However, more research and more genes need to be investigated to interpret this AOP.

5.5.2 Evaluation of gene expression

Earlier studies have indicated that mRNA expression is a relevant tool for investigating DNT endpoints in key neurodevelopment processes recapitulated in the NSC model after exposure to chemicals with the potential to induce DNT effects (149).

When assessing biological relevance to results obtained from gene expression it is common to use the 2-fold change and/or p-value thresholds (117). It has been implicated that small changes in gene expression, under 2-fold change, also could be of biological relevance and should not be left unnoticed. Chemical exposure is particularly harmful to the developing brain and the CNS (27), and small alternations in gene expression may cause harmful effects and therefore be of importance. The dataset has a lot of variances and the variability is quite high. To correct for these variabilities the experiments could have been performed with a higher number of replicates. More replicates could have resulted in statistically significant experiments that showed close to or a 2-fold change in gene expression.

It could also be speculated that the critical windows for PAH exposure are other time points and that alterations in gene expression could occur at other time points than tested in this experiment. The chemical exposure was added to the medium at the earliest 2 days before collecting the sample for gene expression. It may therefore be suggested that if the alternations in gene expression were transient, it has not been detected with our experimental setup. To detect these possible changes, gene expression should be performed shortly after last exposure on NSCs undergoing differentiation. Even though no remarkable change was found for the genes analyzed in this experiment, it cannot be ruled out that other genes related to neurodevelopmental processes could be changed due to exposure to the PAHs.

5.6 Immunocytochemical visualization of protein markers related to neurodevelopment

For immunocytochemistry, different protein markers for neurodevelopment were selected to be used for staining, and later analysis with high content imaging. The aim was to determine whether the markers gave changes related to neurodevelopment and morphology after exposure to the PAHs. The markers were chosen based on their relevance to neurodevelopment with the characterization of different subtypes and synaptogenesis. As described in 1.5.1 Pistollato et al. (2017) have characterized these markers in the NSC model (5, 81). Results obtained in our study were only qualitative and should be accompanied by quantitative analysis. Quantitative analysis is a complicated analysis with algorithms, and such a method first needs to be optimized for the NSC model. This analysis is currently under development at The Norwegian Radium hospital in a collaboration project with the NIPH and therefore only qualitative images

were obtained for this thesis. The images obtained in this master project are supposed to be used for quantitative analysis when the analysis is optimized and developed.

NSCs undergoing differentiation for 14 and 21 days with or without exposure, are shown in Figure 24 and Figure 26. The DAPI staining confirmed the presence of cells and MAP2 confirmed that the cells detected were neurons. The high presence of nestin and the cell cycle marker, Ki67 indicate a high proportion of NSCs still dividing after 21 days of differentiation (Figure 26 A). Nevertheless, the observed presence of dopaminergic, synaptogenesis-related proteins and neurite formation by neurite outgrowth indicate that the NSCs have differentiated into more mature neurons and different subpopulations of neurons. This is in accordance with the previous characterization of the NSCs undergoing differentiation, showing a decent proportion of NSCs as well as GABAergic, glutamatergic, dopaminergic neurons, and glial cells present after 21 days of differentiation, however, user-dependent variability and passage differences may be observed (5). A noticeable difference in the complexity of network formations can be seen between NSCs differentiating for 14 and 21 days (Figure 24 and 26 B and C). These observations are in line with the previous characterization of the NSC model, where a detectable difference in protein expression of markers related to differentiation neurite outgrowth and synaptogenesis between 14 and 21 days of differentiation were determined (81).

It is challenging to observe differences between exposed and unexposed cells in the images with the naked eye. The observed differences in intensity could be explained by how qualitative images are produced. Each image is presented as one Z-section of the differentiated NSCs in one well. As a result, the images may not necessarily be taken in the same cellular plane. A difference in protein expression could therefore be misinterpreted due to differences in how the images are taken. It could therefore be argued that qualitative images are inconclusive and should only be taken under consideration when supported with quantitative data. The differences observed could perhaps indicate the differences expected to be found upon quantification.

The observed fluorescence intensity in MAP2 upon exposure to pyrene for 14 days (Figure 24 B and C) with a further following increase after 21 days (Figure 26 B and C), is in concordance with the tendency towards a concentration-dependent upregulation in gene expression seen for the same time points, however not significant (Figure 22 B). A more prominent difference is seen after 21 days than 14 days of differentiations. The higher presence of the neurite and dendritic marker, MAP2 can indicate differentiation, more mature neurons and an increased neurite outgrowth compared to control. A study conducting POPs found a similar increase in

MAP2+ cells after 28 days of differentiation (138). The same study also found an increase in nestin and Ki67 positive cells upon prolonged exposure indicating proliferating NSCs, a tendency of the observable increase in intensity is also seen in our study. It could therefore be postulated that micromolar concentrations of the PAHs can possibly increase the proportion of NSC proliferating cells, that pyrene possibly inhibit the normal occurring apoptosis leading to an elevated percentage of neurons and an altered differentiation.

5.6.1 Evaluation of immunocytochemistry

The methodological principle behind immunocytochemistry has several essential steps that can affect the results. The fixation and staining procedures are rough procedures for the cells, with layers of liquid and aspiration. We discovered that some cells were lost during these steps, the number of cells in each well are therefore might not be representable for the entire group.

Since the primary antibodies are recovered and re-used, this may cause weak staining when the primary antibodies are used for the second or third time. Some of the markers were stained poorly, this is especially seen for NSCs undergoing differentiation for 21 days with or without exposure (Figure 26), and exemplified in Figure 25 for GABA and PSD95, in this could be due to the reuse of primary antibodies. When staining the NSCs undergoing differentiation for 21 days, cells were stained with antibodies used two times before and this resulted in weak staining for some markers. For further studies, it will be smart to avoid the use of primary antibodies for the third time. Bleaching of the fluorochrome-conjugated secondary antibodies could also be one of the reasons for weak staining or that the secondary antibodies were not mixed well before staining. It is important to avoid light when performing this procedure, if not the secondary antibodies will not be detected and hence not the targets. Other effects that could have affected the antibodies are storage conditions and batch effects, however, there were no batch shifts during this procedure.

5.7 Weakness and limitations with the NSC model and experimental design

Testing over prolonged periods with low concentrations of the PAHs in a dynamic test system could suggest being the explanation for not observing the classical dose-response association. The NSCs undergoing differentiation to neurons and glia cells for 21 day involve changes in the proportion of different cell subpopulations over time, as described in 1.5.1. Compensatory and adaptative mechanisms, especially in long-term exposure (14 and 21 days) may therefore

play an important role. The high variability of data observed may therefore be explained by these suggestions. The observed variability was most prominent for 14 and 21 days of exposure and not so much for 3 days exposure as the cells are less differentiated. However, it is important to have dynamic systems like these, starting from NSCs proliferation to the start of synaptogenesis which reflects brain development processes occurring *in vivo.*

The gene expression analysis indicated no expression of *GFAP* (or lower LOD) in neither control nor exposed samples. GFAP has been found with a progressive increase of mRNA expression when the NSCs have been differentiated for 21 days (5, 81). This thus indicates that a better characterization of the model should have been performed before conducting the experiments performed in this thesis at the NIPH. However, GFAP protein expression has been detected with immunocytochemistry, this could suggest that the expression of GFAP in the model is low and that protein expression is the most suitable method to test for its expression. GFAP has been shown to increase during brain development and is most abundant in the human adult brain (84). A previous study done by Pistollato et al. (2017) on this model detected that astrocytes are less vulnerable to cell death than neurons induced by oxidative stress, with the expression of Nrf2 which is a protein regulating the antioxidant defense system (81). Astrocytes have different functions in the human brain, regulating the BBB, protect neurons from excessive neurotransmitters, and regulating synapse formation. Mutations in the *GFAP* gene are associated with neurodegenerative diseases and high levels of *GFAP* have been associated with damage to the CNS (84). This finding is in line is in support with the ongoing characterization project of the NSC model at the NIPH. The presence of astrocytes in the culture is essential for DNT testing and possibly normal development and function of the neurons in our culture. For further testing, it should be included other genes specific for astrocytes and protein markers to conclude whether astrocytes are present or not in the culture.

The wells in a 96-well plate are small, isolate and contain small volumes, and tend to evaporate during incubation at 37 °C. As seen by the results in Figure 18 A, the relative fluorescence was lower for the cell control placed at the edge of the plate compared to cell control placed inside the plate surrounded by other wells. This happened although they were treated and seeded out the same way. The edge effect observed can be due to evaporation of cell medium which can alter the cell viability negatively and give false negative measurements of mitochondrial activity. A study done by Lundholt et al. (2003), found a similar effect during their experiments, they hypothesized that cell attachment was inhibited due to rapid heating of the wells after seeding, and cells were observed in the periphery of the wells in the edge wells compared to

wells inside the plate (150). When the 96-well plate was framed in PBS the observed effect was no longer seen (Figure 18 B). The observed edge effect was most prominent for NSCs at early differentiation time points and one possible reason could be when NSCs undergoing long time differentiation the cells have the time to make up for cells initially lost. The edge effect possibly affecting the highest concentration was normalized to edge wells of solvent control.

5.8 *In vitro* studies for developmental neurotoxicity effects

This study supports that human NSC-derived neural and glia cultures are relevant *in vitro* models. These models are suitable to test the toxic effects of environmental chemicals to support epidemiological findings that link chemical exposure to abnormal neurodevelopment. *In vitro* studies can give important and valuable information to *in vivo* studies with animal models, by using *in vitro* models we can contribute to the 3Rs. *In vitro* studies are less costly compared to animal studies and are less time-consuming. However, *in vitro* systems have less metabolic capacity and cannot show cell-to-cell interactions, and toxicokinetic are limited compared to *in vivo* studies (77). *In vitro* studies can be a good supplement to human epidemiological studies, because in epidemiological studies it can be hard to identify the confounding factor and investigate the effects that already have taken place. They are not able to identify the toxicological hazards before the effects occur. Experimental studies opposite to epidemiological studies show the possible effects before they occur in humans and can possibly find the causality rather than the correlation (151).

6 CONCLUSION

This master thesis was part of a larger project aiming at establishing the Neural Stem cell (NSC) mode at the Norwegian Institute of Public Health (NIPH). Visual inspection with phase-contrast microcopy supported by gene expression of markers related to neurodifferentiation showed that the model developed as expected. The optimization of the cell viability assay ensured reliable results of cell viability upon exposure. Thus, the model seems to be well-established at the NIPH, and trustworthy and suitable to test key events after chemical exposure to environmental contaminants such as PAHs.

In this thesis, we found that exposure of PAHs (B[a]P, β-NF, and pyrene) in NSCs undergoing differentiation affected the cell viability differently. The most apparent results were seen for early time points, where β-NF and pyrene gave an overall increase in cell viability, effects seen already at nanomolar concentrations, possibly due to increased cell number as a result of increased proliferation/impaired differentiation. The mechanisms involved may include AhR. B[a]P was the PAH that most markedly reduced cell viability. Cytotoxicity seen at higher concentrations is presumably due to reactive metabolites. Although, more direct effects of the lipophilic PAHs on the cellular membranes negatively affected the cell viability the most cannot be excluded.

Minor changes in gene expression were found, with some trends indicting an upregulation of gene expression upon exposure to the PAHs. The neurite outgrowth marker, *GAP43* was found statistically significantly expressed compared to control with a 2-fold upregulation, possibly interfering with neurite outgrowth. *AHR* gene expression showed a trend indicating upregulation upon exposure. However, the low AhR expression may reflect the minor changes found in the gene expression analysis. Expression of *GFAP* was not detected over LOD with gene expression. The presence of astrocytes in the NSC model is important and for its use with DNT testing. Further studies with GFAP as a protein marker with immunocytochemistry should be performed to confirm the presence of astrocytes in the model.

The immunocytochemistry confirmed the expression of protein markers related to neurodevelopment and morphology in both unexposed and in PAH exposed cells. The results obtained were qualitative, and therefore inconclusive and must be supported with quantitative determinations to obtain reliable results upon exposure.

7 FUTURE ASPECTS

Further studies are needed to determine if the changes in mitochondrial dehydrogenase activity caused by PAH exposure are due to impaired differentiation, causing an increase in cell number or, increased metabolic activity. This could be investigated by flow cytometry to examine if the changes were due to increased proliferation or decreased apoptosis. Studies could also include analysis of the expression of genes known to be involved in cell proliferation, the apoptotic process, or expressed as a result of mitochondrial dysfunction. It would also be interesting to explore this issue by flow cytometry to detects apoptotic cells as well as cells in various parts of the cell cycle.

In future studies it would be interesting to combine the PAHs and test it as a human relevant mixture in the NSC models, to better reflect the real-life situation. The simultaneous exposure to PAHs could potentially cause additive or synergic effects. A study conducting this on rat embryonic stem cells found that the mixture enhanced the NSC differentiation and suppressed the glial phenotype and B[a]P alone did not (36). Other PAHs should also be included.

Further analysis of additional gene expression markers related to neurodevelopment and cellular pathways that could be disturbed upon exposure to PAHs should be included in further studies with the NSC model. This could possibly give more answer about the effects reported in epidemiological studies. It would be beneficial to use the gene expression results obtained in this thesis to be repeated. This is to reduce the variance and furthermore increase the statistical power. Thereby a better assessment of the possible human relevant alteration is given consideration. The experimental design should be altered so changes shortly after exposure could be investigated, in addition to long-term effects.

A thorough investigation of the gene *BNDF* would be of particular interest, as it is shown to be disturbed in cases of learning and memory impairment upon binding of chemicals to the AhR receptor (30), and is central in the AOP framework (148). Ca^{2+} measurement after exposure to the PAHs may give mechanistic information, especially regarding pyrene which has shown to increase the cytoplasmic concentration and activated the non-genomic AhR pathway (52). Such measurements are also interesting as interference with NMDAR may modify Ca^{2+} intracellular concentrations. Intracellular calcium levels have been linked to BNDF production which is important for synaptogenesis and neuronal network, and implications for memory and learning (7).

It would be interesting to differentiate the cells for a longer period than 21 days to conduct changes that can occur at a later stage of neuro differentiation and neurodevelopment after PAH exposure. Experiments could be performed using even more complex neuron/glia models such as 3D brain organoids. A culture like this is suggested to reflect the complex interactions of neurons and glia better than a 2D culture (152).

Astrocytic presence in the culture is an important feature of the NSC model and should be investigated thoroughly with alternative genes for gene expression and protein markers for astrocytes.

The immunocytochemical experiments should be completed with quantitative determinations of the qualitative images. Quantitative investigations of protein expression would give a more complete examination of the possible effects the PAHs had on neurodevelopment, differentiation, and synaptogenesis. A marker for the glutamatergic neurons should be included, namely the vesicular glutamate transporter 1(81). Additional proteins linked to neuronal subpopulations, cellular pathways and, oxidative stress could help to better define the specificity of the NSC model.

8 REFERENCES

1. Qiagen. RNeasy Mini Handbook. 2019.

2. Hessel EVS, Staal YCM, Piersma AH. Design and validation of an ontology-driven animal-free testing strategy for developmental neurotoxicity testing. Toxicol Appl Pharmacol. 2018;354:136-52.

3. Silbereis JC, Pochareddy S, Zhu Y, Li M, Sestan N. The Cellular and Molecular Landscapes of the Developing Human Central Nervous System. Neuron. 2016;89(2):248-68.

4. Bal-Price A, Meek MEB. Adverse outcome pathways: Application to enhance mechanistic understanding of neurotoxicity. Pharmacol Ther. 2017;179:84-95.

5. Pistollato F, Canovas-Jorda D, Zagoura D, Price A. Protocol for the Differentiation of Human Induced Pluripotent Stem Cells into Mixed Cultures of Neurons and Glia for Neurotoxicity Testing. J Vis Exp. 2017(124).

6. Cohen AJ, Brauer M, Burnett R, Anderson HR, Frostad J, Estep K, et al. Estimates and 25-year trends of the global burden of disease attributable to ambient air pollution: an analysis of data from the Global Burden of Diseases Study 2015. The Lancet. 2017;389(10082):1907-18.

7. Myhre O, Lag M, Villanger GD, Oftedal B, Ovrevik J, Holme JA, et al. Early life exposure to air pollution particulate matter (PM) as risk factor for attention deficit/hyperactivity disorder (ADHD): Need for novel strategies for mechanisms and causalities. Toxicol Appl Pharmacol. 2018;354:196-214.

8. Kim KH, Jahan SA, Kabir E, Brown RJ. A review of airborne polycyclic aromatic hydrocarbons (PAHs) and their human health effects. Environ Int. 2013;60:71-80.

9. Boström C-E, Gerde P, Hanberg A, Jernström B, Johansson C, Kyrklund T, et al. Cancer risk assessment, indicators, and guidelines for polycyclic aromatic hydrocarbons in the ambient air. Environmental Health Perspectives. 2002;110(suppl 3):451-88.

10. Øvrevik J, Refsnes M, Låg M, Brinchmann BC, Schwarze PE, Holme JA. Triggering Mechanisms and Inflammatory Effects of Combustion Exhaust Particles with Implication for Carcinogenesis. Basic Clin Pharmacol Toxicol. 2017;121 Suppl 3:55-62.

11. Kelly FJ, Fussell JC. Air pollution and airway disease. Clin Exp Allergy. 2011;41(8):1059-71.

12. Schwarze PE, Ovrevik J, Låg M, Refsnes M, Nafstad P, Hetland RB, et al. Particulate matter properties and health effects: consistency of epidemiological and toxicological studies. Hum Exp Toxicol. 2006;25(10):559-79.

13. Brook RD, Franklin B, Cascio W, Hong Y, Howard G, Lipsett M, et al. Air pollution and cardiovascular disease: a statement for healthcare professionals from the Expert Panel on Population and Prevention Science of the American Heart Association. Circulation. 2004;109(21):2655-71.

14. Risom L, Møller P, Loft S. Oxidative stress-induced DNA damage by particulate air pollution. Mutat Res. 2005;592(1-2):119-37.

15. Oudin A, Forsberg B, Adolfsson AN, Lind N, Modig L, Nordin M, et al. Traffic-Related Air Pollution and Dementia Incidence in Northern Sweden: A Longitudinal Study. Environmental Health Perspectives. 2016;124(3):306-12.

16. Tzivian L, Dlugaj M, Winkler A, Weinmayr G, Hennig F, Fuks KB, et al. Long-Term Air Pollution and Traffic Noise Exposures and Mild Cognitive Impairment in Older Adults: A Cross-Sectional Analysis of the Heinz Nixdorf Recall Study. Environmental Health Perspectives. 2016;124(9):1361-8.

17. Power MC, Adar SD, Yanosky JD, Weuve J. Exposure to air pollution as a potential contributor to cognitive function, cognitive decline, brain imaging, and dementia: A systematic review of epidemiologic research. Neurotoxicology. 2016;56:235-53.

18. Chen H, Kwong JC, Copes R, Tu K, Villeneuve PJ, van Donkelaar A, et al. Living near major roads and the incidence of dementia, Parkinson's disease, and multiple sclerosis: a population-based cohort study. Lancet. 2017;389(10070):718-26.

19. Lim YH, Kim H, Kim JH, Bae S, Park HY, Hong YC. Air pollution and symptoms of depression in elderly adults. Environ Health Perspect. 2012;120(7):1023-8.

20. Perera FP, Li Z, Whyatt R, Hoepner L, Wang S, Camann D, et al. Prenatal airborne polycyclic aromatic hydrocarbon exposure and child IQ at age 5 years. Pediatrics. 2009;124(2):e195-202.

21. Landrigan PJ. What causes autism? Exploring the environmental contribution. Curr Opin Pediatr. 2010;22(2):219-25.

22. Perera FP, Tang D, Wang S, Vishnevetsky J, Zhang B, Diaz D, et al. Prenatal polycyclic aromatic hydrocarbon (PAH) exposure and child behavior at age 6-7 years. Environ Health Perspect. 2012;120(6):921-6.

23. Edwards SC, Jedrychowski W, Butscher M, Camann D, Kieltyka A, Mroz E, et al. Prenatal exposure to airborne polycyclic aromatic hydrocarbons and children's intelligence at 5 years of age in a prospective cohort study in Poland. Environ Health Perspect. 2010;118(9):1326-31.

24. Pedersen CB, Raaschou-Nielsen O, Hertel O, Mortensen PB. Air pollution from traffic and schizophrenia risk. Schizophr Res. 2004;66(1):83-5.

25. Rice D, Barone S. Critical Periods of Vulnerability for the Developing Nervous System: Evidence from Humans and Animal Models. Environ Health Perspect. 2000;108:511-33.

26. Stiles J, Jernigan TL. The basics of brain development. Neuropsychol Rev. 2010;20(4):327-48.

27. Bal-Price A, Pistollato F, Sachana M, Bopp SK, Munn S, Worth A. Strategies to improve the regulatory assessment of developmental neurotoxicity (DNT) using in vitro methods. Toxicol Appl Pharmacol. 2018;354:7-18.

28. Dat ND, Chang MB. Review on characteristics of PAHs in atmosphere, anthropogenic sources and control technologies. Sci Total Environ. 2017;609:682-93.

29. Some non-heterocyclic polycyclic aromatic hydrocarbons and some related exposures. IARC Monogr Eval Carcinog Risks Hum. 2010;92:1-853.

30. Chepelev NL, Moffat ID, Bowers WJ, Yauk CL. Neurotoxicity may be an overlooked consequence of benzo[a]pyrene exposure that is relevant to human health risk assessment. Mutat Res Rev Mutat Res. 2015;764:64-89.

31. Authority. EFS. Scientific opinion of the panel on contaminants in the food chain on a request from the European Commission on polycyclic aromatic hydrocarbons in food. The EFSA journal 2008;724:6-114.

32. Singh L, Varshney JG, Agarwal T. Polycyclic aromatic hydrocarbons' formation and occurrence in processed food. Food Chem. 2016;199:768-81.

33. T.Kameda. Atmospheric Chemistry of Polycyclic Aromatic Hydrocarbons and Releated Compounds Journal of Health Science. 2011;57:504-11.

34. Kameda Y, Shirai J, Komai T, Nakanishi J, Masunaga S. Atmospheric polycyclic aromatic hydrocarbons: size distribution, estimation of their risk and their depositions to the human respiratory tract. Sci Total Environ. 2005;340(1-3):71-80.

35. Lai IC, Lee CL, Zeng KY, Huang HC. Seasonal variation of atmospheric polycyclic aromatic hydrocarbons along the Kaohsiung coast. J Environ Manage. 2011;92(8):2029-37.

36. Slotkin TA, Skavicus S, Card J, Giulio RT, Seidler FJ. In vitro models reveal differences in the developmental neurotoxicity of an environmental polycylic aromatic hydrocarbon mixture compared to benzo[a]pyrene: Neuronotypic PC12 Cells and embryonic neural stem cells. Toxicology. 2017;377:49-56.

37. Tang Y, Donnelly KC, Tiffany-Castiglioni E, Mumtaz MM. Neurotoxicity of polycyclic aromatic hydrocarbons and simple chemical mixtures. J Toxicol Environ Health A. 2003;66(10):919-40.

38. Zhang X, Li X, Jing Y, Fang X, Zhang X, Lei B, et al. Transplacental transfer of polycyclic aromatic hydrocarbons in paired samples of maternal serum, umbilical cord serum, and placenta in Shanghai, China. Environ Pollut. 2017;222:267-75.

39. Langlois PH, Hoyt AT, Lupo PJ, Lawson CC, Waters MA, Desrosiers TA, et al. Maternal occupational exposure to polycyclic aromatic hydrocarbons and risk of neural tube defect-affected pregnancies. Birth Defects Res A Clin Mol Teratol. 2012;94(9):693-700.

40. Rodier PM. Developing brain as a target of toxicity. Environ Health Perspect. 1995;103:73-6.

41. Grandjean P, Landrigan PJ. Developmental neurotoxicity of industrial chemicals. Lancet. 2006;368(9553):2167-78.

42. Kishikawa N, Wada M, Kuroda N, Akiyama S, Nakashima K. Determination of polycyclic aromatic hydrocarbons in milk samples by high-performance liquid

chromatography with fluorescence detection. Journal of Chromatography B. 2003;789(2):257-64.

43. Kim SR, Halden RU, Buckley TJ. Polycyclic aromatic hydrocarbons in human milk of nonsmoking U.S. women. Environ Sci Technol. 2008;42(7):2663-7.

44. Miller KP, Ramos KS. Impact of cellular metabolism on the biological effects of benzo[a]pyrene and related hydrocarbons. Drug Metab Rev. 2001;33(1):1-35.

45. Kampa M, Castanas E. Human health effects of air pollution. Environmental Pollution. 2008;151(2):362-7.

46. Juricek L, Coumoul X. The Aryl Hydrocarbon Receptor and the Nervous System. Int J Mol Sci. 2018;19(9).

47. Goedtke L, Sprenger H, Hofmann U, Schmidt FF, Hammer HS, Zanger UM, et al. Polycyclic Aromatic Hydrocarbons Activate the Aryl Hydrocarbon Receptor and the Constitutive Androstane Receptor to Regulate Xenobiotic Metabolism in Human Liver Cells. Int J Mol Sci. 2020;22(1).

48. Akahoshi E, Yoshimura S, Ishihara-Sugano M. Over-expression of AhR (aryl hydrocarbon receptor) induces neural differentiation of Neuro2a cells: neurotoxicology study. Environ Health. 2006;5:24.

49. Latchney SE, Hein AM, O'Banion MK, DiCicco-Bloom E, Opanashuk LA. Deletion or activation of the aryl hydrocarbon receptor alters adult hippocampal neurogenesis and contextual fear memory. J Neurochem. 2013;125(3):430-45.

50. Jiang YZ, Wang K, Fang R, Zheng J. Expression of aryl hydrocarbon receptor in human placentas and fetal tissues. J Histochem Cytochem. 2010;58(8):679-85.

51. Holme JA, Brinchmann BC, Le Ferrec E, Lagadic-Gossmann D, Ovrevik J. Combustion Particle-Induced Changes in Calcium Homeostasis: A Contributing Factor to Vascular Disease? Cardiovasc Toxicol. 2019;19(3):198-209.

52. Brinchmann BC, Le Ferrec E, Bisson WH, Podechard N, Huitfeldt HS, Gallais I, et al. Evidence of selective activation of aryl hydrocarbon receptor nongenomic calcium signaling by pyrene. Biochem Pharmacol. 2018;158:1-12.

53. Larigot L, Juricek L, Dairou J, Coumoul X. AhR signaling pathways and regulatory functions. Biochim Open. 2018;7:1-9.

54. Schroeder H. Developmental Brain and Behavior Toxicity of Air Pollutants: A Focus on the Effects of Polycyclic Aromatic Hydrocarbons (PAHs). Critical Reviews in Environmental Science and Technology. 2011;41(22):2026-47.

55. Knight C, Sorensen A. Windows in early mammary development: critical or not? Reproduction 2001;122(3):337-45.

56. Goasdoue K, Miller SM, Colditz PB, Bjorkman ST. Review: The blood-brain barrier; protecting the developing fetal brain. Placenta. 2017;54:111-6.

57. Munno DW, Syed NI. Synaptogenesis in the CNS: an odyssey from wiring together to firing together. J Physiol. 2003;552(Pt 1):1-11.

58. Keunen K, Counsell SJ, Benders M. The emergence of functional architecture during early brain development. Neuroimage. 2017;160:2-14.

59. Jiang X, Nardelli J. Cellular and molecular introduction to brain development. Neurobiol Dis. 2016;92(Pt A):3-17.

60. Choi H, Jedrychowski W, Spengler J, Camann DE, Whyatt RM, Rauh V, et al. International studies of prenatal exposure to polycyclic aromatic hydrocarbons and fetal growth. Environ Health Perspect. 2006;114(11):1744-50.

61. Sram RJ, Binkova B, Dejmek J, Bobak M. Ambient air pollution and pregnancy outcomes: a review of the literature. Environ Health Perspect. 2005;113(4):375-82.

62. Tan J, Loganath A, Chong YS, Obbard JP. Exposure to persistent organic pollutants in utero and related maternal characteristics on birth outcomes: a multivariate data analysis approach. Chemosphere. 2009;74(3):428-33.

63. Tang D, Li TY, Liu JJ, Chen YH, Qu L, Perera F. PAH-DNA adducts in cord blood and fetal and child development in a Chinese cohort. Environ Health Perspect. 2006;114(8):1297-300.

64. Ivanovic DM, Leiva BP, Perez HT, Olivares MG, Diaz NS, Urrutia MS, et al. Head size and intelligence, learning, nutritional status and brain development. Head, IQ, learning, nutrition and brain. Neuropsychologia. 2004;42(8):1118-31.

65. Perera FP, Wang S, Vishnevetsky J, Zhang B, Cole KJ, Tang D, et al. Polycyclic aromatic hydrocarbons-aromatic DNA adducts in cord blood and behavior scores in New York city children. Environ Health Perspect. 2011;119(8):1176-81.

66. Perera FP, Chang HW, Tang D, Roen EL, Herbstman J, Margolis A, et al. Early-life exposure to polycyclic aromatic hydrocarbons and ADHD behavior problems. PLoS One. 2014;9(11):e111670.

67. Perera FP, Wheelock K, Wang Y, Tang D, Margolis AE, Badia G, et al. Combined effects of prenatal exposure to polycyclic aromatic hydrocarbons and material hardship on child ADHD behavior problems. Environ Res. 2018;160:506-13.

68. Margolis AE, Herbstman JB, Davis KS, Thomas VK, Tang D, Wang Y, et al. Longitudinal effects of prenatal exposure to air pollutants on self-regulatory capacities and social competence. J Child Psychol Psychiatry. 2016;57(7):851-60.

69. Perera FP, Rauh V, Whyatt RM, Tsai WY, Tang D, Diaz D, et al. Effect of prenatal exposure to airborne polycyclic aromatic hydrocarbons on neurodevelopment in the first 3 years of life among inner-city children. Environ Health Perspect. 2006;114(8):1287-92.

70. Polanczyk G, de Lima MS, Horta BL, Biederman J, Rohde LA. The worldwide prevalence of ADHD: a systematic review and metaregression analysis. Am J Psychiatry. 2007;164(6):942-8.

71. Guang S, Pang N, Deng X, Yang L, He F, Wu L, et al. Synaptopathology Involved in Autism Spectrum Disorder. Front Cell Neurosci. 2018;12:470.

72. Mooney LA, Santella RM, Covey L, Jeffrey AM, Bigbee W, Randall MC, et al. Decline of DNA damage and other biomarkers in peripheral blood following smoking cessation. Cancer Epidemiol Biomarkers Prev. 1995;4(6):627-34.

73. Perera F, Li TY, Zhou ZJ, Yuan T, Chen YH, Qu L, et al. Benefits of reducing prenatal exposure to coal-burning pollutants to children's neurodevelopment in China. Environ Health Perspect. 2008;116(10):1396-400.

74. Backes CH, Nelin T, Gorr MW, Wold LE. Early life exposure to air pollution: how bad is it? Toxicol Lett. 2013;216(1):47-53.

75. Chen C, Tang Y, Jiang X, Qi Y, Cheng S, Qiu C, et al. Early postnatal benzo(a)pyrene exposure in Sprague-Dawley rats causes persistent neurobehavioral impairments that emerge postnatally and continue into adolescence and adulthood. Toxicol Sci. 2012;125(1):248-61.

76. Fritsche E, Grandjean P, Crofton KM, Aschner M, Goldberg A, Heinonen T, et al. Consensus statement on the need for innovation, transition and implementation of developmental neurotoxicity (DNT) testing for regulatory purposes. Toxicology and Applied Pharmacology. 2018;354:3-6.

77. Di Consiglio E, Pistollato F, Mendoza-De Gyves E, Bal-Price A, Testai E. Integrating biokinetics and in vitro studies to evaluate developmental neurotoxicity induced by chlorpyrifos in human iPSC-derived neural stem cells undergoing differentiation towards neuronal and glial cells. Reprod Toxicol. 2020;98:174-88.

78. Kirk RGW. Recovering The Principles of Humane Experimental Technique: The 3Rs and the Human Essence of Animal Research. Sci Technol Human Values. 2018;43(4):622-48.

79. Knudsen LE, Smith A, Tornqvist E, Forsby A, Tahti H. Nordic symposium on "toxicology and pharmacology without animal experiments-Will it be possible in the next 10 years?". Basic Clin Pharmacol Toxicol. 2019;124(5):560-7.

80. Takahashi K, Yamanaka S. Induction of pluripotent stem cells from mouse embryonic and adult fibroblast cultures by defined factors. Cell. 2006;126(4):663-76.

81. Pistollato F, Canovas-Jorda D, Zagoura D, Bal-Price A. Nrf2 pathway activation upon rotenone treatment in human iPSC-derived neural stem cells undergoing differentiation towards neurons and astrocytes. Neurochem Int. 2017;108:457-71.

82. Lov om humanmedisinsk bruk av bioteknologi m.m. (bioteknologiloven) Oslo: Lovdata.no; 2003, reviced 2020 [

83. Pistollato F, de Gyves EM, Carpi D, Bopp SK, Nunes C, Worth A, et al. Assessment of developmental neurotoxicity induced by chemical mixtures using an adverse outcome pathway concept. Environ Health. 2020;19(1):23.

84. Middeldorp J, Hol EM. GFAP in health and disease. Prog Neurobiol. 2011;93(3):421-43.

85. Dehmelt L, Halpain S. The MAP2/Tau family of microtubule-associated proteins. Genome Biol. 2005;6(1):204.

86. Grasselli G, Strata P. Structural plasticity of climbing fibers and the growth-associated protein GAP-43. Front Neural Circuits. 2013;7:25.

87. Iovino L, Tremblay ME, Civiero L. Glutamate-induced excitotoxicity in Parkinson's disease: The role of glial cells. J Pharmacol Sci. 2020;144(3):151-64.

88. Lee SE, Lee Y, Lee GH. The regulation of glutamic acid decarboxylases in GABA neurotransmission in the brain. Arch Pharm Res. 2019;42(12):1031-9.

89. Shen K, Cowan CW. Guidance molecules in synapse formation and plasticity. Cold Spring Harb Perspect Biol. 2010;2(4):a001842.

90. Marin O. Interneuron dysfunction in psychiatric disorders. Nat Rev Neurosci. 2012;13(2):107-20.

91. Chinta SJ, Andersen JK. Dopaminergic neurons. Int J Biochem Cell Biol. 2005;37(5):942-6.

92. Coley AA, Gao WJ. PSD95: A synaptic protein implicated in schizophrenia or autism? Prog Neuropsychopharmacol Biol Psychiatry. 2018;82:187-94.

93. Glantz LA, Gilmore JH, Hamer RM, Lieberman JA, Jarskog LF. Synaptophysin and postsynaptic density protein 95 in the human prefrontal cortex from mid-gestation into early adulthood. Neuroscience. 2007;149(3):582-91.

94. Spinu N, Bal-Price A, Cronin MTD, Enoch SJ, Madden JC, Worth AP. Development and analysis of an adverse outcome pathway network for human neurotoxicity. Arch Toxicol. 2019;93(10):2759-72.

95. Dutta K, Ghosh D, Nazmi A, Kumawat KL, Basu A. A common carcinogen benzo[a]pyrene causes neuronal death in mouse via microglial activation. PLoS One. 2010;5(4):e9984.

96. Vondracek J, Machala M. The role of metabolism in toxicity of polycyclic aromatic hydrocarbons and their non-genotoxic modes of action. Curr Drug Metab. 2020.

97. Szychowski KA, Rybczynska-Tkaczyk K, Gminski J, Wojtowicz AK. The interference of alpha- and beta-naphthoflavone with triclosan effects on viability, apoptosis and reactive oxygen species production in mouse neocortical neurons. Pestic Biochem Physiol. 2020;168:104638.

98. Singh VK, Patel DK, Ram S, Mathur N, Siddiqui MK, Behari JR. Blood levels of polycyclic aromatic hydrocarbons in children of Lucknow, India. Arch Environ Contam Toxicol. 2008;54(2):348-54.

99. Pistollato F, Louisse J, Scelfo B, Mennecozzi M, Accordi B, Basso G, et al. Development of a pluripotent stem cell derived neuronal model to identify chemically induced pathway perturbations in relation to neurotoxicity: Effects of CREB pathway inhibition. Toxicology and Applied Pharmacology. 2014;280(2):378-88.

100. Scientific TF. Aseptique Technique 2021 [cited 2021 Jan 22]. Available from: https://www.thermofisher.com/no/en/home/references/gibco-cell-culture-basics/aseptic-technique.html.

101. Rampersad SN. Multiple applications of Alamar Blue as an indicator of metabolic function and cellular health in cell viability bioassays. Sensors (Basel). 2012;12(9):12347-60.

102. Zachari MA, Chondrou PS, Pouliliou SE, Mitrakas AG, Abatzoglou I, Zois CE, et al. Evaluation of the alamarblue assay for adherent cell irradiation experiments. Dose Response. 2014;12(2):246-58.

103. O'Brien J, Wilson I, Orton T, Pognan F. Investigation of the Alamar Blue (resazurin) fluorescent dye for the assessment of mammalian cell cytotoxicity. Eur J Biochem. 2000;267(17):5421-6.

104. Alberts B, Johansen A, Lewis J, Morgan D, Raff M, Roberts K, et al. Molecular Biology of The Cell 6. edition ed. New York Garland Science 2015.

105. Munshi S, Twining RC, Dahl R. Alamar blue reagent interacts with cell-culture media giving different fluorescence over time: potential for false positives. J Pharmacol Toxicol Methods. 2014;70(2):195-8.

106. Gibson UE, Heid CA, Williams PM. A novel method for real time quantitative RT-PCR. Genome Res. 1996;6(10):995-1001.

107. Holland PM, Abramson RD, Watson R, Gelfand DH. Detection of specific polymerase chain reaction product by utilizing the 5'----3' exonuclease activity of Thermus aquaticus DNA polymerase. Proc Natl Acad Sci U S A. 1991;88(16):7276-80.

108. Scientific T. NanoDrop 1000 Spectrophotometer V3.8 user manual 2010.

109. Eppendorf. Eppendorf Concentrator plus™:

Easy handling, broad versatility. In: Eppendorf, editor. Hamburg Eppendorf 2013.

110. Nolan T, Hands RE, Bustin SA. Quantification of mRNA using real-time RT-PCR. Nat Protoc. 2006;1(3):1559-82.

111. Livak KJ, Schmittgen TD. Analysis of relative gene expression data using real-time quantitative PCR and the 2(-Delta Delta C(T)) Method. Methods. 2001;25(4):402-8.

112. Brooks SA. Basic immunocytochemistry for light microscopy. Methods Mol Biol. 2012;878:1-30.

113. Im K, Mareninov S, Diaz MFP, Yong WH. An Introduction to Performing Immunofluorescence Staining. Methods Mol Biol. 2019;1897:299-311.

114. Fox CH, Johnson FB, Whiting J, Roller PP. Formaldehyde fixation. J Histochem Cytochem. 1985;33(8):845-53.

115. Promega. CellTiter-Blue Cell Viability assay 2016.

116. Fisher T. Alamar Blue Cell Viability reagent 2019.

117. St Laurent G, Shtokalo D, Tackett MR, Yang Z, Vyatkin Y, Milos PM, et al. On the importance of small changes in RNA expression. Methods. 2013;63(1):18-24.

118. Adinolfi M. The development of the human blood-CSF-brain barrier. Dev Med Child Neurol. 1985;27(4):532-7.

119. Wu YK, Tu YK, Yu J, Cheng NC. The Influence of Cell Culture Density on the Cytotoxicity of Adipose-Derived Stem Cells Induced by L-Ascorbic Acid-2-Phosphate. Sci Rep. 2020;10(1):104.

120. Slotkin TA, Seidler FJ. Benzo[a]pyrene impairs neurodifferentiation in PC12 cells. Brain Res Bull. 2009;80(1-2):17-21.

121. Cullen DK, Gilroy ME, Irons HR, Laplaca MC. Synapse-to-neuron ratio is inversely related to neuronal density in mature neuronal cultures. Brain Res. 2010;1359:44-55.

122. Courchesne E, Mouton PR, Calhoun ME, Semendeferi K, Ahrens-Barbeau C, Hallet MJ, et al. Neuron number and size in prefrontal cortex of children with autism. Jama. 2011;306(18):2001-10.

123. Raefsky SM, Mattson MP. Adaptive responses of neuronal mitochondria to bioenergetic challenges: Roles in neuroplasticity and disease resistance. Free Radic Biol Med. 2017;102:203-16.

124. Chang DTW, Reynolds IJ. Differences in mitochondrial movement and morphology in young and mature primary cortical neurons in culture. Neuroscience. 2006;141(2):727-36.

125. Kang RR, Sun Q, Chen KG, Cao QT, Liu C, Liu K, et al. Resveratrol prevents benzo(a)pyrene-induced disruption of mitochondrial homeostasis via the AMPK signaling pathway in primary cultured neurons. Environ Pollut. 2020;261:114207.

126. Nie JS, Zhang HM, Zhao J, Liu HJ, Niu Q. Involvement of mitochondrial pathway in benzo[a]pyrene-induced neuron apoptosis. Hum Exp Toxicol. 2014;33(3):240-50.

127. Kajta M, Wojtowicz AK, Mackowiak M, Lason W. Aryl hydrocarbon receptor-mediated apoptosis of neuronal cells: a possible interaction with estrogen receptor signaling. Neuroscience. 2009;158(2):811-22.

128. Yang K, Jiang X, Su Q, Wang J, Li C, Xia Y, et al. Disruption of glutamate neurotransmitter transmission is modulated by SNAP-25 in benzo[a]pyrene-induced neurotoxic effects. Toxicology. 2017;384:11-22.

129. Wei H, Alberts I, Li X. The apoptotic perspective of autism. Int J Dev Neurosci. 2014;36:13-8.

130. Kole AJ, Annis RP, Deshmukh M. Mature neurons: equipped for survival. Cell Death Dis. 2013;4:e689.

131. Stummann TC, Hareng L, Bremer S. Hazard assessment of methylmercury toxicity to neuronal induction in embryogenesis using human embryonic stem cells. Toxicology. 2009;257(3):117-26.

132. Ramesh A, Inyang F, Hood DB, Archibong AE, Knuckles ME, Nyanda AM. Metabolism, bioavailability, and toxicokinetics of benzo(alpha)pyrene in F-344 rats following oral administration. Exp Toxicol Pathol. 2001;53(4):275-90.

133. Wang W, Osenbroch P, Skinnes R, Esbensen Y, Bjoras M, Eide L. Mitochondrial DNA integrity is essential for mitochondrial maturation during differentiation of neural stem cells. Stem Cells. 2010;28(12):2195-204.

134. Griffiths KK, Levy RJ. Evidence of Mitochondrial Dysfunction in Autism: Biochemical Links, Genetic-Based Associations, and Non-Energy-Related Mechanisms. Oxid Med Cell Longev. 2017;2017:4314025.

135. Julien C, Marcouiller F, Bretteville A, El Khoury NB, Baillargeon J, Hebert SS, et al. Dimethyl sulfoxide induces both direct and indirect tau hyperphosphorylation. PLoS One. 2012;7(6):e40020.

136. Adler S, Pellizzer C, Paparella M, Hartung T, Bremer S. The effects of solvents on embryonic stem cell differentiation. Toxicol In Vitro. 2006;20(3):265-71.

137. Zhang C, Deng Y, Dai H, Zhou W, Tian J, Bing G, et al. Effects of dimethyl sulfoxide on the morphology and viability of primary cultured neurons and astrocytes. Brain Res Bull. 2017;128:34-9.

138. Davidsen N, Lauvas AJ, Myhre O, Ropstad E, Carpi D, Gyves EM, et al. Exposure to human relevant mixtures of halogenated persistent organic pollutants (POPs) alters neurodevelopmental processes in human neural stem cells undergoing differentiation. Reprod Toxicol. 2021;100:17-34.

139. Kaneko Y, Tajiri N, Yu S, Hayashi T, Stahl CE, Bae E, et al. Nestin overexpression precedes caspase-3 upregulation in rats exposed to controlled cortical impact traumatic brain injury. Cell Med. 2012;4(2):55-63.

140. Christen V, Rusconi M, Crettaz P, Fent K. Developmental neurotoxicity of different pesticides in PC-12 cells in vitro. Toxicol Appl Pharmacol. 2017;325:25-36.

141. Ryan KR, Sirenko O, Parham F, Hsieh JH, Cromwell EF, Tice RR, et al. Neurite outgrowth in human induced pluripotent stem cell-derived neurons as a high-throughput screen for developmental neurotoxicity or neurotoxicity. Neurotoxicology. 2016;53:271-81.

142. Casanova EL, Casanova MF. Genetics studies indicate that neural induction and early neuronal maturation are disturbed in autism. Front Cell Neurosci. 2014;8:397.

143. Gassmann K, Abel J, Bothe H, Haarmann-Stemmann T, Merk HF, Quasthoff KN, et al. Species-specific differential AhR expression protects human neural progenitor cells against developmental neurotoxicity of PAHs. Environ Health Perspect. 2010;118(11):1571-7.

144. Brown LA, Khousbouei H, Goodwin JS, Irvin-Wilson CV, Ramesh A, Sheng L, et al. Down-regulation of early ionotrophic glutamate receptor subunit developmental expression as a mechanism for observed plasticity deficits following gestational exposure to benzo(a)pyrene. Neurotoxicology. 2007;28(5):965-78.

145. Grova N, Schroeder H, Farinelle S, Prodhomme E, Valley A, Muller CP. Sub-acute administration of benzo[a]pyrene (B[a]P) reduces anxiety-related behaviour in adult mice and modulates regional expression of N-methyl-D-aspartate (NMDA) receptors genes in relevant brain regions. Chemosphere. 2008;73(1 Suppl):S295-302.

146. McCallister MM, Maguire M, Ramesh A, Aimin Q, Liu S, Khoshbouei H, et al. Prenatal exposure to benzo(a)pyrene impairs later-life cortical neuronal function. Neurotoxicology. 2008;29(5):846-54.

147. Grova N, Valley A, Turner JD, Morel A, Muller CP, Schroeder H. Modulation of behavior and NMDA-R1 gene mRNA expression in adult female mice after sub-acute administration of benzo(a)pyrene. Neurotoxicology. 2007;28(3):630-6.

148. Sachana M, Rolaki A, Bal-Price A. Development of the Adverse Outcome Pathway (AOP): Chronic binding of antagonist to N-methyl-d-aspartate receptors (NMDARs) during brain development induces impairment of learning and memory abilities of children. Toxicol Appl Pharmacol. 2018;354:153-75.

149. Hogberg HT, Kinsner-Ovaskainen A, Coecke S, Hartung T, Bal-Price AK. mRNA expression is a relevant tool to identify developmental neurotoxicants using an in vitro approach. Toxicol Sci. 2010;113(1):95-115.

150. Lundholt BK, Scudder KM, Pagliaro L. A simple technique for reducing edge effect in cell-based assays. J Biomol Screen. 2003;8(5):566-70.

151. Xu X, Ha SU, Basnet R. A Review of Epidemiological Research on Adverse Neurological Effects of Exposure to Ambient Air Pollution. Front Public Health. 2016;4:157.

152. Price A, Pistollato F, Munn S, Bopp S, Worth A. Startegies aim for improving the regulatory assessment of Dvelopmental Neurotoxicity (DNT) using non-animal methods European Commision 2018.

Appendix 1: Products and reagents

Reagent name	Catalog number	Supplier/Producer	Area of use
µ-Plate 24 Well Black	82406	Ibidi	Immunocytochemistry
96-deep well plates	732-3323	VWR	Cell cultivation and medium change
Alamar Blue Cell Viability Reagent	DAL1025	Thermo Fisher	Cell viability assessment and optimization
B27 Supplements	17504001	Thermo Fisher	Making ND Incomplete medium
B27 Supplements without Vitamin A	12587001	Thermo Fisher	Making NI Incomplete medium
BDNF	PHC7074	Thermo Fisher	Making NI and ND complete medium
Benzo[a]Pyrene		Sigma-Aldrich	Exposure of cells
bFGF	13256-029	Thermo Fisher	Making NI complete
BioCoat ™ Poly-D-Lysine 96 well Clear Flat Bottom	354461	Corning	Cryopreservation of cells
BRAND cryogenic tube	BR114840-1000EA	Sigma-Aldrich	Cryopreservation of cells
BSA 36%	A7979-50ML	Sigma-Aldrich	Immunocytochemistry
CryoStor Cell Cryopreservation medium	C2874-100ML	Sigma-Aldrich	Cryopreservation of cells
DAPI	62248	Thermo Fisher	Immunocytochemistry
Defined Trypsin Inhibitor (DTI)	R007100	Thermo Fisher	Splitting of cells
DMEM/F12 Glutamax	31331028	Thermo Fisher	Making NI medium
DMSO	D4540-100ML	Sigma-Aldrich	Dilution of the PAHs and for solvent control
EGF	PHG6045	Thermo Fisher	Making NI complete medium
Ethanol 97%	600068	Antibac	Aseptic technique
Falcon ™ Tissue Culture Treated Flasks T25/T75	353108 353136	Falcon	Cell cultivation
Falcon™ tubes 15 mL/50 mL	339650 339652	Falcon	Cell cultivation

Formaldehyde 36%	47609-250ML-F	Sigma Aldrich	Fixation
GDNF	PHC7045	Thermo Fisher	Making ND complete medium
Goat Anti-Chicken IgY H&L (Dyelight 488) preabsorbed	Ab97951	Abcam	Immunocytochemistry
Goat Anti-Mouse IgG H&L (Dyelight 550) preabsorbed	Ab96880	Abcam	Immunocytochemistry
Goat Anti-Rabbit IgG H&L (Dyelight 650)	Ab96902	Abcam	Immunocytochemistry
Hard-Shell® 384-Well PCR Plates	#HSP3805	Bio-Rad	Real-Time PCR
Heparin	H3149-100KU	Sigma-Aldrich	Making NI Incomplete
Ki67 primary antibody	MAB4190	Merck	Immunocytochemistry
Laminin	L2020-1MG	Sigma-Aldrich	Making ND Complete
L-Glutamine	25030024	Thermo Fisher	Making ND Incomplete
LUNA 2-Channel Cell counting slides	L12003-LG	LUNA	Cell passage
MAP2 primary antibody	Ab5392	Abcam	Immunocytochemistry
Matrigel Basement Membrane Matrix	354234	Corning	Coating for flasks
Matrigel Basement Membrane Matrix Reduced Growth Factor	354230	Corning	Coating for plates
Medium Bottle 125 mL/250 mL/500 mL		Fisherbrand™	Preparation of NI and ND medium
N2 Supplements	17502001	Thermo Fisher	Making NI and ND Incomplete medium
Nestin primary antibody	N5413-100UG	Abcam	Immunocytochemistry
Neurobasal Medium	21103049	Thermo Fisher	Making ND medium
Non-essential amino acids (NEEA)	11140-035	Thermo Fisher	Making NI Incomplete
PBS without Ca^{2+} and Mg^{2+}	14190250	Thermo Fisher	Splitting of cells and during experiments to frame the plate
PBS+ (without Ca^{2+} and Mg^{2+})	10010023	Thermo Fisher	Fixation and staining of cells

Penicillin/Streptomycin	15140-122	Thermo Fisher	Making NI and ND Incomplete
PSD95 primary antibody	Ab13552	Abcam	Immunocytochemistry
Pyrene		Sigma-Aldrich	Exposure of cells
QIAshredder	79656	Qiagen	RNA isolation
RNase away	7005-11	Thermo Fisher	RNA isolation
Rneasy Micro Kit	74004	Qiagen	RNA isolation
Rneasy Mini Kit	74106	Qiagen	RNA isolation
TaqMan Gene Expression Assay	4331182	Thermo Fisher	Gene expression analysis
TaqMan Gene Expression Universal Master Mix	4304437	Thermo Fisher	Gene expression analysis
TH primary antibody	AB152	Millipore	Immunocytochemistry
Triton X-100 solution	93442-100ML	Sigma-Aldrich	Immunocytochemistry
Trypan Blue (0,4%)	T8154-100ML	Sigma-Aldrich	Splitting of cells
Trypsin-EDTA (0,5%)	15400054	Thermo Fisher	Splitting of cells
VACUSAFE aspiration system		INTEGRA	Cell cultivation and aseptic technique
β-Naphthoflavone		Sigma-Aldrich	Exposure of cells

Appendix 2: Protocols for cell cultivation

2.1 Coating of labware

Flasks are coated with Matrigel Basement Membrane Matrix (BMM) and plates are coated with reduced Growth Factor (rGF). BMM is a soluble membrane consisting of extracellular matrix protein extracted from Engelbreth-Holm-Swam mouse sarcoma. BMM consist of laminin which is the major component but also other protein and growth factors such as collagen IV, heparan sulfate proteoglycans, entactin/nidogen, TGF-beta, epidermal growth factor (EGF), insulin-like growth factor, fibroblast growth factor (FGF), tissue plasminogen activator and other growth factor that occur naturally in the sarcoma The Matrigel is used for effective attachment for the cells to the bottom surface of the flask.

The plates were initially coated with poly-D-lysine to enhance cell binding, growth, and differentiation to the plate surface. BMM rGF was used as additional coating because it is purified and characterized in a larger extent than the BMM.

This protocol applies to coating of both plates and flasks. Aliquots of BMM and rGF is kept in the freezer at volume 200 µL and 56 µL.

1. Measure out 20 mL cold DMEM/F12 medium per aliquot of matrigel in a falcon tube. If you need more than 20 mL just double/triple the recipe.
2. Dilute one aliquot of BMM (200 µL) or BMM rGF (56 µL) in cold DMEM/F12 medium with chilled pipette tips as matrigel will solidify at 20 °C. Mix gently.
3. Transfer diluted BMM or rGF to flask and/or plates according to Table A2.1.
4. Incubate flasks and plates for 1 h at 37 °C, 5% CO_2 and leave for room temperature for 30 min before adding cells.

Table A2.1: ***Volume added coating for flasks and plates (per well).*** *Aliquots are kept in freezer as 200µL (BMM) and 56µL (rGF) to be diluted in 20mL DMEM.*

Flask size	Matrigel	Volume
T75	BMM	5 mL
T25	BMM	10 mL
Plate size		
96-well	rGF	100 µL/well
24-well	rGF	0,580 mL/well

2.2 Thawing of cryopreserved cells

NSC are cryopreserved in CryoStore Cell cryopreservation media containing 10% DMSO in -150°C. Before the cells can be cultivated the cells must be rinsed free for DMSO and the cells must be viable.

1. Coat a suitable flask according to protocol 2.1
2. Prepare NI medium according to protocol 2.3
3. Take the frozen NSCs and thaw them by transferring them to a water bath at 37 °C for 1-2 min. Add approximal 1 mL of warm NI medium to the cells by drip the medium drop by drop and mix gently by pipetting up and down.
4. Transfer the cells to 5 mL of pre-warm NI medium and mix gently.
5. Centrifuge the tube at 130 g for 4 min and 30 sec in order to remove DMSO form the cryopreservation medium.
6. Aspirate the supernatant and resuspend the pellet by adding 2 mL warm NI medium, drop by drop. Dilute the resuspended cells by adding 4 mL of warm NI medium and mix gently until the cells are completely resuspended.
7. Determine the cell number and cell viability by taking out 20 µL cell suspension and mix it with 20 µL trypan blue (1:2). Assess viability using an automated cell counter and calculate the average cell density (cells/mL).
8. Plate cells in coated flasks according to protocol 2.4 and Table A2.5.

2.3 Culture medium

Incomplete medium can be stored for a few weeks at 4 °C. Complete medium must be prepared fresh for each use and can be stored up to 7-10 days at 4 °C.

Neural Induction medium

We use Neural Induction (NI) medium for expansion of neural stem cells, proliferation without differentiation. The medium uses in flask when we want to expand our population, creating a confluent culture and for the first few days when seeding in plates. NI complete is made from NI Incomplete, see Table A2.2.

Table A2.2: ***Recipe for Neural Induction medium***

NI Incomplete			**NI Complete**		
		Desired concentration		**Desired concentration**	**Dilution**
DMEM/F12 Glutamax	500 mL		NI Incomplete x mL		
B27 Supplements ÷ vit A	10 mL	1x	bFGF	2.5 ng/mL	1:1000
N2- supplements	5 mL	1x	EGF	10 ng/mL	1:1000
Penicillin/Streptomycin	3 mL	1.66x	BDNF	10 ng/mL	1:10000
Non-essential amino acids	5 mL	1x			
Heparin	1 mL	1 mg/mL			

NI complete contains additional growth factors that stimulate proliferation and suppress differentiation: basic Fibroblast Growth Factor (bFGF), Epidermal Growth Factor (EGF) and Brain-derived neurotrophic factor (BDNF). bFGF uses Heparin as a co-factor and helps maintaining cells in undifferentiated state and continued self-renewal of the NSCs. EGF is shown to increase proliferation and survival in NSCs (recommended by EC-JRC). BDNF is an important neuronal growth factor involved in neurite outgrowth, synaptogenesis, synapse maturation and stabilization. BDNF is added to NI Complete in small amounts to aid NSC survival and in necessary for the cells to be representative for hippocampal and/or cortical neurons in the human body.

Neuronal Differentiation medium

The Neuronal Differentiation (ND) medium is used for experimental studies with the aim to differentiate immature neural stem cells into a mixed culture of post-mitotic neurons and astrocytes. ND complete is made from ND Incomplete, see Table A2.3.

Table A2.3: ***Recipe for Neuronal Differentiation medium***

ND Incomplete			**ND Complete**		
		Desired concentration		Desired concentration	Dilution
Neurobasal medium	500 mL		ND Incomplete x mL		
B27 Supplements	10 mL	1x	GDNF	1 ng/mL	1:10000
N2- supplements	5 mL	1x	BDNF	2.5 ng/mL	1:10000
Penicillin/Streptomycin	3 mL	1.66x	Laminin	1 µL/mL	1:1000
L-Glutamine	5 mL	2 mM			

ND Complete contains additional factors that stimulates differentiation and survival of NSC like BDNF, Glial cell line-Derived Neurotrophic Factor (GDNF) and Lamin (1µg/mL). GDNF along with BDNF and the other supplements aids in differentiating the NSC into post-mitotic neurons. Lamin supports growth and differentiation of neural cells and other cells and is the only animal derived product used. Animal derived laminin is used due to its low cost instead of human derived laminin.

2.4 Medium change

Medium change is done three times a week for cells in NI medium and twice a week for cells in ND medium.

1. Prepare the amount of complete medium needed according to Table A2.2 for NI medium and Table A2.3 for ND medium and heat to 37 °C.
2. Aspirate the old cell medium and make sure to not touch cells.
3. Add new medium
    - For flasks: tilt flask on the side, and add medium gently, make sure not to flush cells to roughly to avoid mechanic stress
    - For plates: add medium gently with multipipette while rotating pipette to avoid mechanic stress and ad the medium from one side of the wells.

2.5 Splitting and passaging

Passaging of flask was performed once a week when the NSC culture reached confluency. This happens when the cells are allowed to proliferate until they are covering 100% of the surface of the flask. See Table A2.4 for volumes of solutions needed for cell passaging adjusted to flask size.

Table A2.4: ***Volumes of solutions needed for cell passaging adjusted to flask size.***

Flask size	**T25**	**T75**	**T150**
Trypsin-EDTA (0,5 %)	0,3 mL	1 mL	2 mL
PBS (1X) without Ca^{2+} and Mg^{2+}	3 mL	9 mL	18 mL
Defined Trypsin Inhibitor	2 mL	6 mL	12 mL
NI medium (complete)	3 mL	10 mL	20 mL

1. Coat the appropriate number of flasks, following the protocol described in 2.1.
2. Dilute pre-warmed 0,5 % Trypsin-EDTA (Trypsin) 1:10 in pre-warmed PBS.
3. Aspire the old cell medium from the flask, transfer Trypsin (1:10) to cell flask. Incubate cells for 37 °C for 2 min and inspect in microscope to ensure that all cells are detached from the surface.
4. Transfer the dissolved cell suspension to a Falcon tube and wash the flask with Defined Trypsin Inhibitor and transfer to the dissolved cell suspension. Mix gently by pipetting up and down.
5. Centrifuge cells for 4 min and 30 sec at 130 g. Aspirate the supernatant and tap the tube gently to disperse cells across the surface of the bottom of the Falcon tube.
6. Resuspend the cells in NI medium, mix gently a few times making sure no aggregates are left.
7. Count the cells by mixing 1:1 with trypan blue, using an automatic cell counter. Measure both sides of the cell counter slide. Calculate the average from sides A and B.
8. Calculate how much NI medium you need to dissolve cells in to plate right number of cells according to Table A2.5 . Create a new cell suspension with right amount of cells/mL and transfer to flask or plates.

Table A2.5: ***Seeding volume, cell density and medium change volume.***

Flask size	Area (cm^2)	Seeding volume	Cell number	Medium change volume
T25	25	7 mL	$0,33x10^6$ cells	7-10 mL
T75	75	20 mL	$0,8x10^6$ cells	20 mL
Plate size	Area/well (cm^2)			
96-well	0,33	135-150 µL/well	7000 cells/well	135 µL/well
24-well	1,9	0,5 µL/well	24.000 cells/well	0,5 mL/well

Appendix 3: Preparations of sub stock dilutions

1

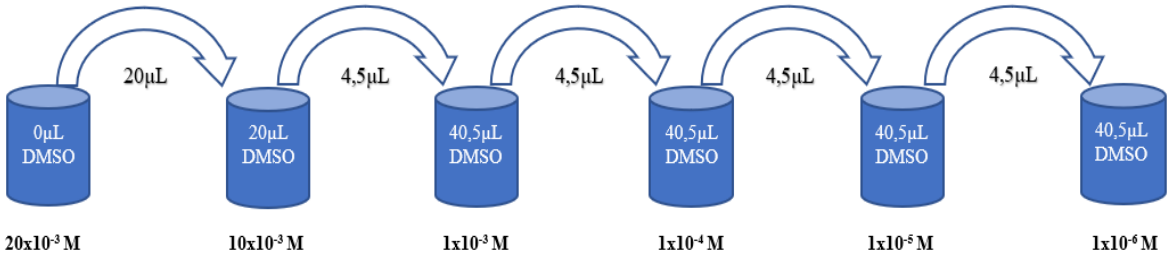

2

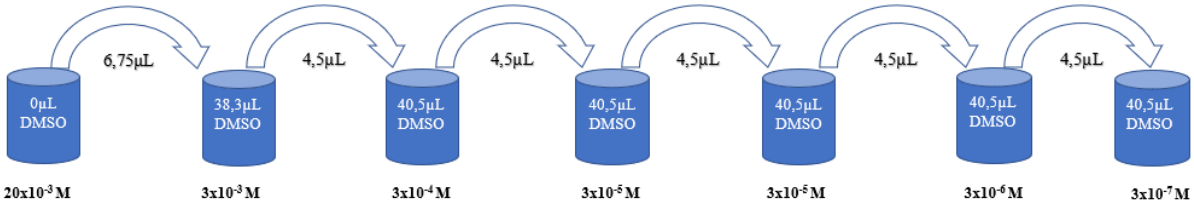

Figure A3.1: ***Preparations of sub stock solutions from original stock solution 2x10^{-3} M for exposure to NSCs undergoing differentiation****. Calculations were done using formula C1*V1=C2*V2 to make sub stock solutions of the PAHs diluted in DMSO. 1: show dilutions making 20x10^{3} to 1x10^{-6} M sub stocks. 2: show dilutions making 3x10^{-3} M to 3x10^{-7} M.*

Table A3.1: ***Dilution of sub stock to ND medium to get a 1:1000 dilution for exposure of NSCs undergoing differentiation.***

Sub stocks:	**20x10^{-3} M**	**10x10^{-3} M**	**3x10^{-3} M**	**1x10^{-3}M**	**3x10^{-4} M**	**1x10^{-4} M**	**3x10^{-5} M**	**1x10^{-5} M**	**3x10^{-6} M**	**1x10^{-6}M**	**3x10^{-7} M**
Dilution in ND medium	1:1000	1:1000	1:1000	1:1000	1:1000	1:1000	1:1000	1:1000	1:1000	1:1000	1:1000
Concentration in medium	2x10^{-5} M	1x10^{-5} M	3x10^{-6} M	1x10^{-6} M	3x10^{-7} M	1x10^{-7} M	3x10^{-8} M	1x10^{-8} M	3x10^{-9} M	1x10^{-9} M	3x10^{-10} M

Appendix 4: Plate layouts

Alamar Blue optimization

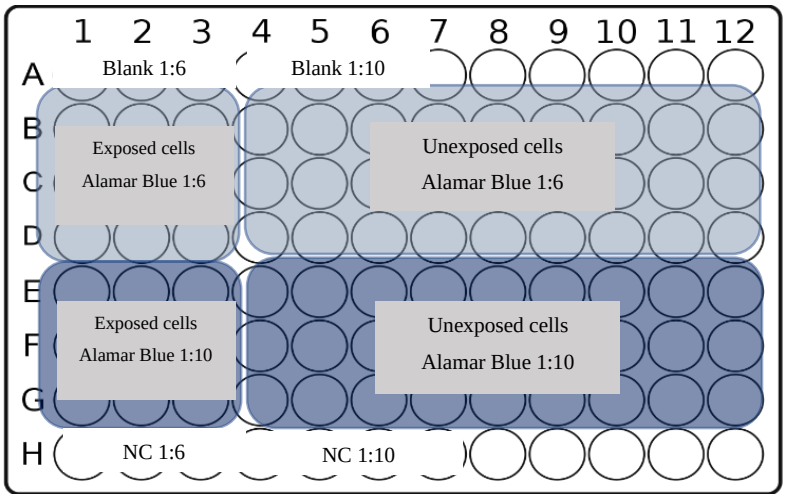

Figure A4. 1: ***Plate layout for Alamar Blue optimization project.*** *Row A, well 1-4 contained blank with the volume for 1:6 dilution of Alamar Blue. Row A, well 5-8 contained volume for 1:10 dilution. Row B to G wells 1-4 contained cells exposed to* $1x10^{-3}$ *M glycidamide in ND medium. Row B to G wells 5-12 contained untreated cells in ND medium that functioned as control cells (positive control). 1:6 dilution of Alamar Blue was added to row B to G wells 1-12. 1:10 dilution of Alamar Blue was added to row E to G wells 1-12. Row H functioned as negative control with the volumes corresponding for 1:6 dilution (well 1-4) and 1:10 (well 5-8) of Alamar Blue.*

Cell viability assay

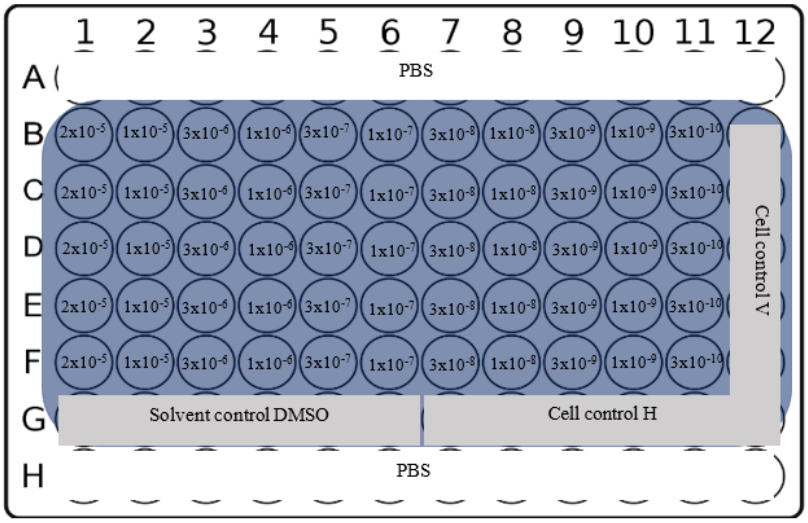

Figure A4.2: ***Plate layout for cytotoxicity experiment of polycyclic aromatic hydrocarbons.*** *Row B1 to F1 contained the highest concentration* $2x10^{-5}$ *M, the concentration decreases for every row down to B11 to F11 that contained the lowest concentration* $3x10^{-10}$ *M. Row G well G1-G6 contained solvent control, cells treated with 0.1% DMSO. Row G well G7-G12 contained cell control horizontal (H) and column 12 contained a cell control vertical (V) both with only in ND medium. Row A and H contained PBS during both proliferation and differentiation. The same set up was used for all three PAH`s, one timepoint correspond to one plate per PAH.*

Gene expression

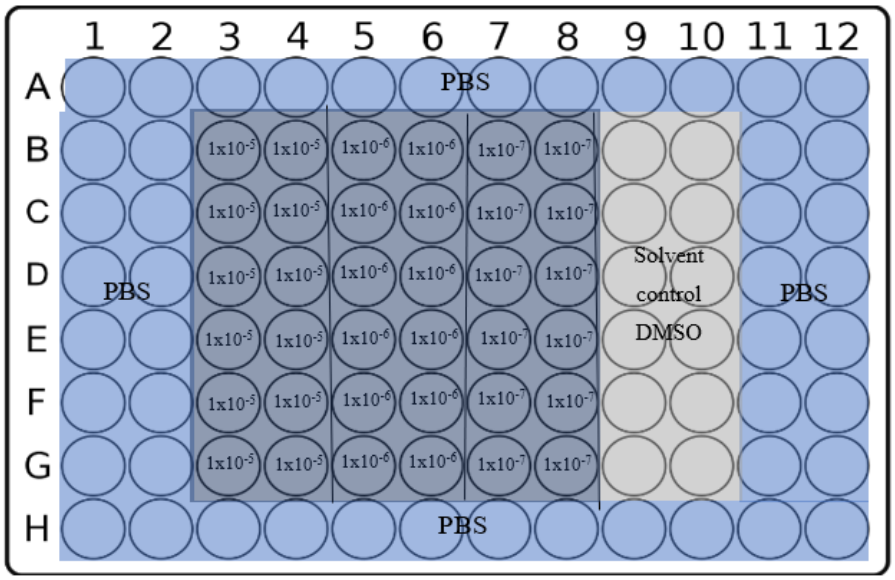

Figure A4.3: ***Plate layout for exposure of cells to gene expression.*** *Row 3-4 contained $1x10^{-5}$ M, row 5-6 contained $1x10^{-6}$ M and row 7-8 contained $1x10^{-7}$ M. Solvent control (0.1% DMSO) was in row 9-10. The plate was framed with PBS. As for β-NF the plate layout was the same, but row 3-4 contained $1x10^{-6}$ M, row 5-6 contained $1x10^{-7}$ M and row 7-8 contained $1x10^{-8}$ M. It was one plate per PAH and per time point.*

Immunocytochemistry

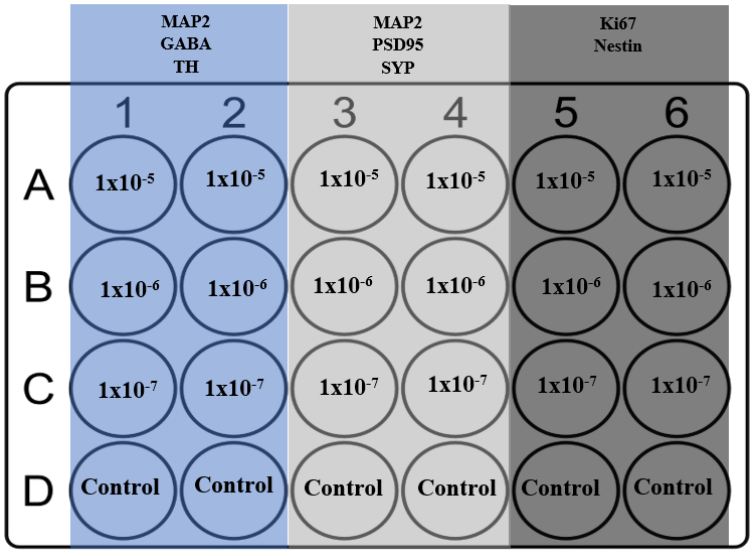

Figure A4.4: ***Plate layout for immunocytochemistry.*** *Column A contained $1x10^{-5}$ M, column B contained $1x10^{-6}$ M, column C contained $1x10^{-7}$ M and column D contained solvent control (0.1% DMSO). As for β-NF the plate layout was the same, but column A contained $1x10^{-6}$ M, column B contained $1x10^{-7}$ M and column C contained $1x10^{-8}$ M. It was one plate per PAH and per time point. Cells were stained with primary antibodies: Row 1-2 was MAP2, GABA and TH. Row 3-4 was stained with MAP2, PSD95 and SYP. Row 5-6 Ki67 and nestin.*